ALKENE EPOXIDATION CATALYSED BY MOLYBDENUM (VI) SUPPORTED ON POLYMERS

A thesis submitted to the Department of Pure and Applied Chemistry, University of Strathclyde, in partial fulfillment of the regulations for the Degree of Doctor in Philosophy in Chemistry

RENE MBELECK

SEPTEMBER 2009

ORIGINAL COPY TIGHTLY BOUND

ACKNOWLEDGEMENTS

First of all, I would like to thank so much Prof. David C. Sherrington FRS for his availability, helpful guidance, his trust and for giving me the opportunity for working in his group.

I also wish to thank Dr. Basu Saha and Dr. Krzysztof Ambroziak for their collaboration and suggestions in this project.

I also wish to thank Dr. Jovita Moreno from Department of Chemical and Environmental Technology, Rey Juan Carlos University, Mosteles, Spain for "*the synthesis of the MCM-41 precursor support and its aminated derivative*".

I particularly thank Pol Besenius for his help in the lab.

To finish with, I wish to thank Dr. Peter Cormack, Gavin, Iain, Arlene and Mol for providing a good working environment.

To my mother Mrs. widow NGO INYOUMA BAKEBECK Marie, Prof. David. C. SHERRINGTON FRS, Dr. Emmanuelle SCHULZ, Dr. Jacqueline COLLIN and Mrs. Marie-Jo NELSON

ABSTRACT

In 1963, Bruce Merrifield introduced the solid-phase peptide synthesis technique using an insoluble macromolecular protecting group for synthesising peptides[1]. Since then organic chemistry involving solid supports has been developed as an efficient technique for the synthesis of a large number of organic compounds, and therefore a significant interest has been raised in catalysis.

This thesis deals with the synthesis of new supported Mo catalysts active, selective and stable for the epoxidation of olefins on an industrial scale using a continuous reactive distillation rig and also in multi-step fine chemical syntheses.

Here I report on the immobilisation of molybdenum (VI) complexes supported on polymer beads or resins and an inorganic MCM-41 support for the catalytic epoxidation of alkenes with alkyl hydroperoxides as the oxidants. Specifically $MoO_2(acac)_2$ has been successfully supported on a commercially sourced polybenzimidazole (PBI) resin using a simple ligand exchange reaction. In addition a number of chloromethylated polystyrene resins has been synthesised by suspension copolymerisation of appropriate mixture of vinyl benzyl chloride (VBC) and divinylbenzene (DVB), in the presence of porogenic solvents when required. The VBC residues have been reacted with several different donors ligands 2-aminomethylpyridine (AMP), 2-aminophenol (2-AMPH), glycine (GLYC), iminodiacetic acid (IMDA) ethylenediaminetetraacetic acid (EDTA) and phenylalanine (Phe) in order to create binding sites for the metal on each polymer matrix. However the inorganic MCM-41 support was first modified with aminopropyl trimethylsilane, then the thiophene-2-carboxyaldehyde ligand was attached in order to generate binding sites for the metal on this support. Ligand exchange with $MoO_2(acac)_2$ again allows Mo (VI) species to be supported on these supports. Each resin supported Mo has been activated by treatment with t-butylhydroperoxide (TBHP) and then investigated as a heterogeneous catalyst in the epoxidation of cyclohexene and styrene using TBHP. An ^1H NMR spectroscopic analytical procedure has been used to monitor the progress of each epoxidation.

In order to check the stability of each of these supported Mo catalysts prior to using them in a reactive distillation column, extensive study of recycling of each support Mo catalyst was undertaken by monitoring the use of a sample of each in up to 5-10 successive batch epoxidations. At the same time the supernatant solution from each epoxidation has been isolated, reduced to a dry residue, and the latter employed as a potential catalyst in an epoxidation reaction. The latter procedure is a very powerful methodology for the detection of low levels of catalyst (Mo) leaching in the heterogeneous reactions.

PBI.Mo, polystyrene-supported Mo and inorganic supported Mo catalysts have proved to be very active, maintaining this activity over 5 to 10 cycles. However, the residues from supernatant solutions have also proved to be catalytically active demonstrating the occurrence of Mo leaching from **PBI.Mo** and polystyrene-supported Mo catalysts. In the case of the PBI supported Mo catalyst (**PBI.Mo**), the level of leaching fell substantially over 10 cycles until the rate of epoxidation was close to that of a control epoxidation reaction carried out in the absence of any Mo species. Leaching from one of the polystyrene-supported **Ps.AMP.Mo** (25) catalysts was more pronounced and remained significant even after several cycles. However, a second sample of polystyrene-supported **Ps.AMP.Mo** (26) with a higher ligand: metal ratio showed a much lower tendency to leach. This result has now been confirmed with a third sample of this type of polymer catalyst (**Ps.AMP.Mo** (27)).

Other polystyrene resin supported Mo catalysts employing the 2-AMPH, GLYC, IMDA and EDTA ligands have also been tested. These are all very active cyclohexene epoxidation catalysts and extensive recycling and leaching experiments have also been carried out in order to assess again if these ligands offer improved stability towards Mo leaching. A similar study has also been carried out with the inorganic **MCM-41.SB.Mo** (32) catalyst.

Several of these supported Mo catalysts have also been assessed on a small scale e.g. for fine chemical syntheses, and they also show relatively good conversion of olefins to their corresponding epoxides using different solvents or no solvent.

PBI.Mo has also been tested in a reaction distillation column. It shows very high reproductive conversion and good selectivity in the case of cyclohexene epoxidation with conversion of TBHP up to 97% after 1 h.

Abbreviations

Abbreviations and acronyms used in this thesis are :

Experimental terminology

AAS	Atomic Absorption Spectroscopy
BET	Brunauer, Emmett and Teller
FTIR	Fourier Transform Infrared spectroscopy
NMR	Nuclear Magnetic Resonance Spectroscopy
rpm	Revolution per minute

Chemicals

acac	acetylacetone
AIBN	azo-bis(isobutyronitrile)
AMP	aminomethyl-2-pyridine
2-AMPH	aminophenol
APTMS	3-aminopropyl-trimethoxysilane
CMS	chloromethylstyrene
CTAB	cetyltrimethylammonium bromide
DCC	dicyclohexylcarbiimide
DCE	1,2-dichloroethane
DMA	dimethylamine
DMF	dimethylformamide
DVB	divinylbenzene
EDTA	ethylenediaminetetraacetic acid
GLYC	glycine
IMDA	iminodiacetic acid
Phe	(L)-phenylalanine
St	styrene
TBAI	tetrabutylammonium iodide
TBHP	tert-Butyl hydroperoxide
TEA	triethylamine
TEOS	tetraethoxysilane
THF	tetrahydrofuran
VBC	vinyl benzyl chloride

supports

PBI	polybenzimidazole resin
Ps	chloromethylated polystyrene resin
MCM-41	MCM-41

Chelated supports

The functionalized supports were named as shown in the following fashion:

Ps.AMP	chloromethylated polystyrene resin with aminomethyl-2-pyridine ligand
Ps-2-AMPH	chloromethylated polystyrene resin with aminophenol ligand
Ps.GLYC	chloromethylated polystyrene resin with glycine ligand
Ps.IMDA	chloromethylated polystyrene resin with iminodiacetic ligand
Ps.EDTA	chloromethylated polystyrene resin with ethylenediaminetetraacetic ligand
Ps.Phe	chloromethylated polystyrene resin with (L)-phenylalanine ligand
Ps.SB	chloromethylated polystyrene resin with Schiff base ligand
MCM-41.SB	MCM-41 with thiophene-2-carboxyaldehyde ligand

Supports metal complexes

The resulting Mo complexes were named as shown:

PBI.Mo	polymer-supported molybdenum (VI) complex (imidazole ligand)
Ps.AMP.Mo	polymer-supported molybdenum (VI) complex (aminomethyl-2-pyridine)
Ps.2-AMPH.Mo	polymer-supported molybdenum (VI) complex (aminophenol)
Ps.GLYC.Mo	polymer-supported molybdenum (VI) complex (glycine)
Ps.IMDA.Mo	polymer-supported molybdenum (VI) complex (iminodiacetic acid)
Ps.EDTA.Mo	polymer-supported molybdenum (VI) complex (ethylenediaminetetraacetic acid)
Ps.Phe.Mo	polymer-supported molybdenum (VI) complex ((L)-phenylalanine)
Ps.SB.Mo	polymer-supported molybdenum (VI) complex (2,4-dihydroxylbenzaldehyde (L)-phenylalanine)
MCM-41.SB.Mo	inorganic support molybdenum (VI) complex (thiophene-2-carboxyaldehyde)

The molecular structures of the supported Mo complexes

The molecular structures of the supported Mo complexes are drawn as shown:

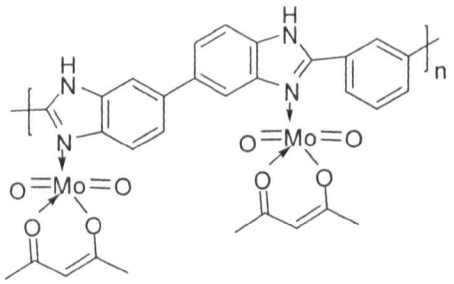

PBI.Mo

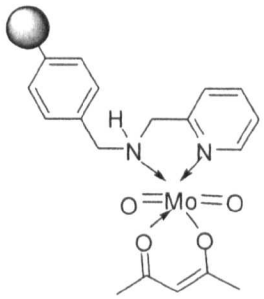

Ps.AMP.Mo

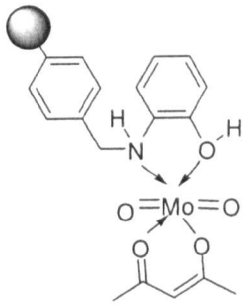

Ps.2-AMPH.Mo

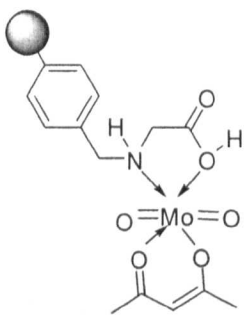

Ps.GLYC.Mo

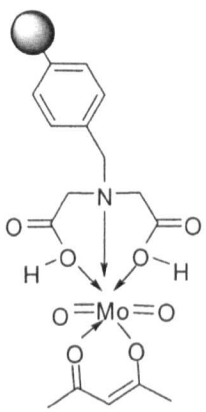

Ps.IMDA.Mo

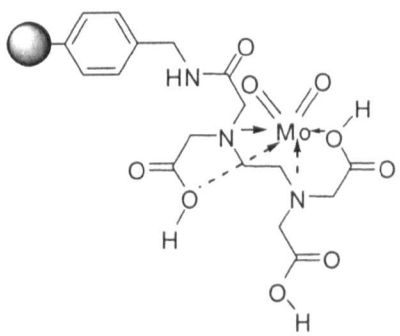

Ps.EDTA.Mo

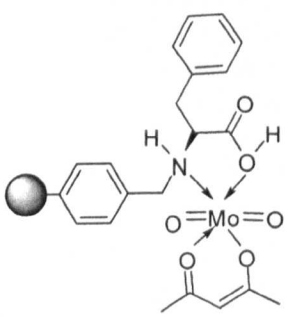

Ps.Phe.Mo

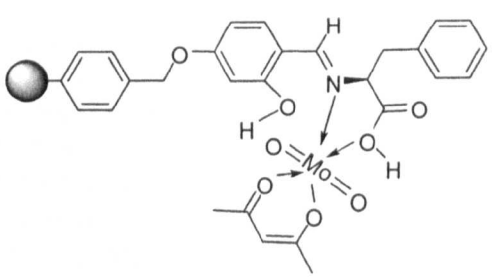

Ps.SB.Mo

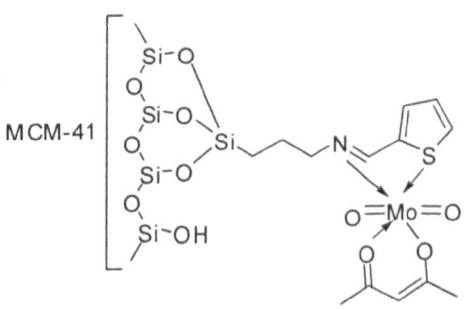

MCM-41.SB.Mo

Table of contents

Chapter 1

Introduction

1 INTRODUCTION

In general, alkenes are derived from natural resources or generated as products of the chemical industry, and they are found in great abundance in many organic molecules. One of the most useful transformations of alkenes is epoxidation (Scheme 1.1).

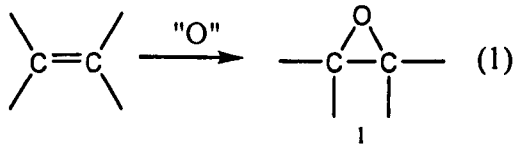

(1)

Scheme 1.1 Schematic representation of the epoxidation of an alkene.

Epoxidation is an important reaction in organic synthesis because the epoxides formed are intermediates that can be converted into a variety of products such as alcohols, alkanolamines,etc. Some reactions of epoxides are shown in scheme 1.2.

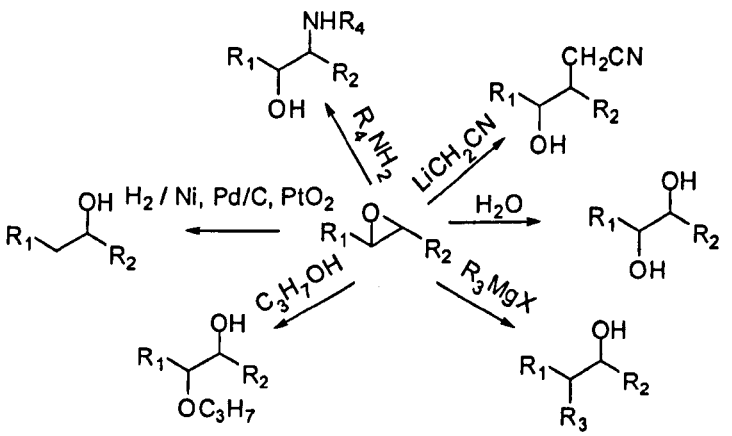

R_1, R_2 : H, alkyl, phenyl, ar, etc.

Scheme 1.2 Some reactions of epoxides.

In addition, epoxidation is also very attractive in the case of in asymmetric reactions since it can lead to two chiral carbon atom in one step[2].

The direct oxidation of two adjacent carbon atoms from alkenes has been known for the last century by the use of peracids as oxidant. The rate of epoxidation by peracids is not very sensitive to steric hindrance but it is sensitive to electronic changes. This means that increasing the electron density of the alkene or decreasing that of the peracid can increase the reaction rate. Despite the absence of full understanding of the mechanism of epoxidation by peracids (Scheme 1.3), this dependence on the electronic effect provides scope for the epoxidation of many of the lower alkenes.

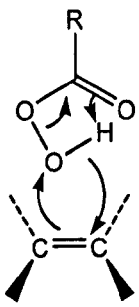

2

Scheme 1.3 Suggested mechanism of the epoxidation of alkenes by peracids.

1.1 Background Concepts in Catalysis

The problem of the dependence on electronic effects has been overcome by the use of transition-metal complexes as catalysts for epoxidation of alkenes. In general the phenomenon of catalysis was recognized over 150 years ago by Berzelius[3] who referred to the catalytic power of substances that were able to awake or to speed up reactions. But the lack of understanding of how catalysts are able to increase the reaction rate without changing the free energy of either reactants or products remained a mystery for many years. Only in the last few decades, once the principles of thermodynamics and the concept of equilibrium had been established was it that chemists began to elucidate mechanistic pathways involving catalysts by using other tools such as kinetics, stereochemical studies and spectroscopy. They discovered that catalysts interact with

reactants to provide a reaction pathway with a significant lower free energy of activation than the corresponding un-catalysed pathway as shown in Scheme 1.4.

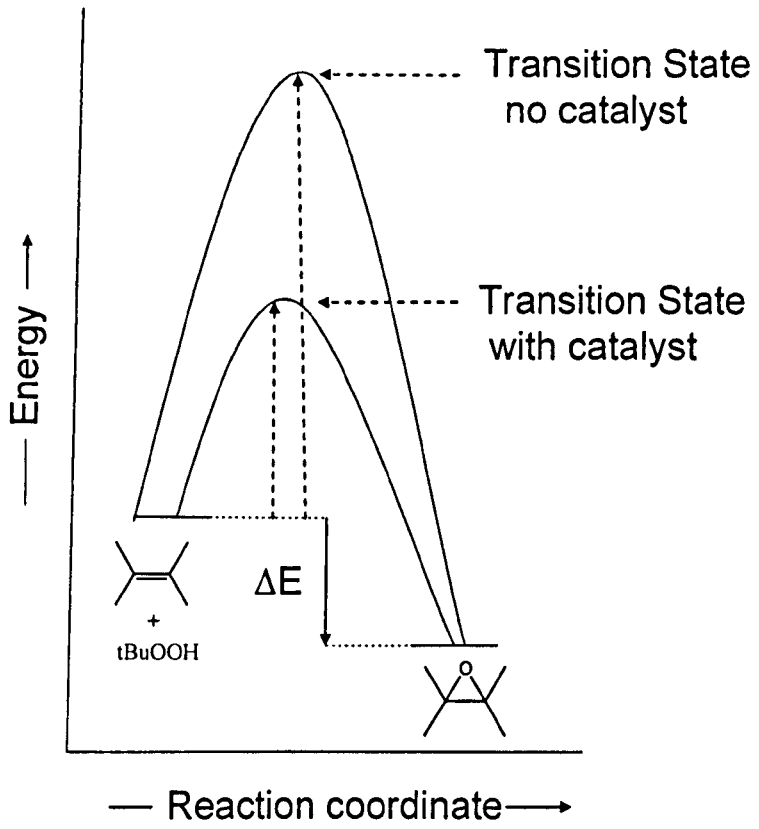

***Scheme 1.4** Epoxidation reaction energy profile diagram.*

In addition, the presence of a catalyst can influence initial product distributions by allowing the preferential formation of a product that may be less stable thermodynamically than another. This is well-known as selectivity. There are several kinds of selectivity that can be by induced by catalysts: chemoselectivity, regioselectivity and stereoselectivity (enantio and diastereoselectivity). From this point of view, the use of transition-metal complexes as catalysts for the synthesis of organic products has received increasing interest not only to obtain good yields and high selectivity of the desired organic products in a clean process, but also to minimise the cost of such processes by recycling metals used such as molybdenum, vanadium and titanium. The

use of transition-metal complexes as catalysts can be divided in two categories: homogeneous catalysts and heterogeneous catalysts.

In general, homogeneous catalysts usually have several advantages over their heterogeneous counterparts. The main advantages are that homogeneous catalysts are soluble in the reaction medium along with the reactants, and the catalytic processes often show high activity, good reproducibility and high selectivity under mild conditions. These qualities are created by the uniformity of the well-defined active sites of homogeneous catalysts in the reaction mixture. In addition, because homogeneous catalysts are discrete molecules with well-defined active sites, they are relatively easy to characterise by standard spectroscopic techniques, such as NMR and IR. Thus it is relatively easy to study and understand the mechanisms of homogenous catalysts by conventional methods.

Heterogeneous catalysts, on the other hand, exist as another phase in the reaction medium, typically as a solid in the presence of a liquid or gaseous mixture of reactants. Thus, the active sites on heterogeneous catalysts are difficult to characterise because they are not discrete molecular entities. This can also lead to low activity, low selectivity and low reproducibility. In addition, it is often difficult to determine the mechanisms involving heterogeneous catalysts due to the constitution of their active sites not being well-defined.

Upon the evidence presented above, homogeneous catalysts would seem to be the best option. However, industrial use of homogeneous catalysts is relatively limited, because homogeneous catalysts suffer from one key disadvantage. They are often difficult to separate from reaction products i.e. catalyst recovery is often problematic. In addition it is also very difficult to engineer *continuous* reaction processes when the catalyst is a soluble metal complex In contrast, the use of heterogeneous catalysts in liquid phase processes usually allows catalyst recovery by simple filtration and in this manner, it is easy to obtain desired pure products. Furthermore *continuous* reaction processes are

relatively easily engineered by packing the heterogeneous catalyst in some suitable column and flowing reaction components through the column.

1.2 Transition-Metal-Catalyzed Epoxidations

1.2.1 Oxygen atom sources

For transition-metal-catalysed epoxidations various oxygen sources such as molecular oxygen, peracetic acid, hydrogen peroxide and alkyl peroxides have been used. Molecular dioxygen is very cheap especially it can be used as air and indeed it is required as pure O_2. However it is well known that catalytic reactions using molecular dioxygen usually proceed by a free radical autoxidation mechanism and are often non-selective[4] because of the existence of a competition in the chain propagation step between addition of the radical, $RO_2^{\bullet}$, to the C=C double bond and hydrogen abstraction at a reactive C-H bond. Scheme 1.5 shows this for propylene autoxidation.

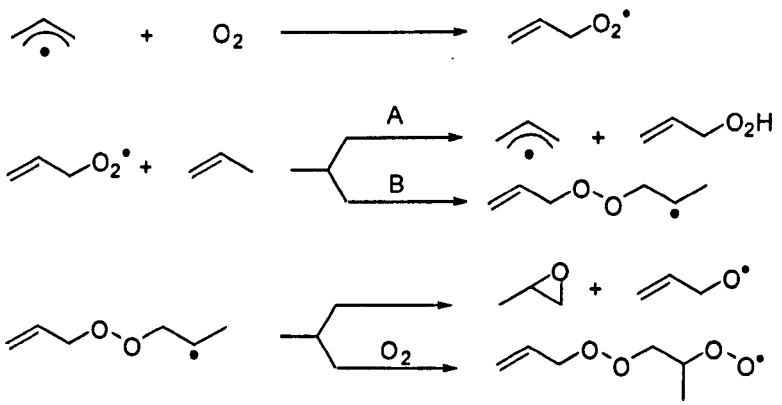

Scheme 1.5 Autoxidation of propylene with molecular dioxygen:
A- H abstraction; B-radical addition.

Peracetic acid is also cheap, but it is more dangerous in almost every situation because it is very unstable thermally and readily decomposes violently. For example the 40%

solution grade of peracetic acid in acetic acid can be transported only by truck, and even then only in small drums or smaller containers.

Hydrogen peroxide is also cheap and it is, in principle, also very stable thermally, but it is more sensitive to violent decomposition catalysed by trace metallic impurities. For this reason it is often difficult to handle it safety.

Alkyl peroxides such as cumene hydroperoxide (CHP), pinane hydroperoxide (PHP) and in particular tert-butyl hydroperoxide (TBHP) have several practical advantages over other oxygen sources[5] in oxidation reactions:

- TBHP is more selective than peracetic acid , hydrogen peroxide.
- TBHP is less sensitive to contamination by metals than either peracetic acid or H_2O_2, and on this basis is safer to handle.
- TBHP has high thermal stability in dilute solution, for example its half-life is 36 days at 115°C as a 0.2 M solution in benzene.
- TBHP is soluble in various hydrocarbon solvents (e.g. benzene, toluene, dichloroethane, dichloromethane) which is an advantage over H_2O_2.
- TBHP is almost unreactive toward most organic compounds in the absence of catalysts.

1.2.2 Metal catalyzed oxidations using alkyl hydroperoxides.

One of the most common oxygen source for the catalytic oxidation reactions is alkyl hydroperoxides. Alkyl hydroperoxides can react in either a homolytic or heterolytic manner in presence of metal catalysts[5]. In the homolytic decomposition of alkyl hydroperoxides, radicals formed as intermediates react with olefin in the similar manner to that shown in scheme 5. These radicals are formed through the following one electron redox processes[6,11] (Scheme 1.6).

$$M^{n+} + RO_2H \longrightarrow M^{(n-1)+} + RO_2^{\bullet} + H^+$$

$$M^{(n-1)+} + RO_2H \longrightarrow M^{n+} + RO^{\bullet} + OH^-$$

The overall reaction is given by:

$$2\,RO_2H \xrightarrow{[M]} RO_2^{\bullet} + RO^{\bullet} + H_2O$$

M = Co, Mn, Fe, Mo etc.

Scheme 1.6 Metal-catalysed decomposition of an alkyl hydroperoxide.

In addition, alkyl hydroperoxides are known as strong oxidants and weak reducing agents. Hence, their homolytic or heterolytic decomposition depends on the nature of the oxidation potential of the metal catalyst and its Lewis acidity. Then strong oxidants metal catalysts such as Co(III), Mn(III), Ce(IV) and Fe(III) cause and facilitate the homolytic decomposition of alkyl hydroperoxides (Scheme 1.6).
However, in order for the reaction to follow a heterolytic decomposition of alkyl hydroperoxides the metal catalyst must be a Lewis acid to allow coordination of organic substrates to the metal centre during the reaction and must be a weak oxidising agent in order to avoid catalysing the homolytic decomposition of alkyl hydroperoxides reactions.

1.2.3 Metal catalyzed epoxidations using alkyl hydroperoxides or hydrogen peroxides as oxidants.

It is well-known that certain transition-metal complexes such as molybdenum(VI), vanadium(V), tungsten(VI) and titanium(IV) catalyse the liquid phase epoxidation of alkenes with alkyl hydroperoxides[7,9,10], although in the last decade the use of rhenium(VII) complexes such as methyltrioxo-rhenium (MTO) as oxidation catalysts has been developed[8]. A number of mechanisms have been proposed for transition-metal-catalysed hydroperoxide epoxidation of olefins. These may be separated into two main types, both invoking the initial formation of a catalyst-hydroperoxide complex. Mimoun

et al[9] suggest a mechanism which proceeds via prior co-ordination of the olefin to the metal hydroperoxide **A**, followed by insertion to form a cyclic intermediate **C** and thereafter elimination of the epoxide **D**. However, Sharpless et al[10] propose a mechanism which proceeds in a concerted way via transition state **E** (Scheme 1.7) where the olefin attacks an oxygen atom of a peroxo group. In addition, in both mechanisms, the oxo-metal bond (M=O) remains intact during the process, and the metal alkoxide bond formed undergoes exchange with alklyl hydroperoxide to regenerate the peroxo-metal complex.

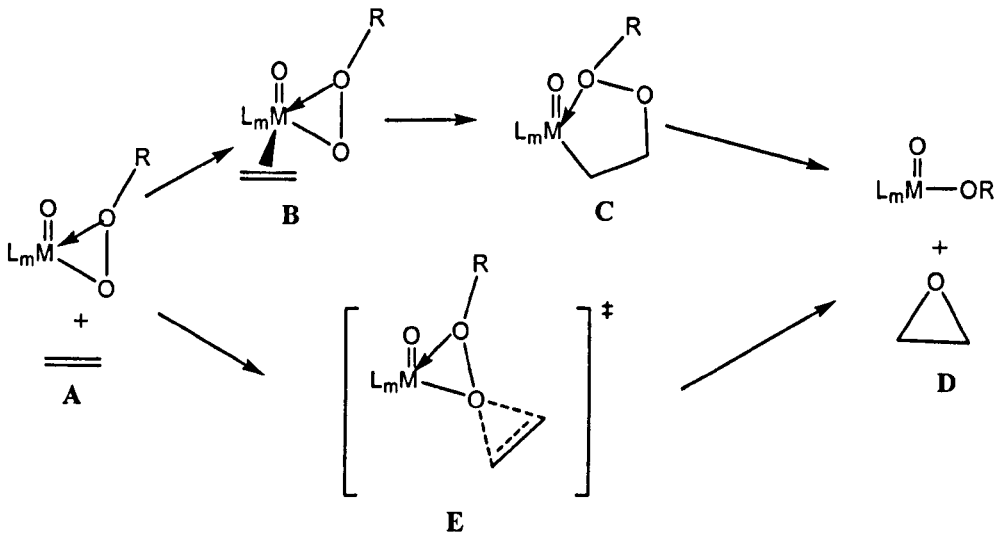

Scheme 1.7 Schematic Representation of the Reaction Mechanism Suggested by Mimoun (top) and by Sharpless (bottom)

The catalytic properties of these transition-metal complexes are characterised as being Lewis acids in their highest oxidation state-d^0. These Lewis acids have a low redox potential and are labile with respect to ligand substitution. Thus the resulting transition-metal complexes in a high oxidation state can facilitate the heterolysis of alkyl peroxides by forming transition metal-alkyl peroxide complexes which are soluble in non-polar solvents. Both homogeneous and heterogeneous catalysts have been used successfully.

1.2.3.1 Soluble molybdenum oxides

Molybdenum (VI) complexes are probably the best catalysts for epoxidation with alkyl hydroperoxides as oxidants, and an enormous amount of literature is available about molybdenum-catalyzed epoxidations[7,11-14]. Soluble molybdenum complexes, ranging from various molybdenum compounds such as $Mo(CO)_6$, $MoO_2(oxinate)_2$, $MoO_2(acac)_2$ to molybdenum clusters as $[C_5H_5N^+(CH_2)_{15}CH_3]_3[PMo_{12}O_{40}]^{3-}$,[15] and ammonium molybdate $[(NH_4)_6Mo_7O_{24}.4H_2O]$[16] catalyse the epoxidation of many different alkenes in high yield and low yields of by products (e.g. alkylperoxo compounds)[14]. For example propylene oxide is currently manufactured on a large scale by molybdenum-catalyzed epoxidation of propylene with t-butyl hydroperoxide (Reaction 2) or 1-phenylethyl hydroperoxide (Reaction 3) (the Halcon process)[17].

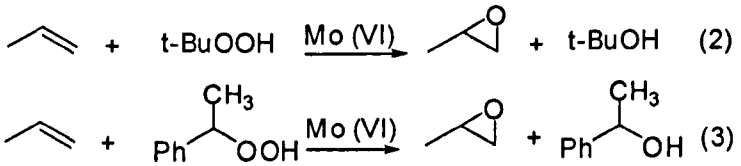

The tert-butyl alcohol co-product in (2) can be recycled by dehydration followed by hydrogenation or converted to methyl tert-butyl ether, a high-octane component used in gasoline. The co-product in (3), 1-phenylethanol, can be dehydrated to styrene or recycled[11]. In addition the catalytic properties of molybdenum complexes are to a certain extent dependent on the ligand attached to molybdenum [13, 18]. It has been observed that a higher epoxidation rate can be achieved by using relatively stable complexes of molybdenum, e.g., $MoO_2(oxinate)_2$, $MoO_2(acac)_2$[18]. It is also well-known that bidentate and tridentate ligands bearing N-, O- and S-electron donors are of interest and have been synthesized in order to stabilize the catalysts and improve the reactivity. For example, the complex dichlorodioxomolybdenum(VI) containing the 2,2-di(1-pyrazolyl)-propane ligand was reported by Kühm et al[19]. This complex displayed a moderate catalytic reactivity (i.e., 65% cyclooctene oxide after 4 h and 100% at 24 h reaction time). However, the stability of the catalyst was only slightly enhanced.

Additionally, complexes of formulas $MoX_2O_2L_2$, where X= Cl, Br, or Me and L_2 = 2,2'-bipyridine or 2,2'-bipyrimidine have been established and appear to be stable catalysts. However, the catalytic reactivity can be considered as moderate, as these catalysts produced only 75% cyclooctene epoxide after 24 h[20, 21].

1.2.3.2 Soluble tungsten oxides

In 1983 Venturello[22, 23] reported the first use of tungstate-phosphate quaternary ammonium chloride ions (Na_2WO_4-H_3PO_4-R_4NCl) and hydrogen peroxide in dichloromethane under acidic conditions for direct epoxidation of olefins. High selectivities to epoxide (80-90%) and good conversion (>93%) were obtained after relatively short reaction times and under mild conditions (40-70°C). But the effectiveness of this method reported appears to be a function of the pH of the aqueous phase. Low pH around 1.6-2 and an excess of alkene seem to be necessary to obtain good yield of epoxide. At the same year, Ishii et al[24] reported the use of W-based heteropoly acids, $H_3PW_{12}O_{40}$ (WPA), and an aqueous hydrogen peroxide, with an appropriate amount of ammononium salts such as cetylpyridinium chloride (CPC), under two-phase conditions using chloroform as solvent. They obtained good conversion to epoxide (>82%) and good selectivity (>98%) after 24h with different terminal alkenes. Despite the success of both procedures, the use of halogen-containing solvents remains an issue of environmental and economic concern. Recently Noyori et al[25] reported a new catalytic system which is a Na_2WO_4 dihydrate, combined with (aminomethyl)phosphoric acid ($NH_2CH_2PO_3H_2$), and methyltri-n-octylammonium hydrogensulfate ([CH_3(n-$C_8H_{17})_3N$] HSO_4) in a 2:1:1 molar ratio and is free from any organic or inorganic choride. High conversion to epoxides and good selectivities were reported for the alkenes (1-octene, 1-decene and 1-dodecene) after 4 h. In contrast styrene and its simple derivatives gave very low conversion to epoxides because they easily undergo the ring opening at the aqueous/ organic interface. Recently, Luck and Jimtaisong[26] reported the synthesis of both Mo (VI), and W (VI) complexes with general formula $MCl_2O_2L_2$ from $MoCl_2$(VI)

and WCl_2(VI) with the bidentate ligand, bis(diphenylphosphino)methane dioxide ($dppmO_2$), which may offer a more stable catalyst. The W (VI) compounds $WCl_2O_2L_2$ were prepared by reaction of WCl_2(VI) with 2 equivalents of the monodentate or bidentate ligands in dichloromethane followed by treatment of the resulting reaction mixture with 2 equivalents of water. These authors, have also discovered that the addition of 1 equivalent of H_2O_2 to $WCl_2O_2L_2$ monodentate or bidentate phosphine oxides, leads to the formation of the oxoperoxo complexes $WCl_2(O)O_2L_2$. The addition of an excess of H_2O_2 to the dioxo compounds bearing the $dppmO_2$ ligand resulted in the formation of the oxodiperoxo, $W(O)(O_2)_2dppmO_2$ compound. The formation of these complexes is summarized in Scheme 1.8.

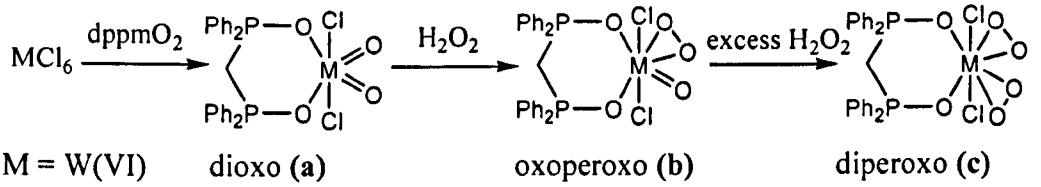

Scheme 1.8 Synthetic pathways to oxo-W (VI) complexes.

Epoxidation of cis-cyclooctene was performed in the presence of TBHP or H_2O_2 as an oxidant. The $WCl_2O_2dppmO_2$ complex **(a)** in the presence of TBHP only gave 52% epoxide conversion at 55°C for 24 h. Raising the temperature resulted in a moderate yield with 70% epoxide conversion at 90°C after 6h. In contrast, the Mo(VI) analogue gave better results with 63% epoxide conversion after 6 h and reached 100% epoxide conversion after 24 h at 55°C. Interestingly, the epoxidation of cis-cyclooctene performed with the $WCl_2O_2dppmO_2$ complex **(a)** in the presence of H_2O_2/EtOH gave higher epoxide conversions, 98% epoxide conversion at 70°C after 6h compared to the Mo(VI) analogue (only 26% epoxide conversion at 70%C after 6 h), i.e. opposite to the TBHP system reported above. The authors[26], postulated that the stability of the W(VI)-based catalysts may be related to the increase in the general metal-ligand bond strength from the first row

down to the third row transition metals. Therefore, the tungsten catalytic species function better in the presence of a strong oxidant such as H_2O_2 and with EtOH as solvent.

1.2.3.3 Soluble rhenium oxides

In the last decade the synthesis of organorhenium(VII) oxides has been carried out by many research groups[27-30]. In 1960, Riedel who was a student of E. O. Fischer at this time, was the first to try to synthesise η^2-$(C_5H_5)ReO_3$ starting from $ClReO_3$ and $Na(C_5H_5)$, but all his attempts failed. However, in 1974, the first organorhenium oxides $(CH_3)_4ReO$ in the oxidation state +VI were prepared by the group of G. Wilkinson[28, 29]. In 1984 Serrano[30], a postdoctoral research associate of W. A. Herrmann, prepared η^5-$(C_5(CH_3)_5)ReO_3$, by oxidising the organorhenium carbonyls (Scheme 1.9).

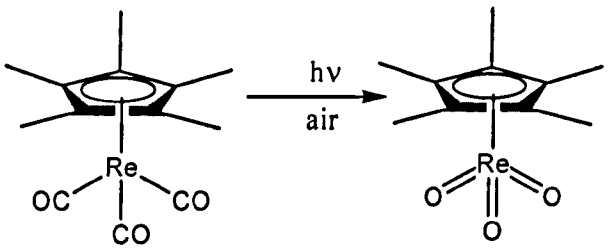

Scheme 1.9 Synthesis of η^5-$(C_5(CH_3)_5)ReO_3$

The importance of the surprisingly stable product was immediately recognized and more direct synthetic approaches were developed[31, 32]. For example the reaction of Re_2O_7 with $Sn(CH_3)_4$ in THF(Scheme 1.10) leads to methyltrioxorhenium(VII) (MTO).

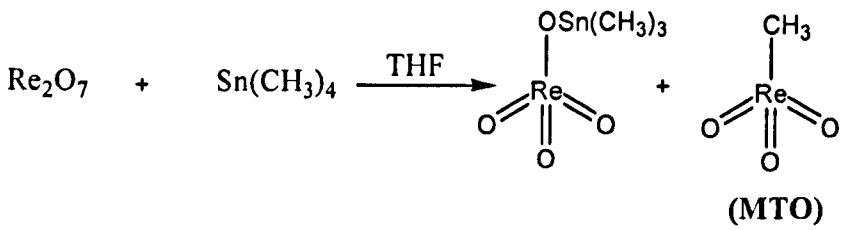

(MTO)

Scheme 1.10 Synthesis of MTO

The resulting compound, methyltrioxorhenium(VII) (MTO) turned out to be stable and, at the same time, a very applicable catalyst. Despite the successful and high yielding syntheses of η^5-$(C_5(CH_3)_5)ReO_3$ η^2-$(C_5H_5)ReO_3$ and (MTO), it had been noticed that it was not possible to generalise these syntheses to other derivatives of organorhenium oxides because the stability of R-ReO_3 depends on the transfer of the alkyl group R. For example the methyl group for MTO, is transferable to Re_2O_7 from a tin precursor only in boiling THF and the more sensitive, but less easily transferable longer chain alkyls cannot be prepared by the Sn route using Re_2O_7 as starting material. However the performance of R-ReO_3 complexes in catalysis is so far only well examined for MTO, since η^5-$(C_5(CH_3)_5)ReO_3$ is not catalytically active in olefin epoxidations and the poor solubility of η^2-$(C_5H_5)ReO_3$ as well as its more pronounced sensitivity to light and temperature prevented the examination of its catalytic behaviour extensively. Methyltrioxorhenium (MTO) is rapidly emerging as a versatile reagent, and in combination with aqueous hydrogen peroxide forms peroxy adducts **A** and **B** which are the catalytically active species as shown in Scheme 1.11.

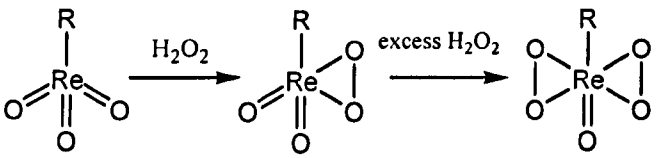

A **B**

Scheme 1.11 *Synthesis of dioxoperoxo Re(VII) (A) and oxodiperoxo Re (VII) (B).*

These species **A** and **B** are capable of the epoxidation of alkenes[33], the oxidation of amines[34,35], sulphides[36,37], phoshines[38],alkynes[39], phenol[40], arenes[41] and oxygen insertion into C-H bonds[42]. However, one the potential shortcomings of this reagent combination, particularly for epoxidation, is the need for a protic solvent (e.g. water or alcohol). Protic solvents may lead to the destruction of sensitive epoxide or a reduction in the stereoselectivity due to competitive hydrogen bonding by the solvent. This epoxide–instability problem has been overcome partially by Spilling et al[43] who reported the use

of the MTO/urea-H_2O_2 system in dichloromethane or ethanol. They obtained high conversion (95% and 100%), in the case of epoxidation of guaiol and cholesterol respectively, without any unwanted diol by-product. However when the epoxidation of cyclohexene was run in ethanol, only products from epoxide ring opening were observed. Two years later, Sharpless et al[44] reported that biphasic systems (water phase/organic phase) and addition of Lewis bases (tertiary nitrogen bases, such as quinuclidine, 2,2'-bipyridine, pyridine) to the system, were found to suppress epoxide ring-opening processes and increase the reaction velocity. In fact Lewis bases such as pyridine play three crucial roles in enhancing this process: (1) they speed up catalytic turnover, (2) they prevent decomposition of the epoxide products and (3) in sufficient concentrations, they increase catalytic lifetime. Another alternative to prevent acid-catalyzed ring opening of sensitive epoxides, was reported by Abu-omar et al[45]. They used (MTO) and urea hydrogen peroxide (UHP) in ionic liquids such as 1-ethyl-3-methylimidazolium tetrafluoroborate ([emim]BF_4) to increase the solubility of the MTO-UHP system, and hence to make this system more homogeneous than the Spilling's procedure described earlier. They obtained high conversion (>95%) and high selectivity (95%-99% epoxide) with several different olefinic substrates after 72 h.

1.2.3.4 Soluble manganese oxides

The interest in manganese complexes as catalysts for alkene epoxidations comes mainly from the relationship of these catalytic systems to the biologically relevant manganese porphyrins. Indeed synthetic metalloporphyrin complexes of iron, manganese and chromium have been the focus of intense studies as models for the monooxygenase enzyme cytochrome P-450. Various oxygen sources have been used such as: iodosylbenzene, sodium hypochlorite, molecular oxygen in the presence of an electron source, alkyl hydroperoxides, N-oxides, potassium hydrogen persulfate, and oxaziridine in the case of manganese porphyrins as epoxidation catalysts.

The presence of porphyrins or salen ligands around the manganese is not necessary to achieve the catalytic properties of manganese since even a soluble manganese salt such as manganese (II) triflate in acetonitrile catalyses the epoxidation of alkenes with iodosylbenzene as oxygen donor[46]. However, the reaction is nonstereopecific since epoxidation of *cis*-stilbene gives a mixture of *cis* and *trans*-stilbene oxide in ratio 35: 65 and also 10% of benzaldehyde[46]. The authors believe that these metal salts in the presence of iodosylbenzene catalyse the isomerisation of (Z) to (E)-stilbene via the participation of a radical intermediate that can rotate freely about the carbon-carbon bond since two other examples of the epoxidation reactions of (Z)-stilbene catalysed by ferric and ferrous triflate give predominantly (Z)-stilbene oxide. However, so far, the most efficient catalytic methods for olefin epoxidation have been obtained with single-oxygen donors such as sodium hypochlorite (NaOCl), iodosylbenzene (PhIO), hydrogen peroxide or alkyl hydroperoxides[47], m-chloro-peroxybenzoic acid (m-CPBA) in the presence of manganese porphyrin complexes as catalyst and in the presence of Lewis bases such as pyridine or N-methylimidazole. These Lewis bases act as axial ligands of the catalyst and increase the reaction rate, the selectivity for epoxide formation. Meunier et al[48] reported that in absence of pyridine the *cis : trans* ratio for epoxidation of *cis*-stilbene is 35: 65, whereas with the pyridine a ratio up to 94: 6 has been obtained.

1.2.4 Polymer-supported metal catalyzed epoxidations using alkyl hydroperoxides or hydrogen peroxides as oxidants.

In terms of polymer-supported systems the most widely investigated are Mo(VI)/ROOH, V(V)/ROOH, W(VI)/H_2O_2, Ti(IV)/ROOH, Mn(III)/RCO_3H and Re(VII)/H_2O_2. The potential technological advantages in converting a process catalysed by a homogeneous metal complex into one involving a heterogeneous polymer-supported analogue have been well argued[49]. Suffice to say that on a laboratory scale supported metal complex catalysts considerably facilitate product work-up and isolation, while on a large scale such heterogeneous species allow processes to be run continuously using packed or

fluidised bed columns with considerable financial advantages (low costs). A wide variety of homogeneous metal complex catalysts have been immobilised on polymers[49] ranging from alkene hydrogenation, hydroformylation, hydrosilylation, isomerisation and polymerisation catalysts to a growing number of alkene oxidation catalysts.

1.2.4.1 Polymer-supported Re(VII) hydrogen peroxide systems

In spite of the progress achieved in the last decade with the use of Re complexes as oxidation catalysts, their heterogenisation as polymer-supported catalysts has received rather scant interest. Neumann et al[50] reported the use MTO supported on silica substituted with polyethers. Using 30% aqueous H_2O_2 as the oxidant in the absence of an organic solvent gave epoxides in high yields by tailoring the hydrophilic-hydrophobic balance of the polyether phase. As represented in the schematic structure, (Scheme 1.12), the authors argued that hydrophobic poly(propylene oxide) (PPO) units may increase the solubility of the alkenes in the solvent anchored phase, whereas poly(ethylene oxide) (PEO) units might serve to dissolve the aqueous hydrogen peroxide oxidant and stabilise the peroxo intermediate responsible for catalytic activity.

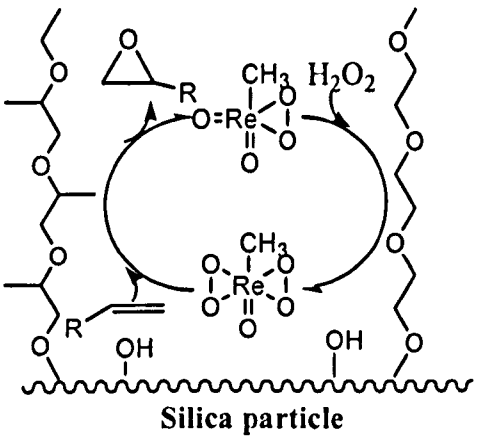

Scheme 1.12 Alkene epoxidation using 30% aqueous H_2O_2 and MTO supported on silica functionalized with polyethers as a catalyst.

The authors demonstrated that the best results were obtained with the heterogeneous system (MTO immobilized on 10% PEO-10% PPO-SiO_2). However, Buffon and Schuchardt[51] reported the use of MTO entrapped in hybrid silica matrices via 4-(3-triethoxysilylpropylamino)pyridine hydrochloride as ligand. The resulting supported catalyst gave relatively moderate conversion (84% epoxide) and moderate selectivity (76%) after 24 h with different alkenes. With styrene, no conversion was observed even after 24 h. However Herrmann et al[52] reported the immobilisation of MTO in the mesoporous silica MCM-41 functionalized with pendant bipyridyl groups of the type [4(-$Si(CH_2)_4$)-4-methyl-2,2-bipyridine] (Scheme 1.13). However the catalytic activity of this system decreases greatly due to a massive leaching of MTO after three runs. In addition the same authors also reported the synthesis of polymer supported derivatives of MTO

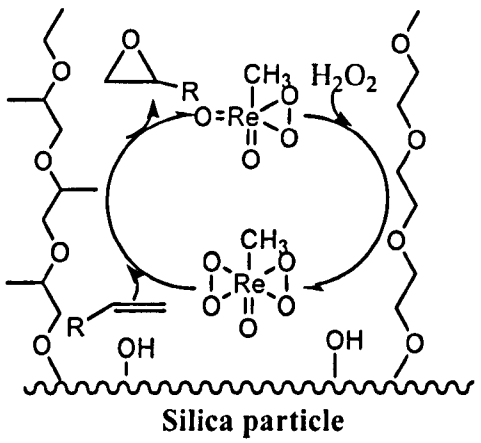

***Scheme 1.13** MTO immobilized on MCM-41 surface by using a bipyridine ligand.*

with poly(4-vinylpyridine) and polystyrene . In the case of poly(4-vinylpyridine)/MTO, the resulting complex proved to be an efficient and selective catalyst for the olefin epoxidation, and the catalytic activity was also reported to be maintained for at least five recycling experiments. Further investigations of poly(4-vinylpyridine)/MTO, poly(4-vinylpyridine-N-oxide)/MTO and polystyrene/MTO as polymeric supports have also been reported recently by Saladino et al[53] (Scheme 1.14).

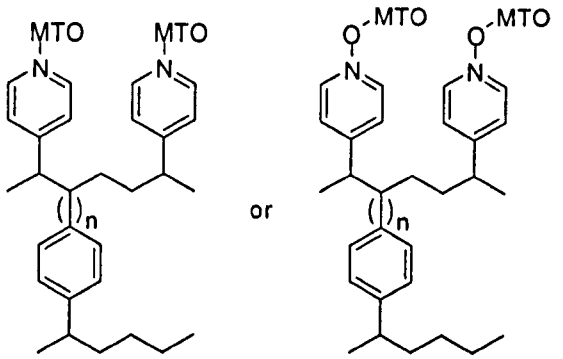

Scheme 1.14 Poly(4-vinylpyridine)/MTO and poly(4-vinylpyridine-N-oxide)/MTO

Epoxidations with 30% aqueous hydrogen peroxide (H_2O_2) were investigated using cyclohexene, cis-cyclooctene, styrene, α-methylstyrene and trans-stilbene as substrates, in a mixture of dichloromethane and acetonitrile as.solvents. The resulting epoxides were obtained with high yields (75%-98%) and good selectivities (78%-100%). For example (95% after 1.5 hour) cyclohexene oxide, (98% after 6 hours) trans stilbene oxide, (98% after 6.5 hours) styrene oxide and (98% after 6.5 hours) α-methylstyrene oxide were obtained with no byproduct using poly(4-vinylpyridine, 25% crosslinked)/MTO as catalyst. Recycling experiments of all these polymer-supported catalysts showed that these catalysts are stable enough to perform at least five recycling experiments with similar conversion and selectivity.

1.2.4.2 Polymer-supported W(VI) hydrogen peroxide systems

The first attempt to produce a polymer-supported analogue of these homogeneous oxidation catalysts was reported by Allen and Neogie[54]. They supported HWO^-_4 on Amberlite IRA-400 ion-exchange resin and used hydrogen peroxide as oxidant. Since this report there have been a number of studies involving the attachment of oxo-metal complexes to ion exchange resins. However, Gelbard et al[55-57] have made perhaps the most important improvement in the immobilisation of W(VI) on polymers. They reported the use of macroporous and gel-type poly(methacrylate)-based quaternary ammonium resins

to immobilise HWO_5^- and they obtained good catalytic activity and moderate selectivity (68%) in the case of the epoxidation of cyclohexene using 70% aqueous H_2O_2. Immobilisation of W(VI) species on polystyrene resins containing pyridinium ion, and pyridine-N-oxide containing gave similar results. Since the above work the same group has also discovered that homogeneous W(VI) complexes with organophosphorous ligands containing the phosphoryl unit P=O (such as hexamethylphosphotriamide, HMPA, trioctyl-phosphine oxide, TOPO) gave better results with H_2O_2 in the epoxidation of simple alkenes and allylic alcohols[56, 57]. Then they reported W(VI) immobilised on polystyrene resins containing phosphine oxide, and phosphonamide functionality by using peroxotungsten acid $H_2W_2O_{22}$[56, 57]. They also reported W(VI) immobilised on polybenzimidazole resin, and polymethylacrylate resin both containing phosphonamide groups[56,57]. Despite the fact that the phosphine oxide-polystyrene supported W(VI) catalyst (**1a**) with 70% aqueous H_2O_2 gave relatively better catalytic activity than the corresponding homogeneous complex with cyclohexene, the latter was too unstable to allow any recycling experiments.

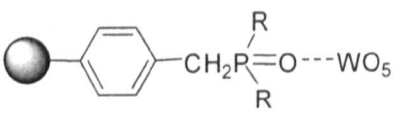

(**1a**)

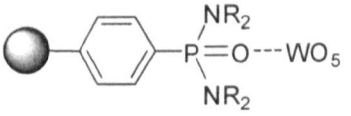

(**1b**)

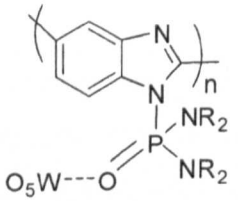

(**1c**)

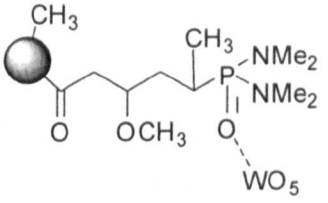

(**1d**)

The corresponding polystyrene-phosphonamide supported W(VI) catalyst (**1b**) gave similar activity and was recycled only twice. However, the polybenzimidazole-phosphonamide supported W(VI) catalyst (**1c**) showed lower activity but good stability.

It was re-used five times without any loss of activity and selectivity. The polymethylacrylate-phosphonamide W(VI) catalyst[56, 57] (**1d**) gave very high selectivity better than the corresponding soluble complex catalyst in the case of the epoxidation of cyclohexene using 65% aqueous H_2O_2.

1.2.4.3 Polymer-supported Mo (VI)/alkyl hydroperoxide systems

Mo(VI) complexes are well known to be potent catalysts for the epoxiation of alkenes using tert-butylhydroperoxide (TBHP) as the oxidant and indeed use of a homogeneous Mo(VI) catalyst is one of the important industrial processes for the epoxidation of propylene, with alkyl hydroperoxides as the oxygen source (Halcon[17]). There have been a number of attempts to immobilise Mo (VI) on polymers in order to generate an active heterogeneous catalyst for this process by the use of electrostatic binding, where cations or anions are bound to resin sites. Ivanov et al[58] have reported the epoxidation of propylene with tert-butyl hydroperoxide in the presence of the modified cation exchange resin Amberlite IRC-50, a copolymer of styrene with acrylic acid possessing the following elementary unit.

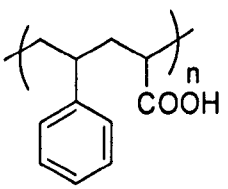

The carboxy cation-exchange resin Amberlite IRC-50 was treated with an alcohol solution of molydenyl chloride ($(MoO_2)_nCl_m$) obtained by evaporation of an acid-salt solution of ammonium molydate ($(NH_4)_6Mo_7O_{24}$). The catalyst seems to be obtained by both Cl^- ions being displaced by the COO^- ions from the exchange resin as shown below.

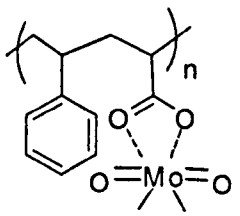

High activities and good yields of alkene oxides (90 to 92 %) were reported by the authors with the propylene under relatively mild conditions (90°C). However, since this earlier work a new strategy has been developed using polymers or resins functionalised with chelating ligands able to bind transition metal ions tightly. Linden and Farona[59] first proposed the use of this kind of polymer containing acetylacetonate, ethylenediamine and pyridine donor ligands to bind oxo-V(IV) ions. The resultant catalysts were active in the epoxidation of cyclohexene using t-butyl hydroperoxide as oxidant. Suzuki et al[60, 61] reported oxo-V(V) and oxo-Mo(VI) catalysts supported on polystyrene resins carrying bis (phosphonomethyl) amino **(2a)**, bis (2-hydroxyethyl) amino **(2b),** and iminodiacetate **(2c)** ligands as shown below.

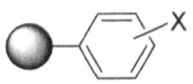

X = $-CH_2N(CH_2CH_2N(CH_2PO(OH)_2)_2)_2$ **(2a)**

$-CH_2N(CH_2CH_2N(CH_2CH_2OH)_2)_2$ **(2b)**

$-CH_2N(CH_2CO_2H)_2$ **(2c)**

They performed the epoxidation of cyclohexene and allylic alcohol substrates with these catalysts in presence of 70 % aqueous tert-butyl hydroperoxide at 80°C. The V based systems were the most effective in the case of allylic alcohol substrates with high conversions (~100 %) and high selectivity (~90 %) whereas the Mo based systems were the most effective in the case of cyclohexene with good conversions up to (90 %). However Gil et al[62] reported epxidation of a series of olefins using a polystyrene Mo resin as support catalyst and with 80 % tert-butyl hydroperoxide (TBHP) in di-tert-butylperoxide and in presence of toluene as solvent at 80°C. The corresponding polymer-supported Mo catalyst was synthesised from a modified Merrifield's polymer 2% crosslinking with ethylenediamine and thioglycolic acid as ligands. The authors claimed to attach successfully first ethylenediame to the resin, thus immobilised Mo on this polystyrene support via a ligand exchange reaction involving displacement of one

acetylacetonate group. Finally the resulting Mo complex was reacted with thioglycolic acid (TGA) to afford a following polymer-supported Mo catalyst **(3d)**:

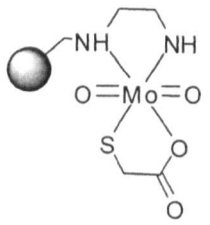

(3d)

Despite good selectivities(>98%) with this polymer catalyst (**d**), modest conversions of alkenes (78% cyclooctene, 65% (E)-cyclododecene, 26% (Z)-stilbene and 10% 1-octene) were obtained after 2 h reaction. No recycling experiments were mentioned. However Arnold et al[63] reported the use of metal-doped epoxy resins (4,4'-methylene-bis-(N,N-didglycidylaniline) (TGMDA) and N,N-diglycidyl--4-glyciloxyaniline (TGAP) as catalysts for the epoxidation of olefins with anhydrous tert-butyl hydroperoxide in toluene (TBHP) as oxidant. These polymer catalysts were obtained in a convenient one-step procedure in which metal complexes (molyldenum 2-ethylhexanoate ($Mo(EH)_n$, or $Mo(OEt)_5$ or a mixture of compounds $Mo[OOCCH(C_2H_5)C_4H_9]_n$) act as both initiators for anionic epoxy resin polymerisation and precursors for the catalytically active species in the resulting polymers. Modest conversions (33% to 86%) and selectivities (75% to 95%) were obtained after 20 consecutive epoxidation reactions when both catalysts were not pre-activated in the case of the epoxidation of cyclohexene. However they claimed that when these catalysts TGMDA-$Mo(OEt)_5$ and TGAP-$Mo(OEt)_5$ were pre-activated for a period of 35 h, the activity and selectivity of these catalysts increase significantly for the epoxidation of olefins. Thus for example good conversions of different alkenes (92% cyclohexene, 66% 1-octene, 93% styrene, 67% propene) and high selectivities (> 95%) were obtained with TGAP-$Mo(OEt)_5$ as catalyst with TBHP after 24 h. Similar results were obtained with TGMDA-$Mo(OEt)_5$ as catalyst at the same conditions. Recycling experiments of these catalysts have shown very low leaching Mo species during the catalytic process. Recently Sherrington et al[64-73] have reported a large number of polymer-supported V and Mo complexes as epoxidation catalysts. The resins used as

supports are polystyrene[65,73], poly(glycidyl methacrylate)[66], polybenzimidazole[64,65, 67,68,71,72,73] (PBI), polyimide[69] and polysiloxane[70] macroporous beads each appropriately functionalised to be used as support material for the homogeneous catalyst. Among these systems, the one based on polybenzimidazole (PBI) showed the best catalytic performance and stability. The PBI.Mo catalyst has proved to be highly active and selective in epoxidation of a range of alkenes, and recycling experiments were carried out using activated PBI.Mo showed, in the case of epoxidation of cyclohexene, no loss of the catalytic activity over 10 successive runs and only traces of leaching Mo which could not be detected by the atomic absorption spectrometer (AAS) instrument. This suggested that PBI.Mo is highly active and stable with regard to metal loss[67, 73]. Recently, Tangestaninejad et al[74] have reported the synthesis of molybdenum hexacarbonyl immobilised on polystyrene (2% cross-linked with divinylbenzene) containing imidazole in THF. The structure of the resulting Mo complex is unclear since the Mo(0) starting material is almost certainly oxidized to Mo(VI) species in the presence of any oxidant. Nevertheless the catalytic activity of the resulting supported catalyst was high, giving high epoxide conversion (>88%) and good selectivity (>88%) after 2.5-20 h in carbon tetrachloride (CCl_4) for a range of alkenes. The recovery and reusability of this supported catalyst also showed, in the case of epoxidation of *cis*-cyclooctene that the catalyst activity does not change even after 10 catalytic cycles. No detail of leaching possibilities was reported. The same group[75] also reported the synthesis of Schiff base molybdenum carbonyl immobilised on chloromethylated polystyrene (2% divinylbenzene) as polymeric support. Chloromethylated polystyrene resin was first oxidised to the aldehyde by reaction with DMSO and $NaHCO_3$ at 155°C for 6 h. The resulting aldehyde polymer was allowed to swell in methanol and a solution of ethylene diamine was added to this over a period of 1 h and then refluxed for 8 h. Finally the resulting polymer-bound Schiff base was reacted with a solution of molybdenum hexacarbonyl in dioxane under reflux conditions to give the corresponding polymer-supported Schiff base Mo complex (**4e**):

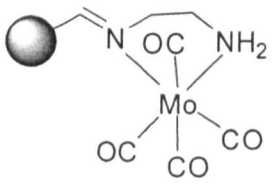

(4e)

The catalytic activity of this supported Schiff base Mo complex **(e)** was tested for epoxidation of a wide range of alkenes in carbon tetrachloride (CCl_4) as solvent and in the presence of TBHP as oxidant. Good conversions (94% *cis*-cyclooctene, 95% styrene, 75% α-methylenestyrene, 100% *cis* and *trans* silbene) and high selectivities (>77%) were obtained with this supported catalyst **(e)**. Recycling experiments of this supported catalyst also showed, in the case of epoxidation of *cis*-cyclooctene that the catalyst still very active even after 8 catalytic cycles. No detail of Mo loss was mentioned.

1.2.4.4. Inorganic MCM-41-supported Mo (VI)/alkyl hydroperoxide systems

On the other hand immobilisation of catalysts on inorganic supports has also several important potential advantages over other approaches such as the use of organic polymer supports. The chemical stability of the inorganic supports is important, particularly with concerned to oxidizing conditions. Their mechanical stability is often excellent, since the problem of swelling depending on solvent conditions can largely be avoided. In addition, inorganic supports also often have superior thermal stability than organic polymer supports.

Since the development of the mesoporous molecular sieve MCM-41 by Mobil company, MCM-41 material has been attracted much attention because of its potential use as catalysts or catalyst supports. The structure of MCM-41 consists of a hexagonal arrays of one dimensional channels of uniform mesoporous with pore diameter in the range 15-100 Å, depending on the nature of the template and synthesis conditions. The presence of these very large uniform pores opens up the possibilities for shape-selective conversions of bulky molecules such as those encountered in the manufacture of fine chemicals and

pharmaceuticals[76]. However the main drawback of MCM-41 support for practical applications is its rather low hydrothermal stability. Rocha et al[77] reported the immobilisation of Mo (VI) on inorganic material MCM-14 and MCM-48, mesoporous siliceous materials possessing very high surface area (1000 m^2), high pore volumes (1 cm^3 g^{-1}) and very narrow pore size distributions (16-100 Å) by direct binding with $MoO_2X_2(THF)_2$ or by using a spacer ligand ($NC(CH_2)_2Si(OEt)_3$) (Scheme 1.15).

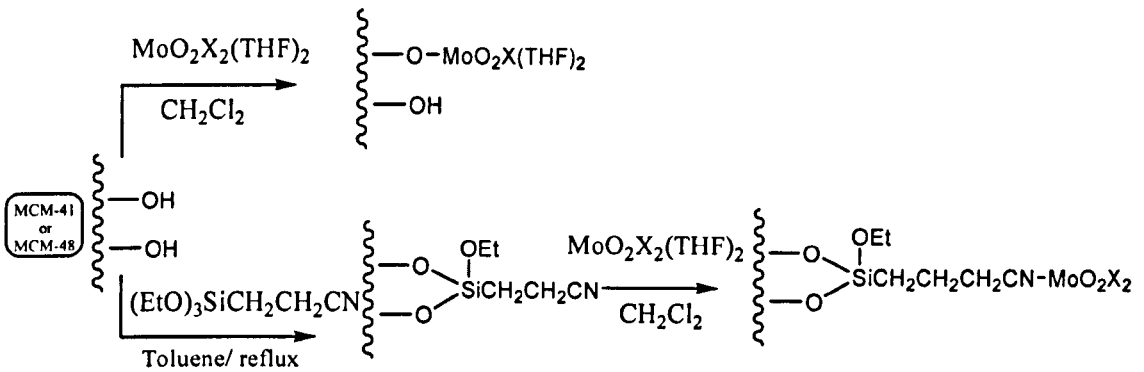

Scheme 1.15 Mo (VI) immobilised on MCM-41/MCM-48.

Both resulting heterogeneous Mo (VI) catalysts gave very high selectivity (100%) and low conversion to epoxide(50%) after 4h in the case of epoxidation of cyclooctene. It seems that the lower epoxide conversion observed, was mainly due to the instability of this catalyst support. To overcome this problem, Masteri-farahani et al[78b] recently reported new heterogeneous systems for stabilizing molybdenum in the structure of catalysts derived from aminopropyl modified MCM-41. A series of novel silica supported molybdenum on MCM-41 catalysts bearing N-N, N-S, and N-O chelating Schiff base ligands derived from reaction of aminopropyl modified silica with different aldehydes and ketones (pyrrolcarbaldehyde, 2-acetylpyrrol, 2-aminoacetophone, salicylaldehyde, acetylphenone) were synthesised. The catalytic activities of these Mo catalysts were investigated in the epoxidation of cyclooctene, cyclohexene, 1-octene and 1-hexene with TBHP as oxidant and in chloroform as solvent. Good conversions (>94%) and high selectivities (>98%) were only observed with cyclic olefin after 7 h reaction time whereas modest conversions (>40%) were obtained with terminal olefins after 10 h reaction time. No recycling experiment was mentioned. However Thiel et al[79,80] reported a new

heterogeneous Mo catalyst synthesised from the modified ordered mesoporous silica MCM-41 with a pyrazolylpyridine ligand. Postsynthetic silylation using trimethylsilane chloride (Me_3SiCl) was also carried out to remove the residual silanol groups on the surface of the mesoporous MCM-41 material prior to immobilise covalently Mo complex onto it.

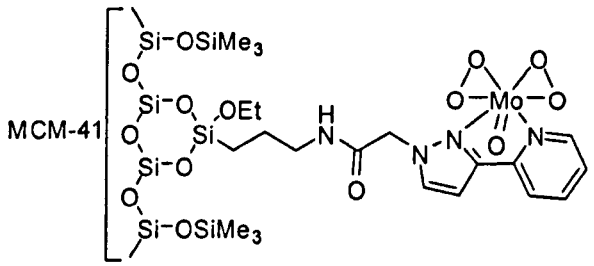

(5f)

The resulting inorganic supported Mo complex **(5f)** was tested as catalyst for the epoxidation of cyclooctene with TBHP as oxidant and in the presence of chloroform as solvent. Good conversions (100%) and high selectivities (nearly 100%) were observed after 7 h reaction time at a reaction temperature of 61°C. This catalyst has been recycled twice with no change of its activity. The authors suggested that the good activity and recyclability (only twice runs tested) of this supported Mo catalyst were attributed by removing or decreasing of the number of the residual Si-OH groups on the surface of the mesoporous material using Me_3SiCl as the silylating agent, which could be unfavourable for the catalytic reaction. Trimethylsilylation may have other advantages, such as making the surface of mesoporous catalyst more hydrophobic and improving its solubility and stability during the catalytic process. Further investigations of this same type inorganic supports have been recently reported by Goncalves et al[81]. Two supported Mo complexes **(5 g)** and **(5 h)** (one of two Mo complexes was postsynthesised with Me_3SiCl to remove the residual silanol groups **(5 h)**) were tested as catalysts for the liquid phase epoxidation of a series of olefins using TBHP as oxidant at 55°C without additional solvent.

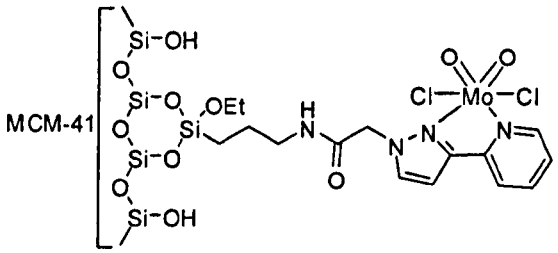

(5 g)

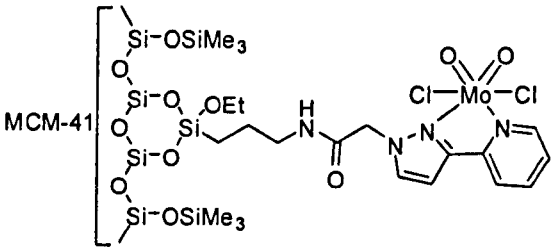

(5 h)

Better conversions (93% cyclooctene, 75% limonene, 31% trans-2-octene, 4% 1-octene) and high selectivities (100% cyclooctene oxide, 90% limonene oxide, <80% linear olefin oxides) were obtained after 8 h reaction time with the catalyst postsynthesis trimethylsilylation step with Me_3SiCl **(5 h)**. In addition leaching tests were performed for both catalysts by filtering the reaction mixture and assaying the molybdenum present, showed that the catalyst postsynthesis trimethylsilylation step **(5 h)** did not loss Mo species whereas the catalyst **(5 g)** lost 6% of its Mo content. These results indicate and confirm the positive influence of trimethylsilylation which was also reported by Thiel et co-workers[79,80] for the epoxidation of cyclooctene in the presence of the oxodiperoxo molybdenum chelate complexes covalently anchored onto the surface of mesoporous MCM-41 material.

1.2.5 Asymmetric-epoxidation

Catalytic asymmetric epoxidation of alkenes presents a powerful strategy for the synthesis of enantiomerically enriched epoxides. Among the several catalytic methods, asymmetric epoxidation of unfunctionalised alkenes catalyzed by chiral (salen)-Mn(III) complexes (Scheme 1.16), developed by Jacobsen et al[82-85], is one of the most reliable methods because of it is easy to synthesise and gives very high enantioselectivities up to 92% e.e, are obtained for *cis*-disubstituted and tri-substituted olefins.

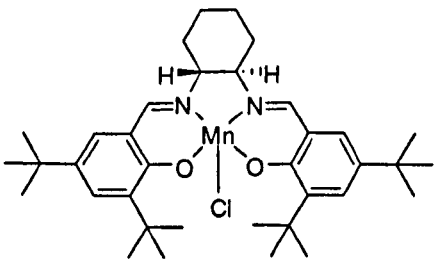

Scheme 1.16 (R,R)- Jacobsen's Mn(salen) complex

High enantioselectivity with this catalyst is attributed to olefin interaction approach with the dissymmetric ligand is maximised[85] (Scheme 1.17).

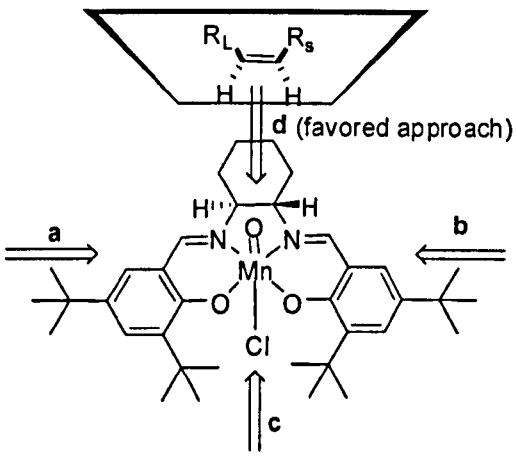

Scheme 1.17 Different approaches of olefins tof (S,S)- Jacobsen's Mn(salen) complex

From this Scheme 1.17 above, four approaches could be envisioned from the approaching olefin. Approach **d** is the most favored approach for optimal alignement of the olefin π-bond to the lone pairs of the oxygen atom. This open quadrant provides the maximisation of the stereochemical communication between ligand and the approaching olefin. This is shown from a top approach of the olefin, taking into consideration the deplacement of R_L (where L= large alkyl or aromatic substitutent) and R_S (S= small alkyl substitutent). The olefin positions in which the R_L group is on the left side the olefin allow maximum stabilisation of energy because of less steric repulsions from the axial hydrogen on the

opposing side. Approach **c** is disfavoured because of the presence of bulky groups (tert-butyl groups) which prevents olefin approach to the oxygen atom. Approaches **a** and **b** are also disfavoured not only by steric repulsions between the approaching olefin and bulky groups but also by repulsive π-π interactions between the approaching olefin and electron rich nature of the salen ligands[86, 87].

1.2.5.1 Asymmetric polymer-supported Mn (III)/ mCPBA /NMO or PhIO systems

Although the typical Jacobsen- type catalysts such as (R,R)-Mn(salen) catalyst shown above in Scheme 1.16, are easy to obtain, several attempts to immobilise Jacobsen's catalysts have been made[88-97]. Several strategies have been developed to immobilise this Jacobsen's Mn(salen) complex into insoluble supports: the covalent attachment of the complex to insoluble organic polymers[88,89,92,93,94] or inorganic supports[98-105], the ion exchange of Mn(III) complexes into the intracrystalline space of mesopores materials[103,104, 109], the physical entrapment in the poly(dimethylsiloxane) membrane[105, 111] and utilising a fluorous biphasic system[106, 107] or ionic liquids[108,110].

Salvadori et al[93] reported the first successful, reusable, polystyrene-supported Mn(Salen) complex by replacing two para tert-butyl group of Jacobsen's Mn(salen) catalyst by vinyl groups(Scheme 1.18).

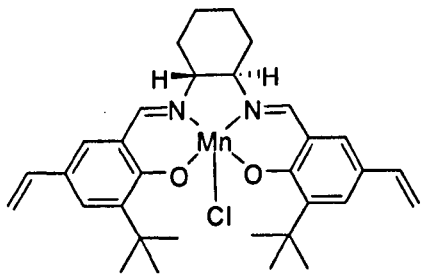

Scheme 1.18 Modified (R,R)- Jacobsen's Mn(salen) complex

Then they carried out the polymerisation of this modified Jacobsen's Mn(salen) with styrene and DVB to afforded the immobilised catalyst, which in the presence of mCPBA

and NMO afforded the epoxides of styrene and *cis*-methylstyrene in 99% yield (15% e.e.) and 95% yield (41% e.e.) respectively. This polymer-supported catalyst retained its efficiency in terms of yield and e.e. after five recycles. In order to increase the enantioselectivity of this polymer-supported Mn(salen) catalyst, the same group[93] reported the synthesis of other polystyrene Mn(salen) complexes with longer spacer groups between the active metal center and the polymeric backbone (Scheme 1.19)

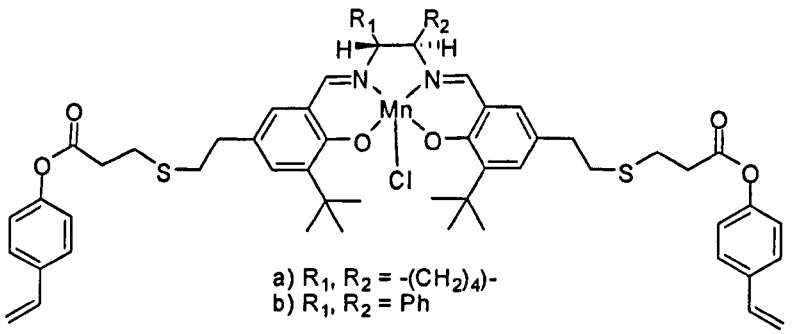

***Scheme 1.19** Modified (R,R)- Jacobsen's Mn(salen) complex*

They obtained a slightly improvement of the enantiomeric excess for *cis*-β methylstyrene oxide (62% e.e.) with the catalyst **a)** and for styrene oxide (26% e.e.) with the catalyst **b)**. It becomes clear that immobilised catalysts containing a spacer group between the active metal center and the polymeric backbone afford epoxides with better e.e. than these without the spacer group. Although the slight improvement of the e.e. was observed with these catatysts containing the spacer group, these e.e were still significantly lower than the homogeneous Mn(Salen) catalyst. Sherrington[89,91] suggested that low enantiomeric.excesses. were observed when two polymerisable double bonds were present in the active monomer as the ligands would be placed on crosslinks inhibiting the formation of a nonplanar transition state which was thought to be responsible for high level of asymmetric induction[87] (e.e.). However Sherrington[89, 91, 94] has also suggested the key design criteria for immobilising salen complexes on polymer supports which are that (a) the complex should be attached to the support through a single flexible linkage to minimise any local steric restriction, (b) the complex should be attached to the support in a reasonably low loading to ensure site isolate of the metal centers, thus limiting the possibility of oxo-bridged dimer formation, responsible to loss of catalytic activity during

the course of reaction, and (c) the morphology of the support should be such that all active site are available. In 2000 Sherrington[88, 89, 91, 94] reported the synthesis of a series of pendant fashion of polystyrene polymer-supported analogues of Jacobsen's chiral Mn salen complexes and one of that series of complexes, a polystyrene methacrylate Mn (salen) catalyst displays for the first time enantioselectivity as high as the soluble jacobsen's complex for the epoxidation of 1-phenylcyclohex-1-ene (91% e.e.) whereas the other catalysts of the same series show modest enantioselectivity (46%-66% e.e) for the epoxidation of 1-phenylcyclohex-1-ene. However recycling experiments with the best catalyst a macroporous polystyrene methacrylate Mn (salen) complex showed a significant decrease of activity and selectivity between the first and the second recycles. Sherrington concluded that the stability of the manganese complex was too low to allow viable recycling. However Suresh et al[95] reported the synthesis of tartrate-functionalized polymers which were prepared by attaching tartaric acid onto 1 and 2% divinybenzene (DVB) and tetraethylenediacrylate (TEGDA) crosslinked polystyrene. They claimed that the resulting immobilised Mn(salen) catalysts gave good yields (up to 74%) and high enantiomeric excess (up to 66%) in the case of the epoxidation of *trans*-cinnamate. They also noticed that the catalysts containing very low crosslinker (1% DVB and 1% TEGDA) gave the best enantiomeric excess (90% e.e. and 91% e.e.) respectively. Although TEGDA polymer supports catalysts proved slightly to be more active the corresponding DVB supports catalysts, all these catalysts were reused successfully three times under the same reaction conditions. Suresh[95] suggested that the lower crosslinked and more flexible polymers afforded higher enantiomeric excess.

1.2.5.2 Asymmetric inorganic-supported Mn (III)/ mCPBA /NMO or PhIO systems

With the successful immobilisation of Jacobsen's type catalyst on organic supports, parallel attempts were carried out on inorganic supports. Several different approaches have also been attempted. In the first approach, chiral Mn(salen) complexes were heterogenised via a covalent link. First Salvadori et al[98, 99] reported a covalent bound Mn (salen) complex on silica gel. The resulting inorganic catalyst displayed high activity in

the asymmetric epoxidation of some aromatic olefins (1,2 dihydronaphthalene, indene, and 1-phenylcyclohexene) using mCPBA/NMO as the oxidant system in acetonitrile. The reaction was complete within 10 min at 0°C for all these substrates examined. However, much lower enantiomeric excess (up to 58% e.e. for 1-phenylcyclohexene) were observed than those obtained in homogeneous counterparts. In addition neither recycling experiments nor leaching studies were reported. However Kim et al[100,101] described that the unsymmetrical chiral Mn(salen) complexes immobilised by a covalent link to the siliceous MCM-41 displayed slightly improved enantioselectivities when compared with the homogeneous counterparts in the epoxidation of styrene and α-methylstyrene with mCPBA/NMO as the oxidant system. For the example, using the inorganic catalyst a) styrene at 0°C and α-methylstyrene at -78°C were epoxidised with 70% and 56% e.e respectively whereas the homogeneous analogue gave the corresponding epoxides with 65% and 43% e.e respectively. In addition, they also claimed that these immobilised complexes were reused four times without the loss of catalytic activity and selectivity, but no data of recycling experiments were reported. In addition to the above ways of immobilising chiral Mn(salen) complexes via a covalent bound, Zhou et al[102] reported the immobilisation of a Cr-binaphthyl Schiff base by coordination to a terminal amino group which had been attached covalently to the walls of a MCM-41 support. Although the heterogenised catalyst was slightly improved enantioselectivities than the homogenous analogue, the level of asymmetric induction of this inorganic catalyst was still modest. For example the epoxidation of 4-chlorostyrene and cis-β-methylstyrene with isosylbenzene (PhIO) at 20°C using the inorganic catalyst gave 4-chlorostyrene oxide and cis-β-methylstyrene oxide in 65% and 73% enantiomeric excess respectively whereas the homogenous analogue gave only for 4-chlorostyrene oxide (17% e.e.) and cis-β-methylstyrene oxide (19% e.e.). They claimed this inorganic catalyst was reused four times with a significant drop both activity and e.e values. However Hutchings et al[103, 104] reported immobilisation method of for jacobsen's Mn(salen) complex based on ion-exchange. Salen ligand, (R.R)-(-)N,N-bis(3,5-di-tert-butylsalicylidiene)cyclohexene-1,2-diamine was heated under reflux with a Mn-exchange al-MCM-41 in such way that

10% of the Mn was ligated. The corresponding Mn-Al-MCM-41-salen catalyst was reported to yield cis and trans to give (70% e.e.) in the epoxidation of *cis*-stilbene using PhIO as oxygen donor and to yield the mixture of *cis* and *trans* epoxide. In addition no recycling experiments were examined.

1.3. Choice of polymer support

Crosslinked polymers derived from vinyl monomer units were used as one of supports for the metal complexes in this present work. It is important to highlight the synthesis of these polymers used as support materials.

Polymers are synthesised by either polycondensation or addition polymerisation. Polycondensation is usually defined as the repetition of an elementary condensation reaction between two difunctional monomers which results in the production of long chain molecules. For examples polyesters are the outcome of the polycondensation between diacids and diols whereas polyamides are obtained from diacids and diamines. High molecular weight with low polydispersity polymer are usually obtained with this technique because of the difunctionality of each monomer unit involved, polycondensation reaction occur at each end of the growing polymer chain. However the main drawback with polycondensation polymers is that they are often difficult to functionalise in order to obtain good polymer-supported catalysts.
Addition polymerisation can be obtained either anionic, cationic, free radical initiators and by Ziegler-Natta type catalysts. However, each of these methods of polymerisations follows analogue mechanisms where propagation, transfer and termination steps all plays a important role in producing polymers with a wide range of molecular weights. Alkene monomers are usually used in addition polymerisations, but certain cyclic monomers such as tetrahyfuran (THF) can be polymerised via a ring opening ionic mechanism. However, polymers obtained from vinyl monomers are most commonly used as catalyst supports, and they are produced via free radical polymerisation.

A free radical polymerisation method is so far the technique the most used in addition polymerisation. Both homogeneous and heterogeneous polymerisation systems use generally a free radical polymerisation method. However, heterogeneous polymerisation system which includes (precipitation polymerisation, dispersion polymerisation, emulsion polymerisation and suspension polymerisation) is so far the technique the most employed in industrial polymerisation since it involves water as solvent which is cheap and which can absorb the exothermic heat generated during the free radical copolymerisation reactions.

As this present work is based on suspension polymerisation, further explanations of the suspension polymerisation system will be highlighted.

Suspension polymerisation is one of the most popular and effective technique to synthesise polymers as spherical form or beads. They are two main types of suspension polymerisation available depending on the nature of the monomers. For hydrophilic monomers such as acrylamide, the monomer is suspended in a hydrocarbon or chlorinated hydrocarbon bulk liquid phase, and this technique is well-known as inverse suspension polymerisation. In contrary, for hydrophobic monomers such as styrene and divinylbenzene, the bulk liquid phase used, is water. The latter technique is used in this present work.

Polymer resins derived from vinyl monomers such as styrene and methacrylates are conveniently made in as spherical form by suspension polymerisation. They are also very versatile supports because they are easily derivatised with a wide range of functional groups for an equally wide range of applications. Ion exchange resins are perhaps the most ubiquitous. The main disadvantage of vinyl polymer supports is their limited thermo-oxidative stability. Decomposition in the absence of O_2 takes place above ~ 200°C, but in the presence of O_2 the upper limit is significantly lower, perhaps ~130°C. Despite this, these polymers are potentially applicable even as oxidation catalyst supports for reactions performed up to ~100°C.

1.3.1 Synthesis polystyrene resins.

Polystyrene resins are prepared by a free radical addition suspension polymerisation methodology (Scheme 1.20). The method uses a baffled glass reactor typically of ~1 litre in the laboratory with a monomer/ water ratio of around 1/ 20 v/v. On an industrial scale, similar steel reactors which are employed capable of handling a comonomer batch size of ~ 1000 kg with a much smaller aqueous phase (monomer/water ~ 1/3)[112]. The technique consists of first mixing the hydrophobic organic monomers (styrene, vinyl chloride and divinylbenzene) with a porogen if required (such as toluene, 2-ethylhexan-1-ol) and a free radical initiator such as AIBN. The resulting organic mixture is dispersed with strong stirring in an aqueous phase containing a stabiliser e.g. polyvinyl alcohol. This creates a suspension of liquid monomer droplets. The polymerisation is initiated by free radicals generated thermally by heating the reaction vessel. The free radicals generated from AIBN attack the monomer vinyl groups. The resultant monomer radical species proceed to attack other monomer groups in the propagation process and produce solid polymer beads. These beads can be as small as around 5μm and up to 1mm in diameter depending on application intended. Once the reaction is completed, the resulting polymer particles are filtered off and washed with water, methanol and with acetone in a Soxhlet extractor in order to remove any impurities. Finally the beads are dried in a vacuum oven.

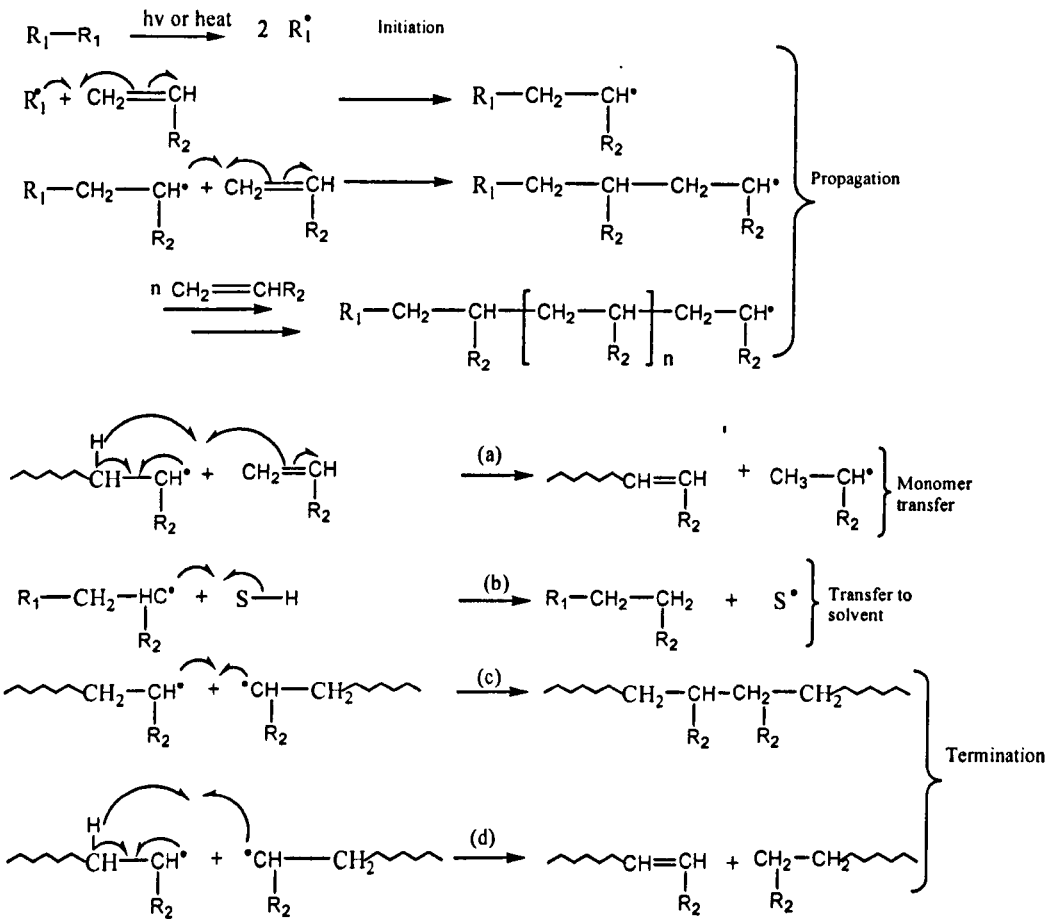

Scheme 1.20 *Free radical vinyl polymerisation mechanism, (a) transfer to monomer, (b) transfer to solvent, termination by (c) combination and (d) disproportionation.*

In the case of resins destined to be used as supports, it is important that the polymer is crosslinked to form an infinite network. This is achieved by using a difunctional comonomer e.g. divinylbenzene (DVB) (Scheme 1.21). This ensures that the polymer particles do not dissolve even when exposed to solvents that would normally dissolve the analogous linear polymer.

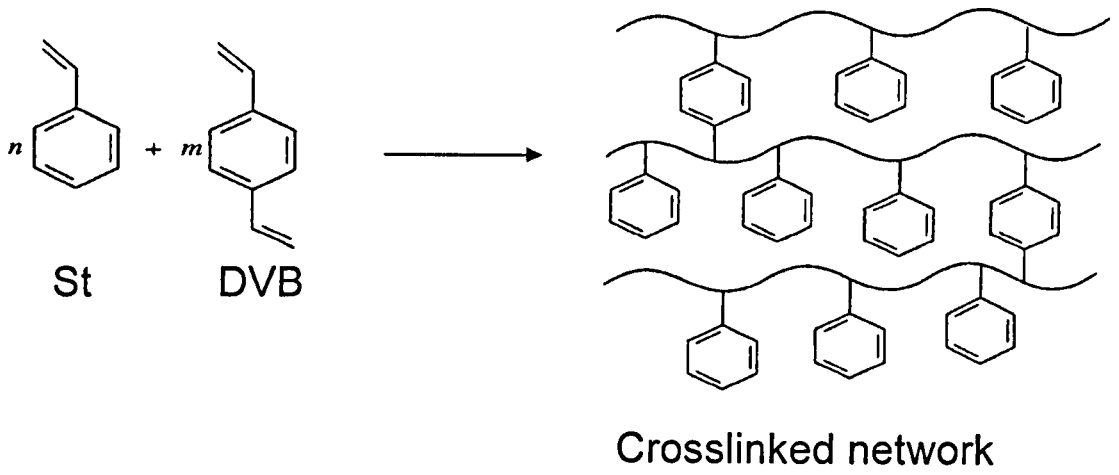

Scheme 1.21 Polymerisation of styrene and DVB to form a polymer crosslinked network

1.3.2 Polymer particle size and shape.

The uniformity and size of polymer particles or beads obtained from suspension polymerisation depend on many factors such as an impeller diameter, reactor shape, porogen, stirrer speed and other the operating parameters used.

The use of a baffled stirred reactor with monomer/ water around 1/ 20 v/v is necessary to minimize unfavourable surface interactions between particles. The vessel must be a cylindrical shape with an almost flattened base and an impeller with blades oriented approximately 45° such that, when rotated, it exerts a rotation of liquid from a top to bottom in order to minimize collision between particles formed and the reactor wall. The rate of stirring must be high (500-600 rpm) to avoid aggregation of the polymer beads. A typical suspension polymerisation process is illustrated in Scheme 1.22.

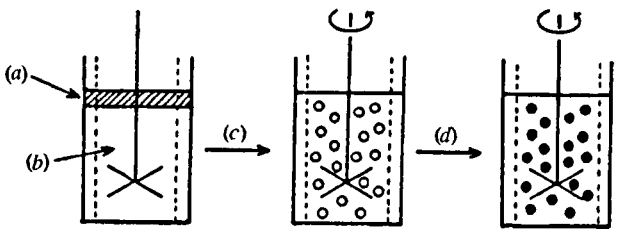

Scheme 1.22 Schemetic representation of suspension polymerisation: (a) organic comonomer mixture with porogen containing dissolved initiator; (b).aqueous continous phase containing dissolved polymeric suspension stabiliser; (c)shearing to form comonomer liquid droplets; (d)thermal plymerisation to form solid polymer resin beads.

The aqueous phase is also a crucial factor for the formation of uniform and spherical beads. An excess of aqueous phase used during the suspension polymerisation acts as a heat transfer medium. It allows the heat produced during the exothermic polymerisation process to dissipate. In addition the aqueous phase contains suspension stabilisers such as a water soluble synthetic polymer (for example polyvinylalcohol) which aids the uniformity and spherical nature of the polymer beads by reducing the tendency of the suspended beads to aggregate. The stabiliser functions by increasing the viscosity of the aqueous phase and surrounding the droplets surface, thus forming a protective layer which acts as a cushion which absorbs any collisions during the suspension polymerisation process.

There are mainly two types stabilisers available for suspension polymerisations: organic and inorganic stabilisers.
Organic stabilisers are synthetic polymers such as poly(vinyl alcohol) and poly(vinyl pyrrolidone) or natural high molecular weight polymers such as gums, starch[113]. However, synthetic polymers have the advantage of being commercial available in a range of weight and with varying degrees of hydrolysis that is why they are widely one of the most used stabilisers. In addition organic stabilisers are more effective than their inorganic counterparts since the use of the inorganic stabilisers sometimes requires the addition of small amounts of additional organic surfactant.

Nevertheless, organic stabilisers which are inorganic oxides and salts such as tricalcium phosphate, magnesium carbonate or betonite[114-116] have the advantage to produce larger beads (250-1000 μm)[117, 118] than their organic counterparts such as poly(vinyl alcohol) (100-200 μm). In addition it is also possible to synthesise small beads (10-100 μm) with inorganic stabilisers such as sodium dodecyl sulphate as surfactants[119,120].

In the case of inverse suspension polymerisation systems, stabilisers facilitating the formation of water-in-oil suspensions are required and cellulose acetate butyrate[121], sortitan trioleate[122] and poly(cetyl methacrylate)[123] have been used with some success.

However, polymer beads from suspension polymerisation generally have a finite particle size distribution, though a surprisingly narrow range which can sometimes be completed in a single polymerization. Normal suspension techniques can produce average particle diameters of between ~50 μm and ~1 mm, though the range 100-300 μm is more common. The final spherical form of particle (d) size depend on many parameters such as reactor design, suspension stabilisers, stirrer speed, but the relationship between these parameters can be formulated and generalised as a mathematical equation using dipersion theory as follows:

$$d \propto \frac{K, \sigma, \phi}{L, N, \rho}$$

where K = is the shape factor (depending on the reactor used)

σ = is the interfacial tension between the bulk and dispersed phases

□ = is the volume fraction of the dispersed phase

L = is the impeller diameter

N = is the stirrer speed

ρ = is the droplet density

From this equation, the influence of various factors on particle size may be predicted. Thus beads size can be reduced by reducing the surface tension (achieved normally by the use of stabilisers) and/or volume fraction of comonomers (volume of the dispersed phase). Increasing the droplet density, impeller size and/or the rate of stirring

speed will also have the same effect. It is also possible to reduce stirrer speeds and simultaneously imcrease the impeller diameter[123] without changing the particle size of the product too dramatically. Although higher shear produces small particles, there is a finite limit to the stirrer speed nevertheless, because the higher rate of the shear can increase the vortex formation which can result in the destruction of the controlled suspension.

1.3.3 Control of the internal porous structure of polymer resins.

The porous morphological structure of polymer resin beads depends on the amount of crosslinking groups present and the type of organic solvent or porogen if any, incorporated into the monomer mixture. The first parameter controls the degree of crosslinking and thus determines the level of swelling of the polymer. However, the second parameter, when present in the reaction mixture, can create pores and control the pore size, pore volume and surface area of the polymer beads.

1.3.4 Gel-type resins

When the comonomer mixture in a suspension polymerisation consists only of styrene and divinylbenzene, plus initiator and with no porogen, the product generally consists of hard glassy transparent resin beads which are known as gel-type (left-hand sample Scheme 1.23).

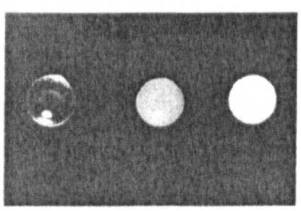

Scheme 1.23 *Optical photograph of (left) gel-type bead, (right) macroporous bead, and (centre) mixed morphology.*

The percentage of crosslinking such as DVB can be varied in principle from 0-100% but typically but for most resin applications the range 0.5-20% is more usual and for gel-type resins is generally around 0.5-2%. Gel-type resins possess essentially no porous structure in their dry state, with very low surface area < 10 $m^2.g^{-1}$ and very low pore volume. These characteristics of gel-type resins prevent any incorporation of a new molecule within their dry polymer network. To overcome this problem, the gel-type resins must first be immersed in a suitable, thermodynamically good solvent. The polymer chains are thus completely solvated and the beads can swell to more than ten times their initial dry state. Thus chemical reactions can take place within the beads at reactive sites in the resins because reagents can penetrate the polymer network. The swelling process occurs largely in the good solvent from the outside to the interior that means the polymer network on the geometric exterior of resin beads becomes swollen first, forming an expanded pellicular layer and leaving a central unswollen glassy core. Thus when the thickness of the swollen layer increases, the central core gradually shrinks and finally disappears[112] as shown in Scheme 1.24.

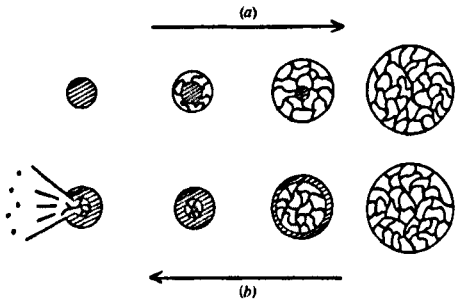

***Scheme 1.24** (a) swelling process of gel-type bead in a good solvent; (b) deswelling of gel in a bad solvent*

However the reverse of the swelling process can also take place if a gel-type resin is fully swollen in a good solvent and then introduced into an excess of bad solvent and the resin starts to shrink. This reverse process can damage the resin for example the resin particles can fracture or burst. Gel-type resins are only useful if they are able to undergo many cycles of swelling and deswelling without mechanical damage and in fact the swelling

behaviour of the gel-type resin limit their use in many applications for example their use in packed columns. However many restrictions of gel-type resins can be overcome by the use of macroporous resins.

1.3.5 Macroporous resins

When a suspension polymerisation of a comonomers of a styrene and with high level of crosslinking (such as divinylbenzene ≥ 20 %) mixture is carried out with an appropriate organic solvent or porogen such as toluene, 2-ethylhexan-1-ol, the product generally obtained consists of spherical beads or pearls which are known as macroporous resins. Macroporous resins possess permanent porosity in their dry state, with high surface area up to ~700 m^2g^{-1} and high pore volume. In contrast to gel-type resins, these materials do not need to swell in any solvents (good or bad solvents) to allow access to the interior because they possess a permanent porous structure. These characteristics of macroporous resins facilitate any reagents to penetrate within the empty pore structure of the polymer beads. In addition, macroporous resins are also the rigid materials because they possess a high degree of crosslinking. Their rigidity and pore structure allow them to be used with any solvents. This specific characteristic may lead to further applications of macroporous resins for example as supports, for packing into small or large columns.

The search for thermally stable resins re-usable several times for chemical transformations at high temperature and for long periods of time has been given an impetus as a result of the high performance materials needs of the electronics and aerospace industries.

Thermally stable polymers should have the following properties:

i. high melting or softening points
ii. low weight loss
iii. structures that are not susceptible to degradative chain scission or intra- or intermolecular bond formation

iv. chemically inert, especially to oxygen and moisture

v. structures which have a highly resonance-stabilized system or an aromatic or other thermally unreactive ring structure as a major portion of the polymer composition.

In view of these requirements, the most promising thermally stable polymers are: the polybenzimidazoles, polyimides and polysiloxanes. Polybenzimidazoles will be discussed here since the other species are not relevant to the present project.

1.3.6 Polybenzimidazoles

As mentioned previously, polybenzimidazoles could offer several advantages as reactive polymer supports and their method of synthesis is of relevance.

Polybenzimidazoles (PBI) were first reported by Brinker and Robinson[124]. Later, further studies were carried out by Vogel and Marvel[125], who reported the preparation of fully aromatic polybenzimidazoles by the melt condensation of aromatic tetramines with an aromatic dicarboxylic acid or derivatives as shown in Scheme 1.25.

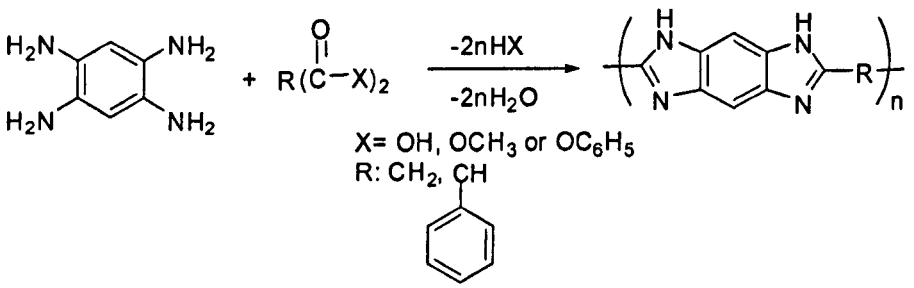

Scheme 1.25 *Synthesis of polybenzimidazoles by melt condensation of aromatic tetramines with a dicarboxylic acid or derivatives.*

Poly[2,2′-(m-phenylene)-5,5′-bibenzimidazole] is the form of polybenzimidazole that is commercially available and it is produced by the Celanese Corporation, USA via

condensation of 3,3′,4,4′-tetraaminobiphenyl (TAB) with diphenyl isophthalate (DPIP), as shown in Scheme 1.26.

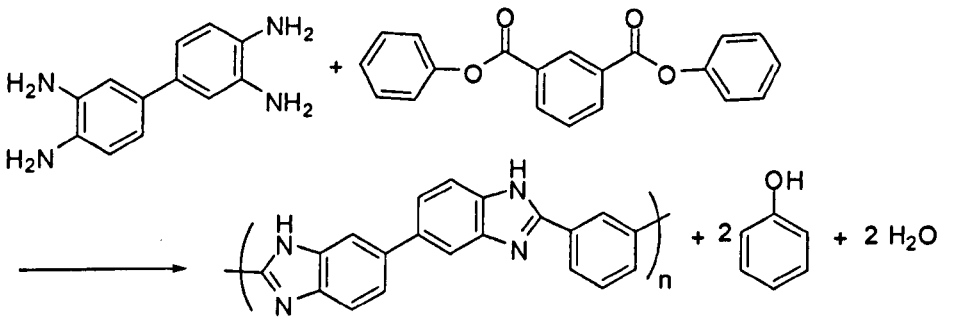

PBI

Scheme 1.26 Synthesis of poly(2,2′-(m-phenylene)-5,5′-bibenzimidazoles (PBI).

The material (PBI) is produced in a spherical particulate form which is convenient for application as a support. Further studies were carried out by Iwakura et al[126] who reported that polybenzimidazole can be prepared by the solution polycondensation of 3,3′,4,4′-tetraaminobiphenyl tretrahydrochloride and aromatic dicarboxylic derivatives in polyphosphoric acid. This polyphosphoric acid procedure was found to be a most suitable reaction medium for homogeneous-solution polymerisation. Similar material has also been prepared by Sherrington et al[127] using a non-aqueous suspension methodology in which the monomer in this case 3.4-diaminobenzoic acid was suspended in paraffin oil and polyphosphoric acid was slowly added to the reactants (Scheme 1.27), forming a dispersed phase consisting of an acidic solution of monomer, the reaction mixture was kept for several hours at 180-200°C. The authors also reported that the best suspension results were obtained when using a polymeric suspension stabilizer carboxy-terminated polyisobutylene (PIB). The macromolecular product consisted of almost 100% of polybenzimidazole spherical beads in various sizes with a fairly narrow particle size distribution and with very low surface area (1.8 $m^2 g^{-1}$).

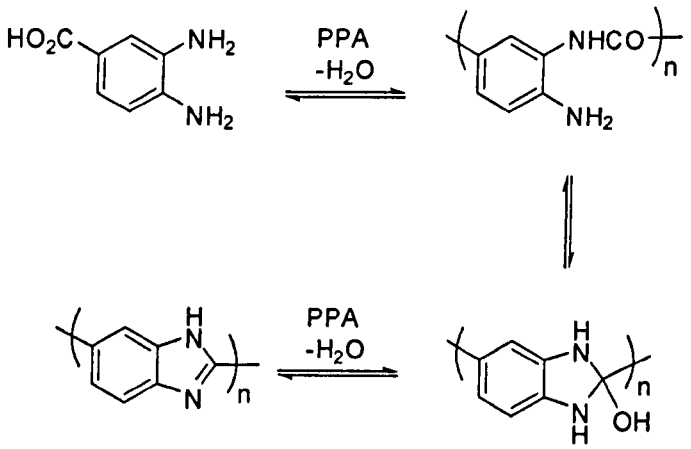

Scheme 1.27 Representation of the synthetic pathway to the preparation of a polybenzimidazole in polyphosphoric acid (PPA).

1.3.6.1 Properties

One of the most outstanding properties of PBI is probably its chemical and high thermal stability. The aromatic structure of the polymer backbone permits extensive electron delocalisation and an outstanding thermal stability allowing this material to be used at high temperature up to 500°C. For example burning tests unveil that PBI resin is intrinsically non-flammable in air[128] because of its relative inertness of the off-gases produced. In addition PBI exhibits outstanding chemical stability in presence of concentrated acids or bases environments[129]. The chemical structure of PBI provides also unique separation opportunities. The polymer can behave as amphoteric ion exchanger (anionic under acid conditions and cationic under basic conditions). Its high thermal stability offers more applications opportunity beyond those of conventional resins, e.g. polystyrene and divinylbenzene. PBI have been tested for various sorption processes involving phenolics and carboxylic acids. Furthermore because of its hydrophilic nature, PBI is also an excellent sorbent for biological separation[130] Celanese reported the separation of fatty acid free bovine serum albumin with PBI at pH 8.0.

1.3.6.2 Applications

The most frequent application of polybenzimidazole is in a fiber form. PBI is frequently made into a fiber with excellent textile and tactile performance, exhibiting exceptional thermal and durability properties not found in other synthetic fibers. For example PBI fiber is currently used as a replacement for asbestos in fire-blocking applications such as thermal protective clothing for fire fighters and race drivers where facial flame protection is required, and also in aircraft furnishings.
Other forms of polybenzimidazole apart from fibers are also commercially available for different applications. For example low molecular weight of fully polymerised PBI into structural shapes has been used in missile hardware allowing this material to perform well at high temperature exposure between 650-1380°C[131-133]. Furthermore, PBI has been used in composite applications such as a resin for filament winding[134], a crosslinkage component of composite matrix[135], ablative heat shields[136], matrix resins[137] and sheet processed from a liquid crystalline solution[138]. PBI also shows promise in other applications such as film, adhesive, foams (where lightweight foams of PBI have been used as high temperature insulation), and microporous absorbent beads of PBI has been used as selective sorbent in medical and biological separations. PBI is also used as a packing in high temperature gas chromatography and in liquid chromatography, where it retards polar compounds from polar solvents, and as an inert substrate for oxidizing and reducing agents[139] or as an ion-exchange resin.

The strategy to be used in the present work is still the same as described above i.e the attachment to polymers or crosslinked polymers and to an inorganic support of organic groups capable of acting as ligands for coordination to transition-metal ions.

Three types of resins have been used as supports in the present work. The first is polybenzimidazole (PBI) and the second are new crosslinked polymers derived from

divinylbenzene (DVB) and vinyl benzyl chloride (VBC) monomers or styrene (St) and the third was an inorganic support MCM-41 modified with aminoproplyl trimethylsilane.

1.4 Introduction to microwave chemistry

Over the past decades, microwave has developed as an established field of science, due to intensified research in the area[140-149]. Microwave chemistry is likely to become one of a preferred method for synthetic reactions and for conducting analytical procedures in laboratories. Initially, microwave chemistry was primarily used to carry out analytical processes such as digestion, extraction, fat analysis and protein hydrolysis. With the development of microwave chemical synthesis, its applications have been extended to include the synthesis of fine chemicals, organometallic chemistry[150, 151]. Microwave chemistry also allows cleaner and more efficient chemical reactions with higher yields to be achieved compared to conventional heating methods[150, 151].

1.4.1 Principles of microwave chemistry

Microwave chemistry involves the use of microwave radiation to conduct chemical reactions[150, 151]. Microwaves lie in the electromagnetic spectrum between infrared waves and radio waves. They have wavelengths between 0.01 and 1 meter, and operate in the frequency range between 0.3 and 30 GHz. However, for their use in laboratory reactions, a frequency of 2.45 GHz is preferred, since this frequency has the right penetration depth for laboratory reaction conditions. Beyond 30 GHz, the microwave frequency range overlaps with the radio frequency range. The microwave electromagnetic spectrum is divided into sub-bands comprising the following frequency ranges as shown in Table 1.4.1.

Table 1.4.1 Microwave frequency bands

bands	Freqeuncy (GHz)
L	1-2
S	2-4
C	4-8
X	8-12
Ku	12-18
K	18-26
Ka	26-40
Q	30-50
U	40-60
V	46-56
W	56-100

The lower microwave frequency ranges (1-2 GHz) are used for the purpose of communication, microwave frequency ranges (2-4 GHz) are used in laboratory reactions, and the higher frequency ranges (56-100 GHz) in the spectrum are used for analytical techniques such as spectroscopy.

However the main effect of microwave heating in chemistry involves agitation of polar molecules or ions that oscillate under the effect of an oscillating electric or magnetic field. In the presence of an oscillating field, particles try to orient themselves or be in phase with the field. However, the movement of these particles is restricted by resisting forces (such as inter-particle interaction or electric resistance), which restrict the movement of particles and generate random agitation, producing heat.

Since the response of various materials to microwave is diverse, not all materials are suitable to microwave heating. Based on their response to microwaves, materials can be broadly classified as follows:

- Materials that are transparent to microwaves, e.g., sulphur
- Materials that reflect microwaves, e.g., copper

- Materials that absorb microwaves, e.g., water

Only materials that absorb microwaves radiation are relevant to microwave chemistry. These materials can be classified according to the three main mechanisms of heating which are:

1. Dipolar polarisation
2. Conduction mechanism
3. Interfacial polarisation

1.4.2 Dipolar polarization method

Dipolar polarization method is a process by which heat is generated in polar molecules. When polar molecules are exposed to an oscillating electromagnetic field of appropriate frequency, they try to follow the field and align themselves in phase with the field. However, because of inter-molecular forces, polar molecules are unable to follow the field completely in phase and this create the random movement of particles which generates heat (Figure 1.4.2). Thus dipolar polarization can generate heat by interaction between polar solvent molecules or interaction between polar solute molecules.

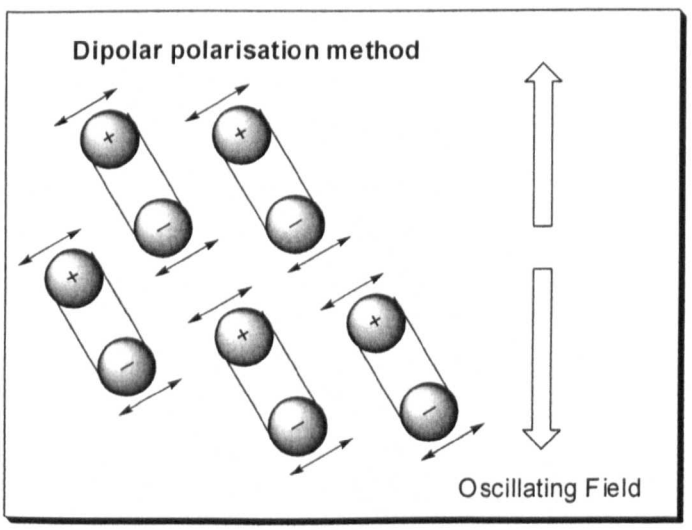

Figure 1.4 2 *Dipolar polarisation method of heating by microwave radiation*

The main requirement for dipolar polarisation is that the frequency range of the oscillating field should be appropriate to enable adequate inter-particle interaction. This means that if the frequency range is very high, inter-molecular forces will stop the movement of a polar molecule before it tries to follow the field, resulting in inadequate inter-particle interaction. On the other hand, if the frequency range is low, the polar molecule gets sufficient time to align itself in phase with the field. Therefore, no random interaction takes place between the adjoining particles. Microwave radiation has the appropriate frequency (0.3-30GHz) to oscillate polar particles and enable enough inter-particle interaction. This makes it an ideal choice for heating polar solutions. Furthermore, the energy of a microwave photon (0.037 kcal/mol) is very low, relative to the typical energy required to break a molecular bond (80-120 kcal/mol). Hence, microwave excitation of molecules does not affect the structure of an individual organic molecule, e.g. no direct bond scission and the interaction is purely intermolecular and kinetic.

1.4.3 Conduction mechanism

The conduction mechanism generates heat through resistance to an electric current. The oscillating electromagnetic field generates an oscillation of electrons or ions in a conductor (Figure 1.4.3), resulting in an electric current. This current faces internal resistance, which heats the conductor.

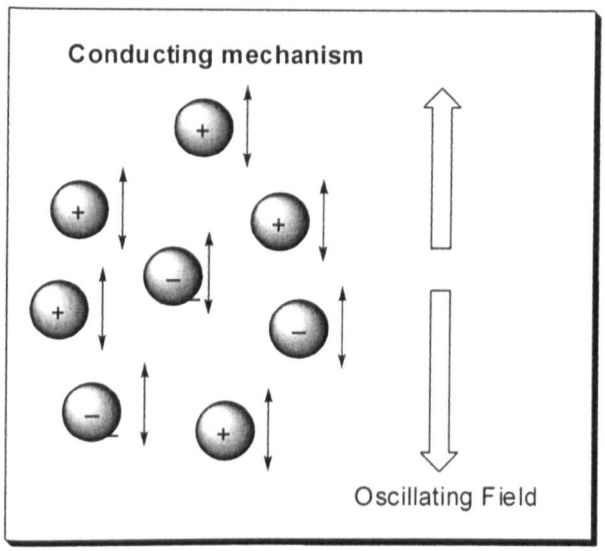

Figure 1.4 3 Conducting method of heating by microwave radiation

The main drawback of this method is that it is not applicable for materials that have high conductivity, since such materials reflect most of the energy that falls on them.

1.4.4 Interfacial polarisation method

The interfacial polarization method can be considered as a combination of the conduction and dipolar polarization methods. With this interfacial polarization technique, it is possible to irradiate metal powder materials. The environment of the metal powder can generate a random motion of ions which can create the heating of the system.

1.4.5 Advantages of microwave chemistry

Microwave radiation has proved to a highly effective heating source in chemical reactions[150, 151]. Microwaves can accelerate the reaction, give better yields and uniform and selective heating, achieve greater reproducibility of reactions, and help in developing cleaner and greener synthetic chemistry reactions.

Microwaves can accelerate the reaction rate. For example, compared to conventional oil bath heating, microwave heating enhances the rate of certain chemical reactions by 10 to 1,000 times. This is due to its ability to substantially increase the temperature of reactions. Thus the rate acceleration in liquid phase reactions, heated by microwave radiation, can be explained to the superheating of solvents, for example, water, when heated by conventional methods, has a boiling point of 100°C. However, when water is used as solvent in microwave, it has been observed that the boiling point of water can reach 119°C when a power input of 500 watts of microwave equipment is employed. Hence, this superheating of solvents enables the reaction to be performed at higher temperatures and results in an increase in the rate of reaction. However, in catalytic reactions, it has been observed that the rate acceleration in solid-state catalytic reactions for example, on exposure to microwave radiation, is attributed to high temperature on the surface of the catalyst. The increase in the local surface temperature of the catalyst results in enhancement of catalytic action, leading to an enhanced rate of reaction. For example, it has been noticed that the rate of heterogeneous oxidation and esterification reactions increases with microwave heating, compared to conventional heating under the same conditions.

In certain reactions, microwave radiation produces higher yields compared to conventional heating methods. In addition, microwave radiation, unlike conventional heating methods, also provides uniform heating throughout a reaction mixture. For example, in conventional heating, the walls of the oil bath get heated first, and then the solvent. As a result of this distributed heating in an oil bath, there is always a temperature difference between the walls and the solvent. In the case of microwave heating, only the solvent and the solute particles are excited, which results in uniform heating of the solvent. This feature permits the placing of reaction vessels at any location in the cavity of a microwave oven. It also proves vital in processing multiple reactions simultaneously, or in scaling up reactions that require identical heating conditions.

Selective heating is based on the principle that different material respond differently to microwaves[151]. Some materials are transparent to microwave radiation whereas others absorb microwave radiations. Hence, microwaves can be used to heat a combination of such materials. For example, the production of metal sulphide with conventional heating requires weeks because of the volatility of sulphur vapours. In addition, rapid heating of sulphur in a closed tube results in the generation of sulphur fumes, which can cause an explosion. However, in microwave heating, since sulphur is transparent to microwaves radiation, only the metal gets heated. Hence, the reaction can be carried out at a much faster rate, with rapid heating, without the threat of an explosion.

Reactions carried out through microwaves are cleaner and more environmentally friendly than conventional heating methods. Microwaves heat the compounds directly, therefore usage of solvents in the chemical reaction can be reduced or eliminated. In addition reactions with microwave heating are more reproducible compared to conventional heating because of uniform heating and better control of process parameters. The temperature of chemical reactions can also be easily monitored. This is of particular relevance in the optimization phase of a drug development process in pharmaceutical companies.

1.4.6 Limitations of microwave chemistry

The limitations of microwave chemistry are related to its scalability, limited application and the hazards involved in its use.

The yield obtained by using microwave equipment available in the market is limited to a few grams. Despite the fact that there have been developments in the recent past, relating to the scalability of microwave apparatus, there is a gap that needs to be filled up to make the microwave technology scalable. This is particularly issue for reactions at the industrial production level.

In addition, the use of microwave as source of heating has limited applicability for materials that absorb them. Microwaves cannot heat materials such as sulphur, which are transparent to their radiation. In addition, although microwave heating increases the rate of certain chemical reactions, it can also produce yield reduction compared to conventional heating methods.

Although manufacturers of microwave heating apparatus have directed their research to make microwaves a safe source of heating, uncontrolled reaction conditions may have undesirable results, for example, chemical reactions involving volatile reactants under superheated conditions may result in explosive conditions. Furthermore, improper use of microwave heating for rate enhancement of chemical reactions involving radioisotopes may result in uncontrolled radioactive decay. In addition, certain reactions, with dangerous end results, have also been observed while conducting polar acid-based reactions. For example, microwave irradiation of a reaction involving concentrated sulphuric acid may damage the polymer vessel used for heating. This is because sulphuric acid is a strong acid and with microwave energy, the reaction temperature can raise to 300°C within the short time. As a result, the polymer microwave heating container may melt with hazardous consequences. In addition, conducting microwave reactions under pressure conditions may also result in uncontrolled reactions and cause explosions. It has also been observed that while microwaves operating at a low frequency range are only able to penetrate the human skin, higher frequency range microwaves can reach body organs. Research has proven that on prolonged exposure microwaves may result in the complete degeneration of body tissues and cells. For example, it has been established that constant exposure of DNA to high frequency microwave during a biochemical reaction may result in complete degeneration of the DNA strand whereas this degeneration of the DNA strand is not observed in conventional heating.

1.4.7 Applications of microwave chemistry

Microwaves have now been successfully applied in varied industries such as the biotechnology, pharmaceuticals, petroleum, plastics, chemicals, etc. However, most of these applications have been limited to small scale use in laboratories and have not been extended to the production level. However the major industrial applications of microwave are :

1. Applications of microwave in analytical chemistry
2. Application of microwave in chemical synthesis

1.4.7.1 Applications microwaves in analytical chemistry

The range applications of microwave radiation in analytical chemistry include the following processes: digestion, extraction, protein hydrolysis, moisture analysis and spectroscopic analysis.

Digestion is the process by which samples are broken down to their basic constituents for chemicals analysis. Microwave digestion systems are used in analytical laboratories for sample decomposition and preparation. Microwave radiation has become the technology of choice for sample preparation trace and ultra trace metals analysis, and it is now used in the digestion of even the toughest organic or inorganic samples in diverse industries.

Furthermore, microwave extraction has proved to be more effective and efficient than its conventional counterpart, the Soxhlet extraction method. Soxhlet extraction, which is a standard technique, is a continuous solvent extraction method. Extraction systems are used to conduct routine solvent extraction of soils, sediments, polymers and plastics, biological tissues, textiles and food samples. In addition, extraction experiments carried

out with microwave use a lesser volume of solvent and sample, and perform extraction at a much faster rate than with the Soxhlet extraction.

Microwave radiation has been found to very useful in protein hydrolysis to achieve precision in amino acid analysis. The general structure of an amino acid is a chemical structure in which a primary amine and a carboxyl group are tied to the same carbon atom. A protein molecule consists of about twenty such amino acids that are linked through peptide bonds. To facilitate the analysis of the amino acid present in a protein molecule, the peptide bond has to be hydrolysed. Conventional hydrolysis methods take hours to break the peptides, whereas microwave protein hydrolysis reduces this to 10-30 minutes by processing samples at elevated temperature up to 200°C. Microwave heating is also able to generate high precision in breaking the peptide structure without causing any damages to the amino acid and is used for protein sequencing and structure studies in biomedical research (such as protein therapeutic agents).

Microwave radiation is also used to analyse the moisture level in many solid compounds for example powders or slurries and it has been found to be highly effective in reducing testing time. Microwave moisture analysis is applied in particular at product development stages such as process and quality control, and to test raw materials, intermediate and finished products. The food and beverage, chemical, environmental, organic and pharmaceutical industries use microwaves for moisture analysis.

1.4.7.2 Applications microwaves in fine chemical synthesis

Microwave organic synthesis is the main part of microwave- assisted chemical synthesis since it includes a large range of organic reactions such as hydrolysis, condensation, protection and deprotection, reduction, epoxidation, etc. Furthermore, organic synthesis reactions can be carried out in microwaves using different reaction conditions such as at atmospheric pressure or at elevated pressure. In addition, application of microwave

radiation in chemical synthesis permits organic reactions to proceed faster and to generate higher yields and increases products purity. Microwave assistance in the epoxidation of cyclohexene and styrene with polymer-supported Mo complexes as catalysts in this present work will be discussed in Chapter 4.

1.5 Catalytic reactions under Reactive Distillation Column (RDC)

The catalytic reactive distillation column system has gained remarkable attention in chemical industries because of its simplicity and high efficiently. The reactive distillation column systems are based on the combination of two simultaneous processes of chemical reaction and distillation in one step. The major advantages of the catalytic distillation include less operational equipment, energy savings, and increased chemical system efficiency due to thermodynamic advantages of in situ removal of products by distillation. The catalytic distillation method is based on the use of catalyst packing within the reactive section of the reactive distillation column. Clearly, effective contact between reactants in the liquid and gas phases in this system has a great influence on the system operation since effective contact not only increases the efficiency of the reactions but also improves the separation of the products.

In order to understand the mechanism of reactive distillation column, Doherty et al[152-154] have first reported a design model for reactive distillation column (RDC) based on equilibrium stage model which means the equilibrium reaction occurs at all stages of the column during the continuous process. Calculating the number of theoretical stages and assuming that the vapor and liquid streams leaving any stage in the column are in the phase as well as reaction equilibrium. They concluded that gas-liquid mass transfer, the presence of the catalysts in the reactive section and reaction kinetics strongly influence the performance of RDC. With this model, it was possible to predict the amount of products attainable for a given feed to a reactive distillation column (RDC) and at the

same time it was possible to visualize the equilibrium states for a lower dimensional reaction system. However, this conventional equilibrium stage model fails to explain and to predict the synthesis of the pure reactions products because of the assumption that the reaction reaches equilibrium instantaneously. However Lee et al[155] suggested that the generalized non-equilibrium model should be preferred for the simulation of a column reactive distillation to the equilibrium model because it gives the accurate prediction of the reaction products. In addition, the non-equilibrium model seems to be better because the model takes into account the technique characteristics of the column (type of plate, of packing).

1.5.1 Applications

The first industrial application of the reactive distillation column system is the etherification of *iso*-olefins with methanol or ethanol to produce fuel additives such as methyl *tert*-butyl ether (MTBE), ethyl *tert*-butyl ether (ETBE), *tert*-amyl methyl ether (TAME) in the presence of an acidic cation exchanged resins catalysts. These important ethers are MTBE, ETBE produced by the reaction of *iso*-butylene and methanol, ethanol respectively, and TAME produced by reacting a mixture of *iso*-amylenes (2-methyl -1-butene and 2-methyl -2-butene) with methanol, are used as oxygenate gasoline additives to prevent evaporation of gasoline which is one of the causes of smog, and also to avoid absorption of moisture from the atmosphere. Jin et al[156] reported the hydrolysis of methyl acetate on the catalytic reactive distillation column. The hydrolysis of methyl acetate is a reversible chemical reaction as shown in Scheme 1.28.

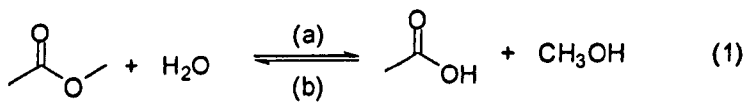

***Scheme 1.28** (a) Hydrolysis of methyl acetate, (b).esterification of acetic acid*

Hence, it is difficult to obtain the methyl acetate high conversion in batch reaction even by using an excess of one of the starting reactants to shift the equilibrium reaction.

However the authors[156] claimed to increase the methyl acetate conversion of hydrolysis process from 34% (the equilibrium conversion of hydrolysis of methyl acetate) to 72 % on reactive distillation column in which reactive section was filled with 1 l of G-26H ion exchange resin produced by Dowex Co (USA). That result also means the catalytic distillation column improves the methyl acetate hydrolysis conversion up to 50 % than its equilibrium conversion. Furthermore it is also possible to obtain good conversion with the inverse reaction (b) which is esterification of acetic acid in presence of methanol via reactive distillation. Schoenmakers and co-workers from Brite-Euram project (European project)[157] reported the production of methyl acetate in a single reactive distillation column in which acetic acid was fed into RDC at the top of catalyst whereas methanol was fed under the catalyst. While the esterification process, the products water and methyl acetate were separated off as low and high boilers, respectively. It was also noticed that the removal of water and methyl acetate at the bottom and at the top of RDC respectively seems to accelerate the esterification reaction. However, it also appears in the literature that long-chain acid esterification is much more difficult to carry out in batch reaction compared to shorter acids such as acetic acid. For example, in typical batch reactions, using solid acid catalysts such as sulfated zirconia catalyst or titania and tin oxide catalysts, and equivalent amounts of dodecanoic acid (fatty acid) with of 2-ethylhexanol were reacted at 160°C for a period of 2 h as shown in Scheme 1.29. Rothenberg et al[158] reported modest conversions (50%-60%) of dodecanoic acid (fatty acid).

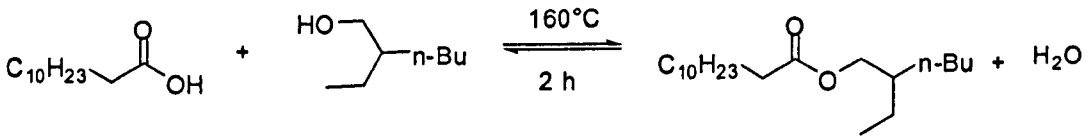

Scheme 1.29 Esterification of dodenoic acid (fatty acid) with 2-ethylhexanol

The resulting 2-ethylhexenyl dodecanoate ester is also a key additive in biodiesel since it also generates 10% oxygen in biodiesel and therefore improves combustion and reduces carbon oxide (CO), soot and hydrocarbon emissions. However, when they carried out this

esterification of dodecanoic acid with 2-ethylhexanol under reactive distillation column. They claimed to obtain a complete conversion of both reactants at the ends of the column with water at the top and 2-ethylhexenyl dodecanoate at the bottom of the column. They also claimed successful esterification reactions with fatty acids and other alcohols such as methanol reacting in stoichiometric ratio with the use solid acid catalysts under reactive distillation column.

In this present work, the epoxidation of cyclohexene with PBI.Mo as catalyst under a reaction distillation column (RDC) will be discussed in Chapiter 4.

Objectives

The first and most important objective of the present work was to reproduce the synthesis of a previously prepared polybenzimidazole supported Mo complex, PBI.Mo, and to investigate in detail its recyclability and long-term activity as a heterogeneous catalyst in the epoxidation of cyclohexene using t-butylhydroperoxide, TBHP, as the oxidant. If sufficiently stable it was further proposed to scale up the synthesis of this and supply the catalyst to our chemical engineering collaborators at the University of Loughborough for them to exploit in a reactive distillation column (RDC) in which cyclohexene was to be epoxidised in a continuous process with simultaneous separation of the products. If sufficient progress was made a visit to Loughborough was to be made to gain experience of the continuous RDC process.

A second objective was to synthesise a range of polystyrene resin supported Mo complexes where the Mo was to be retained employing a novel range of polymer-bound ligands to assess if even more stable cyclohexene epoxidation catalysts could be developed.

The above two objectives were to employ alkene epoxidation conditions similar to those typical of a continuous 'large scale process' i.e. solventless and with a large excess of alkene to oxidant, since these are known to avoid over-oxidation hence improving the selectivity for epoxide formation, and provide safe working conditions. In terms of the epoxidation of alkenes in the fine chemicals industry, for example in the batch synthesis of drugs or their precursors, the alkene substrate is the expensive component and the objective is to try to achieve 100% epoxidation typically employing an alkene/oxidant ratio of 1/1, or even excess oxidant to accomplish this. In addition the (solid) alkene needs to be dissolved in a suitable solvent. A further objective of the present work was therefore to assess the catalytic efficiency of the supported Mo complexes under the conditions of fine chemical synthesis i.e. 'small-scale conditions'.

Finally if time permitted it was planned to synthesis some polystyrene resin supported chiral ligands to which Mo would be bound, and the resultant chiral complexes examined as catalysts in the epoxidation of styrene to assess the level if any of asymmetric induction.

REFERENCES

[1]R. B. Merrifield, *J. Am. Chem. Soc.* **1963,** 85, 2149.

[2]S. Itsuno, M. Sakakura, K. Ito, *J. Org. Chem.* **1990,** 55, 6047.

[3]Taken from a quotation in G.C. Bond, *Homogeneous Catalysis,* Oxford University Press, Oxford, 1987, p2.

[4]R. M Arluck, F. R. Mayo, D.E. Van Sickle and M.G. Syz, *J. Am. Chem. Soc.*, **1967,** 80, 967.

[5]J. K. Kochi and R.A. Sheldon *Advan, Catal.*, **1976,** 25, 344.

[6]]D.J. Rawlinson, and G. Sosnovsky., *Synthesis*, **1972,** 1.

[7]K. B. Sharpless and T. R. Verhoeven, *Aldrichimica Acta*, **1979,** 12, 63.

[8]R. W. Fischer, D. W. Marz, *Angew. Chem. Int. Ed. Engl*, **1991,** 30, 1638.

[9]H. Mimoun, *Angew.Chem. Int. Edn. Eng.;* **1982,** 21, 734.

[10]A.O. Chong and K. B. Sharpless, *J. Org. Chem.* **1977,** 42, 1587.

[11]R. A. Sheldon, J. A. Kochi, Metal-Catalyzed Oxidations of Organic Compounds; Academic Press: New York, 1981.

[12]R. A. Sheldon, J. A. Van Doorn, *J. Catal.* **1973,** 31, 427.

[13]R. A. Sheldon, J. A. Van Doorn, *J. Mol. Catal.* **1980,** 7, 107.

[14]R. A. Sheldon, In *The Chemistry of Peroxides*; Patai, S., Ed.; Wiley: New York, **1983,** 161.

[15]Y. Matoba, H. Inoue, J. I. Akagi, T. Okabayashi, Y. Ishui, M. Ogawa, *Synth. Commun.* **1984,** 14, 865.

[16]B. M. Trost, Y. Masuyama, *Isr. J. Chem.* **1984,** 24, 134.

[17]J. Kollar, U.S. Patent., 3. 360. 584, **1967** to Halcon International.

[18]A. Fusi, R. Ugo, G. M. Zanderighi, *J. Catal.* **1974,** 34, 175.

[19]A. M. Santos, F. E. Kühm, K. Bruus-Jensen, I. Lucas, C. C. Romão, E. Herdtweck, *J. Chem. Soc. Dalton Trans.* **2001,** 8, 1332.

[20]F. E. Kühm, M. Groarke, E. Beneze, E. Herdtweck, A. Prazeres, A. M. Santos, M. J. Calhorda C. C. Romão, I. S. Gonçalves, A. D. Lopes, M. Pilinger, *Chem.Eur. J.* **2002,** 8, 2370.

[21]L. F. Veiros, A. Prazeres, P. J. Costa, C. C. Romão, F. E. Kühm, M. J. Calhorda, *Dalton. Trans.* **2006**, 1383.

[22]C. Venturello, E. Almeri and M. Ricci, *J. Org. Chem.* **1983**, 48, 3831.

[23]C. Venturello, and R. D'Aloisio, *J. Org. Chem.* **1988**, 53, 1553.

[24]Y. Ishii, K. Yamawaki, T. Ura, H. Yamada, T. Yoshida, and M. Ogawa, *J. Org. Chem.* **1988**, 53, 3587.

[25]K. Sato, M. Aoki, M. Ogawa, T. Hashimoto, and R. Noyori, *J. Org. Chem.* **1996**, 61, 8310-8311.

[26]A. Jimtaisong and L. Luck, *Inorg. Chem.* **2006**, 45, 10391.

[27]F. E. Külm, A. M. Santos and W. A. Herrmann, *Dalton. Trans.* **2005**, 2483.

[28]K. Mertis, D. H. Williamson and G. Wilkinson, *J. Chem. Soc., Dalton. Trans.* 1975, 607.

[29]J. F. Gibson, K. Mertis, D. H. Williamson and G. Wilkinson, *J. Chem. Soc., Dalton. Trans.* 1975, 1093.

[30]W. A. Herrmann, R. Serrano and H. Block, *Angew. Chem. Int. Ed. Engl.* **1984**, 23, 383.

[31]W. A. Herrmann, J. G. Kuchler, J. K. Felixberger, E. Herdtweck, and W. Wagner, *Angew. Chem. Int. Ed. Engl.* **1988**, 27, 394.

[32]F. E. Kühm, W. A. Herrmann, R. Hahn, M. Elison, J. Blümel and E. Herdtweck, *Organometallics.* **1994**, 13, 1601.

[33]W. A. Herrmann, R. W. Fischer, D. W. Marz, *Angew. Chem. Int. Ed. Engl.* **1991**, 30, 1638.

[34]Z. Zhu, J. H. Espenson, *J. Org. Chem.* **1995**, 60, 1326.

[35]A. M. Ajlouni, J. H. Espenson, *J. Am. Chem. Soc.* **1995**, 117, 9243.

[36]W. Adam, C. M. Mitchell, C. R. Saha-Möller, *Tetrahedron.* **1994**, 50, 13121.

[37]K. A. Vassel, J. H. Espenson, *Inorg. Chem.* **1994**, 33, 5491.

[38]M. M. Abu-Omar, J. H. Espenson, *J. Am. Chem. Soc.* **1995**, 117, 272.

[39]Z. Zhu, J. H. Espenson, *J. Org. Chem.* **1995**, 60, 7728.

[40]W. Adam, W. A. Herrmann, J. Lin, C. R. Saha-Möller, *J. Org. Chem.* **1994**, 59, 8281.

[41]W. Adam, W. A. Herrmann, J. Lin, C. R. Saha-Möller, R. W. Fischer, J. D. G. Correia, *Angew. Chem. Int. Ed. Engl.* **1994**, 33, 2475.

[42]R. W. Murray, K. Iyanar, I. Cheng, J. T. Wearing, *Tetrahedron Lett.* **1995**, 36, 6415.

[43]T. R. Boehlow, C.D. Spilling, *Tetrahedron Lett.* **1995**, 37, 2717.

[44]J. Rudolph, K. L. Reddy, J. P. Chiang, K. B. Sharpless, *J. Am. Chem. Soc.* **1997**, 119, 6189.

[45]G. S. Owens, M. M. Abu-Omar, *Chem. Commun.* **2000**, 1165.

[46]R. B. Vanatta, C. C. Franklin, J. S. Valentine, *Inorg. Chem.* **1984**, 23, 4121.

[47]R. A. Sheldon, J. A. Kochi, Metal-Catalyzed Oxidations of Organic Compounds; Academic Press: New York, 1981,p275.

[48]B. Meunier, E. Guilmet, M. E. De Carvalho, R. Poilblanc, *J. Am. Chem.* Soc. **1986**, 106, 6668.

[49]C. U. Pittman, in: P. Hodge, D. C. Sherrington (Eds.), *Polymer-supported Reactions in Organic Synthesis*, Wiley, Chichester, 1981; Chap5. p249.

[50]R. Neumann, and T. Wang, *Chem. Commun.* **1997**, 1915.

[51]R. Buffon, and U. Schuchardt, *J. Braz. Chem. Soc.* **2003**, 14, 3, 343.

[52]F. E. Kühm, A. M. Santos and W. A. Herrmann, *Dalton. Trans.* **2005**, 2483.

[53]R. Saladino, V. Neri, A. R. Pellicia, R. Caminiti, C. Sadum, *J. Org. Chem.* **2002**, 67, 1323.

[54]G. G. Allen, A. N. Neogie, *J. Catal.* **1970**, 19, 256.

[55]M. Quenard, V. Bonmarin, G. Gelbard, *Tetrahedron. Lett.* **1987**, 28, 2237.

[56]G. Gelbard, F. Breton, D. C. Sherrington, *J. Mol. Catal.* **2000**, 153, 7.

[57]G. Gelbard, C. R. Acad. Sci. Paris, serie IIc, *Chimie /Chemistry.* **2000**, 3, 757

[58]S. Ivanov, R. Boeva, S. Tanielyan, *J. Catal.* **1979**, 56, 150.

[59]G. L. Linden, M. F. Farona, *J. Catal.* **1977**, 48, 284.

[60]T. Yokoyama, M. Nishizawa, T. Kimura, T. M. Suzuki, *Chem. Lett.* **1983**, 1703.

[61]T. Yokoyama, M. Nishizawa, T. Kimura, T. M. Suzuki, *Bull.Chem. Soc. Jap.* **1985**, 58, 3271.

[62]S. Gil, R. Gonzales, R. Mestres, A. Zapater, *React. Funct. Polym,* **1999**, 42, 65.

[63]U. Arnold, F. Fan, W. Habicht, M. Döring, *J. Catal.* **2007,** 245, 55.

[64]M. M. Miller, D. C. Sherrington, S. Simpson, *J. Chem. Soc. Perkin Trans 2.* **1994,** 2091.

[65]M. M. Miller, D. C. Sherrington, *J. Chem. Soc. Chem. Commun.* **1994,** 55.

[66]S. Simpson, D. C. Sherrington, *J. Catal.* **1991,** 131, 115.

[67]M. M. Miller, D. C. Sherrington, *J. Catal.* **1995,** 152, 368.

[68]G. Olason, D. C. Sherrington, Macromol. Symp. **1998,** 131, 127.

[69]J. H. Ahn, D. C. Sherrington, *Chem. Commun.* **1996,** 643.

[70]K. I. Alder, D. C. Sherrington, *Chem. Commun.* **1998,** 131.

[71]M. M. Miller, D. C. Sherrington, *J. Catal.* **1995,** 152, 377.

[72]K. Ambroziak, R Mbeleck, B. Saha and D. C. Sherrington, *J. Ion. Exchange.* **2007,** 18, 452.

[73]R. Mbeleck, K. Ambroziak, B. Saha and D. C. Sherrington, *React. Funct. Polym.* **2007,** 67, 1448.

[74]G. Grivani, S. Tangestaninejad, M. H. Habili, V. Mirkhani, *Catal. Commun.* **2005,** 6, 375.

[75]G. Grivani, S. Tangestaninejad, M. H. Habili, *Inorg. Chem. Communications.* **2007,** 10, 914.

[76]A. Corma, V. Fornés, T. M. Navarro, J. Péres-Pariente, *J. Catal.*, **1994,** 148, 569

[77]P. Ferreira, I. S. Goncalves, F. E. Kühm, A. D. Lopes, M. A. Martins, M. Pilinger, A. Pina, J. Rocha, C. C. Romao, A. M. Santos, T. M. Santos, A. A. Valente, *Eur. J. Inorg. Chem.* **2000,** 2263.

[78]M. Master-Farahani, F. Farzaneh, M. Ghandi, *J. Mol. Catal. A.Chem.* **2006,** 245, 53.

[79]M. Jia, A. Seifert, W. R. Thiel, *Chem. Mater.* **2003,** 15, 2174.

[80]M. Jia, W. R. Thiel, *Chem. Commun.* **2002,** 2392.

[81]S. M. Bruno, J.A. Fernandes, L. S. Martins, I. S. Goncalves, M. Pilinger, P. Ribeiro-Claro, J. Rocha, A. A. Valente, *Catal. Today.* **2006,** 114, 263.

[82]E. N. Jacobsen, M. H. Wu, Epoxidation of Alkenes Other than Allylic Alcohol. In *Comprehensive Asymmetric Catalysis*, E. N. Jacobsen, A. Pfaltz, H. Yamamoto., Eds, Springer-Verlag: Berlin, **1999**, Vol. 2, P649.

[83]W. Zhang, J. L. Loebach, S. R. Wilson, E. N. Jacobsen, *J. Am. Chem. Soc.* **1990,** 112, 2801.

[84]B. D. Brandes, E. N. Jacobsen, *J. Org. Chem. Soc.* **1994,** 59, 4378.

[85] E. N. Jacobsen, W. Zhang, A. R. Muci, J. R. Ecker, L. Deng, *J. Am. Chem. Soc.* **1991,** 113, 7063.

[86]T. Katsuki, *J. Mol.Catal. A,* **1996,** 113, 87.

[87]T. Hamada, T. Fukuda, H. Imanishi, T. Katsuki, *Tetrahedron* **1996,** 52, 515.

[88]L. Canali, E. Cowan, H. Deleuze, C. L. Gibson, D. C. Sherrington, *Chem. Commun.* **1998,** 2561.

[89]L. Canali, E. Cowan, H. Deleuze, C. L. Gibson, D. C. Sherrington, *J. Chem. Soc.,Perkin Trans 1.* **2000,** 2055.

[90]H. Deleuze, X. Schultze, D. C. Sherrington, *J. Mol.Catal. A-Chem,* **2000,** 159, 257.

[91]L. Canali, D. C. Sherrington, H. Deleuze, *React. Funct. Polym.* **1999,** 40, 155.

[92]M. D. Angelino, P. L. Laibinis, *Macromolecules,* **1998,** 31, 7581.

[93]F. Minutolo, D. Pini, P. Salvadori, *Tetrahedron Lett,* **1996,** 37, 33375.

[94]D. C. Sherrington, *Catal. Today,* **2000,** 57, 87.

[95]P. S. Suresh, M. Srinivasan, V. N. Rajasekharan, *J. Polym. Sci. Pol. Chem* **2000,** 38, 161.

[96]X. Yao, H. Chen, W. Lü, G. Pan, X. Hu, Z. Zheng, *Tetrahedron Lett,* **2000,** 41, 10267.

[97]H. Seller, J. K. Karjalainen, D. Seebach, *Chem. Eur. J,* **2001,** 7, 2873.

[98]F. Minutolo, D. Pini, A. Petri, P. Salvadori, *Tetrahedron Asymmetric,* **1996,** 7, 2293.

[99]D. Pini, A. Mandoli, S. Orlandi, P. Salvadori, *Tetrahedron Asymmetric,* **1999,** 10, 3883.

[100]G. Kim, J. H. Shin, *Tetrahedron Lett,* **1999,** 40, 6827.

[101]G. J. Kim, S. H. Kim, *Catal.Lett.* **1999,** 57, 139.

[102]X. G. Zhou, X. Q. Yu, J. S. Huang, C. M. Che, S. G. Li, L. S. Li, *Chem Commun* **1999,** 1789.

[103]P. Paggio, P. McMorn, D. Murphy, D. Bethell, P. C. B. Page, F. E. Hancock, C. Sly, O. J. Kerton, G. J. Hutchings, *J. Chem. Soc.,Perkin Trans 2.* **2000,** 2008.

[104]P. Paggio, C. Langham, P. McMorn, D. Murphy, D. Bethell, P. C. B. Page, F. E. Hancock, C. Sly, G. J. Hutchings, *J. Chem. Soc.,Perkin Trans 2.* **2000,** 143.

[105]I. F. J. Vankelecom, D. Tas, R. F. Partron, V. Van de Vyver, P. A. Jacobs , *Angew. Chem. Int. Ed. Engl.* **1996,** 35, 1346.

[106]G. Pozzi, F. Cinato, F. Montanari, S. Quici, *Chem. Commun,* **1998,** 877.

[107]M. cavazzini, A. manfredi, F. Montanari, S. Quici, G. Pozzi, *Chem. Commun,* **2000,** 2171.

[108]C. E. Song, E. J. Roh, *Chem. Commun,* **2000,** 837.

[109]J. M. Fraile, J. I. Garcia, J. Massam, J. A. Mayoral, *J. Mol. Catal. A Chem* **1998,** 136, 47.

[110]C. E. Song, E. J. Roh, B. M. Yu, D. Y. Chi, S.C. Kim, K. J. Lee, *Chem. Commun,* **2000,** 615.

[111]K. B. M. Jansen, I. Laquiere, W. Dehean, R. F. Partron, I. F. J. Vankelecom, P. A. Jacobs, *Tetrahedron Asymmetric.* **1997,** 8, 3481.

[112]D. C. Sherrington, *Chem. Commun.* **1998,** 2275.

[113]H. Warson, *J. Polym. Paint. Col.,* **1983,** 24, 541.

[114]W.P. Hohenstein and H. Mark, *J. polym. Sci.* **1940,** 1, 127.

[115]B.W. Brooks, *Makromol. Chem. Makromol. Symp.*, **1990,** 35/36, 121.

[116]H. Bieringer, K. Flatau, D. Reese, *Agnew. Makromol. Chem.,* **1984,** 123/124, 307.

[117]D. C. Sherrington., *Brit. Polymer. J.*, **1984,** 16, 164.

[118]D. C. Sherrington, P. Hodge., *Synthesis and Separation using Functional Polymerss,* Wiley and sons, New york, **1988;** p4

[119]M. Tomoi and W.T. Ford, *J. Am. Chem. Soc.*, **1981,** 103, 821

[120]J.M.J. Frechet, P. Darling, M.J. Farral, *J.Org. Chem.*, **1981,** 46, 728

[121]J. Coupek, M. Krivakova, S. Pakorny., *J. Polym. Sci. Polym. Symp.*, **1973,** 42, 185

[122]E. Atherton, D. Clive, R. C. Sheppard., *J. Am. Chem. Soc.* **1975,** 97, 6584.

[123]R. Epton, S.R. Holding, J.V. McLaren, *Polymer,* **1973,** 17, 843

[124]K.C. Brinker, I.M.Robinson, US, Patent **1959,** 2, 895, 984.

[125]H. Vogel and C. S. Marvel, *J. Polym. Sci.* **1961,** 50, 511.

[126]Y. Iwakura, K. Uno, Y. Imai, *J. Polym. Sci.* **1964,** 12, 2605.

[127]S. Simpson, D. C. Sherrington, *React. Polym.* **1993**, 19, 13.

[128]D. E. Stuetz, A. H. DiEdwardo, F. Zitomer and B. P. Barnes, *J. Polym. Sci. Polym. Chem. Ed.* **1980**, 18, 987.

[129]D. R. Coffin, G.A. Serad, H. L. Hicks and R. T. Montgomery, *Text. Res,* **1982**, 52, 466.

[130]Typical Applications for Celanese *PBI Microporous Resins, Technical Bulletin SF-6.1, Celanese Corp.*, Charlotte, N.C, 1984.

[131]J.F. Jones and co-workers, *Technology Vectors, Proceedings of the 29th National SAMPE Symposium Exhibit,* Society of Aerospace Material Process Engineers, Azusa, Calif., **1984**, p777.

[132]R. Fountain and J. F. Jones, *Society of Manucfacturing Engineers Fabricating Composites Conferences, MF85-505,* SME, Hartford, Conn, June 11-13, **1985**.

[133]J. F. Jones and R. Fountain, *The Use of Polybenzimidazole in Composites, International Conference on Composite Materials,* San Diego, Calif., Aug. 1985

[134]F. J. Reil and S. Litvatk, Advances in Structural Composites, 12th Society of Aerospace Material Process Engineers Nattional Symposium Exhibit, Western Period Co., North Hollywood, Calif, 1967, p5.

[135]U.S. Pat 4,113,683 (Sept.12, 1978), G. J. Breckenridge and I. L. Kalnin (*to Celanese Corp.*).

[136]R. R. Dickey and co-workers, *J. Macromol. Sci. Chem.* **1969**, 3, 601.

[137]U.S. Pat 3,555,108 (Jan.12, 1971), N. Bilow and L. J. Miller (to Hughes Aircraft Co.).

[138] Jpn. Pat 59/184211 A2 [84/184211] (Oct.19, 1984), (to Matsushita Electric Industrial Co., Ltd.).

[139]J. M. J. Frechet and N. Li, *Polym. Prepr. Am. Chem. Soc. Div. Polym. Chem.* **1985**, 26, 251.

[140]A. Loupy, A. Petit, J. Hamelin, F. Texier-Boullet, P. Jacquault, D. Mathe, *Synthesis,* **1998**, 1213.

[141]R. S. Varma, *Pure Appl. Chem,* **2001**, 73, 193.

[142]R. S. Varma, *Tetrahedron,* **2002**, 58, 1235.

[143]L. Perreux, A. Loupy, *Tetrahedron,* **2001**, 57, 9199.

[144]N. Kuhnert, *Angew. Chem. Int. Ed.* 2002, 41, 1863.

[145]C. R. Strauss, *Angew. Chem. Int. Ed.* 2002, 41, 3589.

[146]C. O. Kappe, *Angew. Chem. Int. Ed.* 2004, 43, 6250.

[148]S. Caddick, *Tetrahedron*, 1995, 51, 10403.

[149]R. Gedye, F. Smith, K. Westaway, H. Ali, L. Baldisera, L. Laberge, J. Rousell, *Tetrahedron Lett.* 1986, 27, 279.

[150]H. O. Kappe, A. Stadler, *Microwave in Organic and Medicinal Chemistry*, Wiley-VCH, Weinheim, 2005 (Chapter 2).

[151]H. O. Kappe, D. Dallinger and S. S. Murphree, *Practical Microwave synthesis for Organic Chemists*, Wiley-VCH, Weinheim, 2008 (Chapters 1, 2, 5 and 6).

[152]D. Barbosa, M. F. Doherty, Design and minimum-reflux calculations for single-feed multicomponent reactive distillation columns. *Chem. Eng. Sci.* 1988a, 43, 1523.

[153]D. Barbosa, M. F. Doherty, Design and minimum-reflux calculations for double-feed multicomponent reactive distillation columns. *Chem. Eng. Sci.* 1988b, 43, 2377.

[154]G. Buzad, M. F. Doherty, Design of three-multicomponent kinetically controlled reactive distillation columns using fixed-point methods. *Chem. Eng. Sci.* 1994, 49, 1947.

[155]J. H. Lee, M. P. Dudukovic, A comparision of the equilibrium and non equilibrium models for a multicomponent reactive distillation. *Comp.Chem. Eng.* 1998, 23, 159.

[156]J. Wang, X. Ge, Z. Wang, Y. Jin, *Chem. Eng. Technol.*, 2001, 24 (2), 155.

[157]H. G. Schoenmakers and B. Bessling, *Chem. Eng. Proces.*, 2003, 42, 145.

[158]A. A. Kiss, A. C. Dimian, G. Rothenberg, *Energy & Fuels*, 2008, 22, 589.

Chapter 2

Experimental

2 EXPERIMENTAL

2.1 Materials

2.1.1 Chemicals

The list of liquid and solid chemicals used in this study is found in the following paragraphs. Unless otherwise stated these chemicals were used without purification. All other chemicals used in this study were common laboratory reagents.

2.1.1.i Liquid Chemicals

Chemicals	*Supplier*
2-Amino methylpyridine	Aldrich Chemical Co.
Aminophenol	Aldrich Chemical Co.
Ammonium hydroxide	Aldrich Chemical Co.
Bromobenzene	Aldrich Chemical Co.
Chloroacetic acid	Aldrich Chemical Co.
Cyclohexene[a]	Aldrich Chemical Co.
Cyclohexene oxide	Aldrich Chemical Co.
1,2-Dichloroethane[b]	Aldrich Chemical Co.
Dicyclohexylcarbodiimide	Aldrich Chemical Co.
2,4-dihydroxybenzaldehyde	Aldrich Chemical Co.
Divinylbenzene[c]	BDH Laboratory Chemical.
Ethylenediaminetetraacetic acid	Aldrich Chemical Co.
2-Ethylhexanol	Fisons Laboratories.
Glycine	Aldrich Chemical Co.
Iminodiacetic acid	Aldrich Chemical Co.

Chemicals	*Supplier*
Methanol	Aldrich Chemical Co.
Methylamine 33%	Aldrich Chemical Co.
Phenylalanine	Aldrich Chemical Co.
Styrene	Aldrich Chemical Co.
tert-Butyl hydroperoxide 70%	Aldrich Chemical Co.
Thionyl chloride	Aldrich Chemical Co
Thiophene-2-carboxyaldehyde	Aldrich Chemical Co
Toluene	Aldrich Chemical Co

[a] distilled and the fraction boiling between 82-83°C collected and used.

[b] distilled and the fraction boiling between 83-84°C collected and used.

[c] purified using silica flash column

2.1.1.ii Solids Chemicals

Chemicals	*Supplier*
AIBN[a]	BDH Laboratory Chemical.
Boric Acid	Fisons Laboratories.
Molybdenyl acetylacetonate	Aldrich Chemical Co.
Potassium phthalimide	Aldrich Chemical Co.
Sodium hydroxide	BDH Laboratory Chemical.
Sodium iodide	Aldrich Chemical Co.
Sodium chloride	Aldrich Chemical Co.
Sodium thiosulphate	Aldrich Chemical Co.
Tetrabutylammonium iodide	Aldrich Chemical Co.

[a] recrystallised from methanol.

Chemicals	*Supplier*
MCM-41	our Spanish collaborators
Aminated MCM-41	our Spanish collaborators

2.1.1.iii Surfactants and stabilisers

Chemicals	*Supplier*
Polyvinylalcohol (Mowiol 40-88)	Aldrich Chemical Co.

2.2 Precuror polymer-support resins

2.2.1 Polybenzimidazole resin

The wet polybenzimidazole resin was supplied from the Celanese Corporation. The resin was pre-treated prior to use by stirring it in 1 M NaOH solution overnight, washed with deionised water until the pH of the washings was neutral, washed with acetone, and dried under vacuum at 40 °C.

2.2.2 Synthesis of DVB-co-styrene resins

The syntheses of these macroporous high or low surface area resins were carried out using the suspension polymerisation according to Sherrington's procedure[1] as follows. Initially some preliminary syntheses were carried out in order to establish familiarity with the procedure.

Poly (DVB-co-styrene)-macroporous high surface area resin (1)

For the synthesis of the aqueous continuous phase, the suspension stabiliser PVOH [M_w ~127,000, Mowiol 40-88] (7.5 g) was dissolved in water at ~50°C then the NaCl (33 g) was added . When the NaCl was completely dissolved, the solution was cooled to room temperature, then more water was added until the volume was brought to 1 litre to give a 0.75% PVOH and 3.3% NaCl solution. The resulting solution (650 ml) was added to a 1 litre parallel-sided, jacketed glass baffled reactor, fitted with a condenser, double impeller and mechanical stirrer. The volume ratio of the organic to the aqueous phase was chosen to be 1/20.

The organic phase was prepared by stirring the monomers DVB (75%, 11.25 g, 12.24 ml) and styrene (25%, 3.75 g, 4.12 ml), AIBN (1% by weight of comonomers, 0.15 g), and toluene (1/1 volume ratio weight comonomers, 15.54 ml, 13.44 g) as porogen into a

conical flask (250 ml). The resulting organic phase was then added to the reactor, containing the aqueous phase, and the stirrer started. Nitrogen was bubbled through the stirred suspension for 30 minutes and the supplying needle was removed from its septum before starting the reaction. The suspension polymerisation was carried out under a nitrogen atmosphere and the stirrer speed was 500rpm. The temperature of the reaction was set at 80°C and the resulting polymerisation mixture was left for a period of 6 hours. The resulting beads were filtered off, washed exhaustively with distilled water, and a sonic bath was used to remove all impurities (NaCl, PVOH). The resulting beads were then washed successively with methanol and acetone. The beads were extracted with acetone as solvent in a Soxhlet apparatus for a period of 24 hours before being dried in a 40°C vacuum oven.

Yield: 12.3g (82%)

Elemental microanalysis: 91.49 % C, 7.46 % H, 0 % N, 0 % Cl.

FT-IR (ν_{max} [cm^{-1}]): 3024, 2943, 2169, 1768, 1700, 1630, 1602, 1511, 1493, 1452, 1245, 1221, 1182, 1029, 988, 830, 794, 760, 699.

Poly (DVB-co-styrene)-macroporous low surface area resin (2)

For the synthesis of this macroporous low surface area resin, the same experimental procedure was used, changing the monomer feed to: DVB (15%, 2.25 g, 2.45 ml) and styrene (85%, 12.75 g, 14.03 ml), AIBN (1% weight comonomers, 0.15 g), and 2-ethylhexanol (1/1 volume ratio weight comonomers, 16.48 ml, 17.53 g) as porogen.

Yield: 6.5g (43%)

Elemental microanalysis: 91.43 % C, 7.84 % H, 0 % N, 0 % Cl.

FT-IR (ν_{max} [cm^{-1}]): 3060, 3025, 2922, 1800, 1699, 1601, 1492, 1452, 1181, 1028, 757,703, 650.

Poly (DVB-co-styrene)-macroporous low surface area resin (3)

For the synthesis of this macroporous low surface area resin, the same experimental procedure was used, changing the monomers feed to: DVB (12%, 1.8 g, 1.95 ml) and styrene (88%, 13.20 g, 14.52 ml), AIBN (1% weight comonomers, 0.15 g), and 2-ethylhexanol (1/1 volume ratio weight comonomers, 16.47 ml, 17.53 g) as porogen.
Yield: 6.3g (41%)
Elemental microanalysis: 90.82% C, 7.73 % H, 0 % N, 0 % Cl.
FT-IR (ν_{max} [cm^{-1}]): 3446, 3082, 3025, 2922, 1942, 1601, 1493, 1452, 1028, 757, 705, 606, 539.

2.2.3 Gel-type resin

The synthesis of gel-type resins is slightly different from other macroporous resins because no porogen is involved, and the aqueous continuous phase is slightly different.

Poly (DVB-co-styrene)-gel-type resin (4)

For the synthesis of the aqueous continuous phase, the suspension stabiliser PVOH [M_w ~115,000 g/mol] (14 g) was dissolved in 700 ml distilled water at ~90°C then boric acid (6 g dissolved in 175 ml distilled water) was added only. The solution was then cooled down at room temperature and the water was topped up again to 700 ml. The resulting solution (660 ml) was added to the 1 litre parallel-sided, jacketed glass baffled reactor, fitted with a condenser, double impeller and mechanical stirrer. The volume ratio of the organic to aqueous phase was chosen to be 1/20.

The organic phase was prepared by stirring the monomers DVB (2%, 0.3 g, 0.33 ml) and styrene (98%, 14.70 g, 16.17 ml), AIBN (1% weight comonomers, 0.30 g). The amount of each monomers was doubled to keep the level of the aqueous phase at around 600 ml,

and to have a reasonable yield of the reaction because it is well known that the gel-type polymerisation always give low yields.
Yield: 12.37 g (41%)
Elemental microanalysis: 92.02% C, 7.59 % H, 0 % N, 0 % Cl.
FT-IR (ν_{max} [cm^{-1}]): 3437, 3025, 2919, 2393, 1943, 1870, 1600, 1492, 1451, 1068,1027, 840, 756, 697, 534.

2.2.4 Synthesis of DVB-co-VBC resins

Poly (DVB-co-VBC)-macroporous low surface area resin (5) (25% VBC loaded)

For the synthesis of this macroporous low surface area resin, the same experimental procedure was used, changing the monomers feed to: DVB (75%, 11.25 g, 12.24 ml) and VBC (25%, 3.75 g, 3.49 ml), AIBN (1% weight comonomers, 0.15 g), and 2-ethylhexanol (1/1 volume ratio weight comonomers, 15.73 ml, 16.89 g) as porogen.
Yield: 10.02 g (67%)
Elemental microanalysis: 84.64 % C, 7.54 % H, 0 % N, 5.19 % Cl.
FT-IR (ν_{max} [cm^{-1}]): 3421, 3022, 2928, 1605, 1448, 1267, 1017, 990, 837, 797, 706, 580.

Poly (DVB-co-VBC)-macroporous high surface area resin (6) (25% VBC loaded)

For the synthesis of this macroporous high surface area resin, the same experimental procedure was used, changing the monomers feed to: DVB (75%, 11.25 g, 12.24 ml) and VBC (25%, 3.75 g, 3.49 ml), AIBN (1% weight comonomers, 0.15g), and toluene (1/1 volume ratio weight comonomers, 15.73 ml, 16.89 g) as porogen.
Yield: 10.94 g (73%)
Elemental microanalysis: 86.96 % C, 7.39 % H, 0 % N, 5.01 % Cl.
FT-IR (ν_{max} [cm^{-1}]): 3446, 3021, 2926, 1603, 1446, 1266, 1017, 989, 833, 795, 704, 576.

Poly (DVB-co-VBC)-macroporous low surface area resin (7) (85% VBC loaded)

For the synthesis of this macroporous low surface area resin, the same experimental procedure was used, changing the monomer feed to: DVB (15%, 2.25 g, 2.44 ml) and VBC (85%, 12.75 g, 11.87 ml), AIBN (1% weight comonomers, 0.15 g), and 2-ethylhexanol (1/1 volume ratio weight comonomers, 14.31 ml, 15.36 g) as porogen.
Yield: 9.5 g (63%)
Elemental microanalysis: 77.97% C, 6.94 % H, 0 % N, 14.50 % Cl.
FT-IR (ν_{max} [cm^{-1}]): 3400, 3052, 3024, 2924, 1606, 1446, 1266, 1093, 796, 705, 606, 540.

2.2.5 Synthesis of DVB-co-VBC-co-styrene resins

These resins were again prepared using the free radical addition suspension polymerisation according to the Sherrington procedure[1] employing the monomers : DVB, VBC and styrene. These resins are destined to be aminated with an appropriate ligand and then complexed with Mo.

Poly (DVB-co-VBC-co-styrene)-macroporous high surface area resin (8) (5%VBC loaded)

The aqueous phase was prepared as described in Section 2.2.2.

The organic phase was prepared by stirring the monomers DVB (75%, 11.25 g, 12.24 ml), VBC (5%, 0.75 g, 0.69 ml) and styrene (20%, 3 g, 3.3 ml), AIBN (1% by weight the comonomers, 0.15 g), and toluene (1/1 by volume ratio of the comonomers, 16.24 ml, 14.047 g) as porogen in a conical flask (250 ml). The resulting organic phase was then added to the reactor and the polymerisation reaction and polymer resin work-up and isolation carried out as described in Section 2.2.2.
Yield: 11.4 g (76%)
Elemental microanalysis: 89.61 %C, 7.77 %H, 0 %N, 0.94 %Cl.

FT-IR (ν_{max} [cm^{-1}]): 3446, 3026, 2928, 1604, 1453, 1263, 1030, 989, 836, 796, 700, 540.

Poly (DVB-co-VBC-co-styrene)-macroporous low surface area resin (9) (5% VBC loaded)

For the synthesis of this macroporous low surface area resin, the same experimental procedure was used, changing the monomer feed to: DVB (12%, 1.8 g, 1.95 ml), VBC (5%, 0.75 g, 0.69 ml) and styrene (83%, 12.45 g, 13.69 ml), AIBN (1% by weight of the comonomers, 0.15 g), and 2-ethylhexanol (1/1 by volume ratio of the comonomers, 16.33 ml, 17.53 g) as porogen.
Yield: 6.7 g (44%)
Elemental microanalysis: 84.6 %C, 7.01 %H, 0 %N, 1.15 %Cl.
FT-IR (ν_{max} [cm^{-1}]): 3446, 3028, 3059, 3025, 2922, 1601, 1493, 1452, 1263, 1028, 757, 697,539.

Poly (DVB-co-VBC-co-styrene)-macroporous low surface area resin (10) (25% VBC loaded)

For the synthesis of this macroporous low surface area resin, the same experimental procedure was used, changing the monomer feed to: DVB (12%, 1.8 g, 1.95 ml), VBC (25%, 3.75 g, 3.5 ml) and styrene (63%, 9.45 g, 10.39 ml), AIBN (1% by weight of the comonomers, 0.15 g), and 2-ethylhexanol (1/1 by volume ratio of the comonomers, 16.33 ml, 17.53 g) as porogen.
Yield: 6.8 g (45%)
Elemental microanalysis: 86.57%C, 7.38 %H, 0 %N, 4.72 %Cl.
FT-IR (ν_{max} [cm^{-1}]): 3451, 3024, 2918, 1601, 1492, 1451, 1263, 1027, 797, 758, 697, 535.

Poly (DVB-co-VBC)-macroporous low surface area resin (11) (88% VBC loaded)

For the synthesis of this macroporous low surface area resin, the same experimental procedure was used, changing the monomer feed to: DVB (12%, 1.8 g, 1.95 ml) and VBC (88%, 13.2 g, 12.30 ml), AIBN (1% weight comonomers, 0.15 g), and 2-ethylhexanol (1/1 volume ratio weight comonomers, 14.25 ml, 15.36 g) as porogen.
Yield: 7.9 g (53%)
Elemental microanalysis: 73.75% C, 6.05% H, 0% N, 16.45% Cl.
FT-IR (ν_{max} [cm^{-1}]): 3580, 3331, 3023, 2923, 1605, 1487, 1446, 1265, 1092, 1016, 796, 704, 606, 540.

2.2.6 Synthesis of polymeric ligands derived from precursor chloromethylated polystyrene resin (88% VBC loaded) (11)

2.2.6.1 Functionalisation of poly(DVB-co-VBC)-macroporous low surface area resin (88% VBC loaded) (11) with 2-(aminomethyl)-pyridine (AMP) to yield Ps.AMP (16)

2-(Aminomethyl)-pyridine (AMP) was used directly to derivatise the poly(DVB-co-VBC)-macroporous low surface area resin (11). The polymer resin was reacted with an excess of 2-aminomethylpyridine in the mole ratio resin / ligand = 1/ 4 as shown in Scheme 2.1.

Synthesis of Ps.AMP (16)

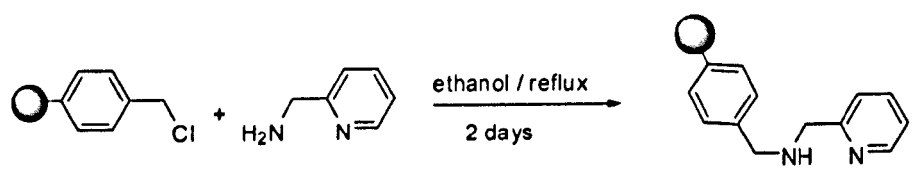

(11) Ps.AMP (16)

Scheme 2.1 Amination of resin (11) with AMP.

Chloromethylated polystyrene resin (**11**) (6 g, 27.8 mmol of $-CH_2Cl$) was heated under reflux with excess 2-aminomethylpyridine (12.05 g, 11.5 ml, 111.2 mmol of AMP) in ethanol (100 ml) for 48 h. After this the beads were filtered off, washed with acetone/water, and then stirred gently overnight in pyridine. The beads were filtered off and washed successively with water, water/methanol and acetone. Finally, they were extracted overnight in a Soxhlet apparatus with acetone before being dried in vacuum oven at 40°C.

Elemental microanalysis : 81.40% C, 5.78% H, 6.46% N, 1.80 %Cl.

FT-IR (ν_{max} [cm^{-1}]): 3453, 3019, 2925, 1634, 1435, 1383, 1118, 1048, 793, 758, 706, 614.

2.2.6.2 Functionalisation of poly(DVB-co-VBC)-macroporous low surface area resin (88% VBC loaded) (11) with 2-aminophenol (2-AMPH) to yield Ps.2-AMPH (17)

Synthesis of Ps.2-AMPH (17)

This ligand was attached to poly(DVB-co-VBC)-macroporous resin in order to produce an aminophenol functionality bonded to the polymer. An excess of 2-aminophenol was reacted with the polymer in mole ratio resin/ ligand 1/4 as shown in Scheme 2.2.

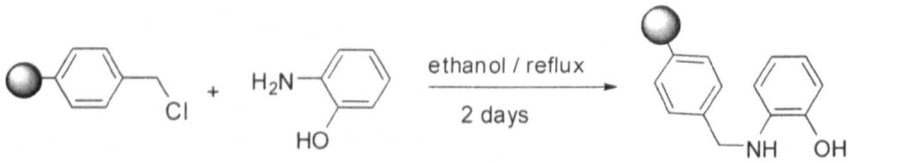

(11) **Ps.2-AMPH (17)**

Scheme 2.2 *Functionalisation of resin (8) with 2-AMPH*

The same experimental procedure was used. Chloromethylated polystyrene resin (**11**) (5 g, 22.3 mmol of $-CH_2Cl$) was heated under reflux with 2-aminophenol (9.73 g, 89.2 mmol of 2-AMPH) in ethanol (80 ml).

Elemental microanalysis : 81.06% C, 7.25% H, 2.90% N, 3.19% Cl.

FT-IR (ν_{max} [cm^{-1}]): 3367, 3023, 2925, 1607, 1511, 1490, 1376, 1249, 1113, 1017, 900, 794, 746, 705.

2.2.6.3 Functionalisation of poly(DVB-co-VBC)-macroporous low surface area resin (88% VBC loaded) (11) with glycine (GLYC) to yield Ps.GLYC (18)

This ligand was attached to the polymer macroporous resin in order to generate an aminocarboxylic acid functionality bonded to the polymer. An excess of glycine was reacted with the polymer in mole ratio resin/ligand 1/4 (Scheme 2.3).

Synthesis of Ps.GLYC (18)

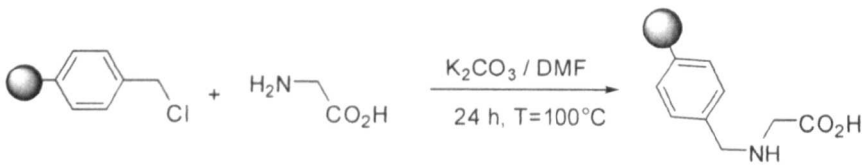

(11) **Ps.GLYC (18)**

Scheme 2.3 *Functionalisation of resin (8) with GLYC*

Chloromethylated polystyrene resin (11) (4 g, 18.58 mmol of $-CH_2Cl$) was heated at 100°C with glycine (5.6 g, 74.32 mmol of GLYC) and an excess of potassium carbonate (20.5 g, 148.6 mmol) in DMF (160 ml) for 24 h. After this the beads were filtered off and washed exhaustively with distilled water. Finally, they were extracted overnight in a Soxhlet apparatus with THF before being dried in vacuum oven at 40°C.

Elemental microanalysis : 72.26% C, 7.21% H, 2.86% N, 0.19% Cl.

FT-IR (ν_{max} [cm^{-1}]): 3405, 3019, 2927, 1739, 1608, 1450, 1379, 1185, 1017, 796, 706.

2.2.6.4 Functionalisation of poly(DVB-co-VBC)-macroporous low surface area resin (88% VBC loaded) (11) with iminodiacetic acid (IMDA) to yield Ps.IMDA (19)

This ligand was attached to the polymer macorporous resin in order to generate an aminodicarboxylic acid functionality bonded to the polymer. An excess of iminodiacetic acid was reacted with the polymer in mole ratio resin/ligand 1/4 (Scheme 2.4) .

Synthesis of Ps.IMDA (11)

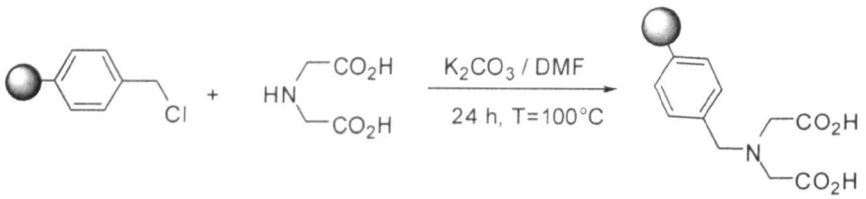

(11) **Ps.IMDA (11)**

Scheme 2.4 *Functionalisation of resin (11) with IMDA.*

Chloromethylated polystyrene resin (**11**) (6 g, 28.32 mmol of $-CH_2Cl$) was heated at 100°C with iminodiacetic acid (15.07 g, 113.28 mmol of IMDA) and an excess of potassium carbonate (31.3 g, 226.6 mmol) in DMF (200 ml) for 24 h. After this the beads were filtered off and washed exhaustively with distilled water. Finally, they were extracted overnight in a Soxhlet apparatus with THF before being dried in vacuum oven at 40°C.

Elemental microanalysis : 70.38% C, 6.84% H, 2.10% N, 3.86% Cl.

FT-IR (ν_{max} [cm^{-1}]): 3410, 3024, 2927, 1742, 1682, 1487, 1449, 1382, 1267, 1181, 798, 707, 579.

2.2.7 Synthesis of poly(4-aminomethyl styrene) resin (12) from poly(DVB-co-VBC)-macroporous low surface area resin (88% VBC loaded) (11)

The Gabriel's procedure[2, 3] was used to transform the chloride functionality contained in the poly(DVB-co-VBC)-macroporous low surface area resin to an amine functionality in a two step reaction as shown in Scheme 2.5.

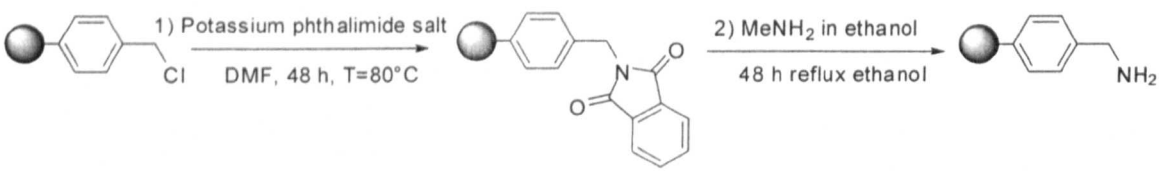

(11) **(12)**

Scheme 2.5 *Synthesis of the poly(4-aminomethyl styrene) resin (12)*

In the first reaction step, chloromethylated polystyrene resin (**11**) (5 g, 21.32 mmol of CH_2Cl) was heated at 80°C with excess potassium phthalimide (15.7 g, 85.1 mmol) in DMF (150 ml) for 48 h. After this the beads were filtered off, washed with 0.2 M of NaOH solution, washed exhaustively with distilled water. Finally, they were extracted overnight in a Soxhlet apparatus with THF before being dried in vacuum oven at 40°C.
Elemental microanalysis : 76.11% C, 5.41% H, 3.83% N, 1.58% Cl.
FT-IR (ν_{max} [cm^{-1}]): 3433, 3025, 2923, 1772, 1711, 1607, 1467, 1429, 1392, 1187, 1085, 953, 793, 710, 528.

The second step, which is the deprotection of the amine, was carried out by refluxing the polymer-phthalimide (6 g, 16.6 mmol) with 33% $MeNH_2$ in ethanol (80 ml, 38.6 mmol) in ethanol for 48 h. Then the beads were filtered off and washed exhaustively with distilled water. Finally, they were extracted overnight in Soxhlet apparatus with THF before being dried in vacuum oven at 40°C.
Elemental microanalysis : 78.25% C, 6.79 % H, 5.17% N, 0.68 % Cl.
FT-IR (ν_{max} [cm^{-1}]): 3370, 3022, 2924, 1771, 1714, 1655, 1541, 1444, 1393, 1187, 1085, 954, 792, 704, 528.

2.2.7.1 Functionalisation of poly(4-aminomethyl styrene)-macroporous low surface area resin (12) with ethylenediaminetetraacetic acid (EDTA) to yield Ps.EDTA (20)

This ligand was attached to the polymer via a selective monoamidation according to Supuran's procedure[4, 5] by reacting the poly(4-aminomethyl styrene) resin (**12**) with ethylenediaminetetraacetic acid (EDTA) in a molar ratio resin:ligand 1: 1 (Scheme 2.6).

Synthesis of Ps.EDTA (20)

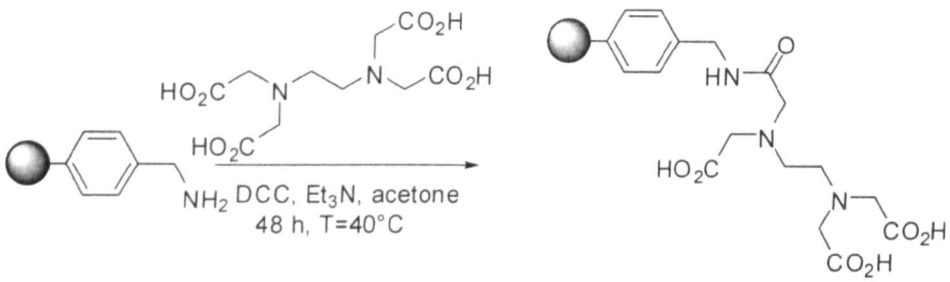

(12) **Ps.EDTA (20)**

Scheme 2.6 *Functionalisation of poly(4-aminomethyl styrene) resin* ***(12)*** *with EDTA.*

Poly(4-amino methyl styrene) resin (**12**) (3 g, 11.1 mmol of amine) was heated at 40°C with the same molar amount of ethylenediaminetetraacetic acid (EDTA) (3.23 g, 11.1 mmol of EDTA) and dicyclohexylcarbiimide (DCC) (2.3 g, 11.1 mmol) in anhydrous acetone (110 ml) for 1 h. Then triethylamine (TEA) (2.24 g, 3 ml, 22.2 mmol) was added and the mixture was left stirring for 48 h. After this the beads were filtered off, washed exhaustively with distilled water until pH = 7. Finally, they were extracted overnight in a Soxhlet apparatus with acetone before being dried in vacuum oven at 40°C.

Elemental microanalysis : 73.05% C, 7.13 % H, 6.77% N, 0.14 % Cl.

FT-IR (ν_{max} [cm^{-1}]): 3327, 3020, 2928, 2850, 1771, 1716, 1625, 1534, 1436, 1394, 1311, 1243, 1088, 794, 707, 640, 530.

2.2.7.2 Functionalisation of poly(4-aminomethyl styrene)-macroporous low surface area resin (12) with glycine (GLYC)

The iminoacetic acid functionality was generated by reacting the poly(4-aminomethyl styrene) resin (**12**) with 1 mole of chloroacetic acid in presence of excess of sodium hydroxide according to Blatt's procedure[6] (Scheme 2.7).

Synthesis of Ps.GLYC (18)

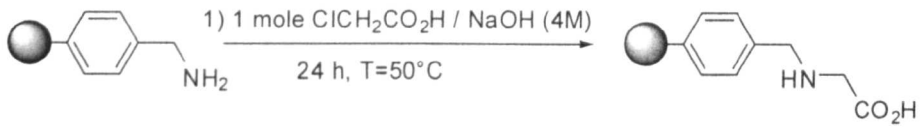

(12) **Ps.GLYC (18)**

Scheme 2.7 *Alkylation of poly(4-aminomethyl styrene) resin* ***(12)*** *with chloroacetic acid.*

Elemental microanalysis : 77% C, 7.08% H, 4.89% N, 0.17% Cl

FT-IR (ν_{max} [cm^{-1}]): 3631, 3261, 3022, 2923, 1770, 1716, 1643, 1557, 1444, 1377, 1307, 1088, 1016, 898, 794, 705, 648, 566.

Note. This version of Ps.GLYC **(18)** was not taken further in forming a Mo complex

2.2.7.3 Functionalisation of poly(4-aminomethyl styrene)-macroporous low surface area resin (12) with glycine (GLYC) or iminodiacetic acid (IMDA)

The iminodiacetic acid functionality was generated by reacting the poly(4-aminomethyl styrene) resin **(12)** with 2 moles of chloroacetic acid in presence of excess of sodium hydroxide according to the Blatt's procedure[6] (Scheme 2.8).

Synthesis of Ps.IMDA (19)

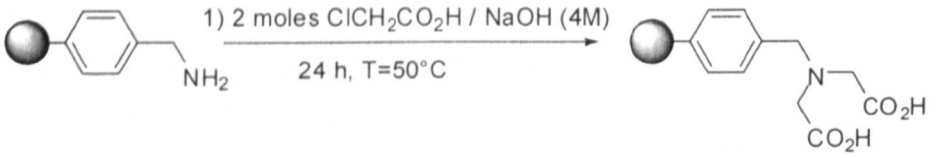

(12) **Ps.IMDA (19)**

Scheme 2.8 *Double alkylation of poly(4-aminomethyl styrene) resin* ***(12)*** *with chloroacetic acid.*

Elemental microanalysis :76.01% C, 7.25 % H, 4.92% N, 0.19 % Cl.

FT-IR (ν_{max} [cm^{-1}]): 3022, 2918, 1771, 1717, 1640, 1558, 1444, 1379 1309, 1166, 1088, 795, 705, 648, 562.

Note. This version of Ps.IMDA (**19**) was not taken further in forming a Mo complex.

2.2.8 Synthesis of (L)-phenylalanine methyl ester

Methyl esterification of (L)-phenylalanine was carried out in the presence of thionyl chloride and dried methanol according to Wang's procedure[7].

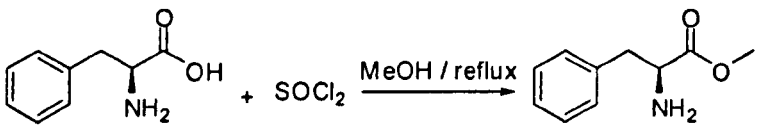

Scheme 2.9 Methyl esterification of (L)-phenylalanine

To a solution of (L)-phenylalanine (5 g, 30 mmol), in 150 ml dried methanol was added dropwise thionyl chloride (17.85 g, 150 mmol) at -30°C. After warming up to room temperature, the reaction mixture was refluxed for 2h. The organic solvent was concentrated under reduced pressure, and then the residue was treated with ammonium hydroxide into pH 9.0. The mixture was extracted three times with Et_2O. The combined organic layers were washed with little saturated NaCl, dried over anhydrous Na_2SO_4 and concentrated under reduced pressure, to obtain 4.88g, 92% yield.

$[\alpha]_D$ +29.45° (c 4.04 g/ 100 ml, CH_3CH_2OH; 20°C).

^1H NMR (500MHz, $CDCl_3$, δ (ppm)): 7.16-7.30 (m, 5H, Ph-H), 3.72 (m, CHN,J= 5.2 Hz), 3.69 (s, CH_3), 3.08-3.05 (dd, 1H, PhCH, J= 10 Hz), 2.85-2.82 (dd, 1H, PhCH, J= 10 Hz), 1.45 (s, 2H, NH_2).

13C NMR (500MHz, $CDCl_3$, δ (ppm)): 41. 12 ($PhCH_2$), 51.91(CH_3O), 55.48 (CHN), 126.80, 128.54, 129.26, 137, 27 (Ph), 175.42 (C=O).

Hydrolysis of (L)-phenylalanine methyl ester

Basic hydrolysis of the methyl ester was carried out in the presence of NaOH and in a mixture of THF: H_2O in proportion 1: 2 according to Lawson's procedure[8]

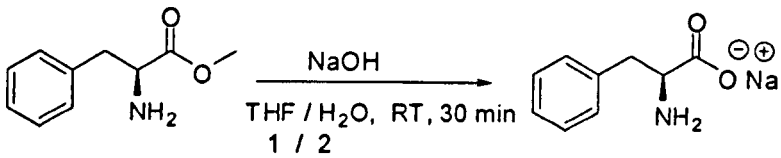

Scheme 2.10 Hydrolysis of (L)-phenylalanine methyl ester

A 50 mL round-bottomed flask containing (L)-phenylalanine methyl ester (0.1 g, 0.5 mmol) and tetrahydrofuran (5 ml) was treated with a solution of NaOH (0.02 g, 0.6 mmol) in water (10 ml). The mixture was stirred at room temperature for 30 min and was concentrated under reduced pressure to give the corresponding sodium salt.

$[\alpha]_D$ +19.8° (c 1 g/ 100 ml, H_2O; 20°C).

^1H NMR (500MHz, DMSO, δ (ppm)): 7.25-7.13 (m, 5H, Ph-H), 3.35 (m, CHN,J= 5.2 Hz), 3.09-3.07 (dd, 1H, PhCH, J= 10 Hz), 3.04-3.02 (dd, 1H, PhCH, J= 10 Hz), 1.3 (s, 2H, NH_2).

^{13}C NMR (500MHz, DMSO, δ (ppm)): 41. 12 ($PhCH_2$), 57.58 (CHN), 125.36, 127.80, 129.20, 141,18 (Ph), 178.16 (C=O).

2.2.9 Functionalisation of poly(DVB-co-VBC)-macroporous low surface area resin (88% VBC loaded) (11) with (L)-phenylalanine methyl ester to yield Ps.Phe (22)

Synthesis of Ps.Phe (12)

The (L)-phenylalanine methyl ester (Phe) ligand was attached to poly(DVB-co-VBC)-macroporous resin (11) in order to produce an amine functionality bonded to the polymer. An excess of (L)-phenylalanine methyl ester was reacted with the polymer in mole ratio resin/ ligand 1/3 as shown in Scheme 2.11.

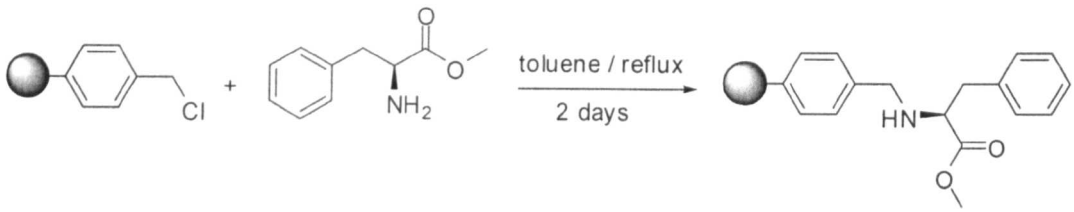

Scheme 2.11 *Amination of resin (11) with (L)-phenylalanine methyl ester*

Chloromethylated polystyrene resin (**11**) (3 g, 14.6 mmol of $-CH_2Cl$) was heated under reflux with excess (L)-phenylalanine methyl ester (7.85 g, 43.75 mmol of Phe) in dried toluene (60 ml) for 48 h *without stirring*. After this the beads were filtered off, washed with THF. Finally, they were extracted overnight in a Soxhlet apparatus with THF before being dried in vacuum oven at 40°C.

Elemental microanalysis: 77.96% C, 6.92% H, 4.09% N, 3.22% Cl

FT-IR (ν_{max} [cm^{-1}]): 3450, 3319, 3203, 3028, 2926, 1734, 1676, 1658, 1604, 1586, 1510, 1488, 1454, 1338, 1267, 1211, 1198, 1092, 1016, 899, 795, 756, 700, 581, 482, 443.

Hydrolysis of methyl ester of Ps.Phe (22)

The basic hydrolysis of the methyl ester was carried out in the presence of NaOH and in a mixture of THF: H_2O in proportion 1: 2 according to Lawson's procedure[8].

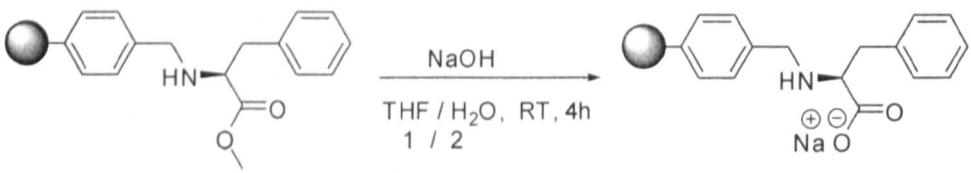

Scheme 2.12 *Hydrolysis of methyl ester of polymer Ps.Phe*

A 100 mL round-bottomed flask containing polymer methyl ester (2 g, 5 mmol) and tetrahydrofuran (20 ml) was treated with a solution of NaOH (0.2 g, 5 mmol) in water (40 ml). The mixture was stirred at room temperature for 4 h and then beads were filtered off and dried under vacuum 40°C.

Elemental microanalysis: 77.84% C, 6.56% H, 4.20% N, 2.57% Cl

FT-IR (ν_{max} [cm^{-1}]): 3203, 3028, 2926, 1735, 1672, 1661, 1604, 1496, 1460, 1338, 1268, 1211, 1092, 1016, 899, 798, 756, 700, 581, 482, 443.

2.2.9.1 Functionalisation of poly(DVB-co-VBC)-macroporous low surface area resin (88% VBC loaded) (11) with 2,4-dihydroxybenzaldehyde

The 2,4-dihydroxybenzaldehyde ligand was attached to the poly(DVB-co-VBC)- resin (**11**) in presence of excess of sodium hydroxide and tetrabutylammonium iodide

Synthesis of functionalised Ps (11)

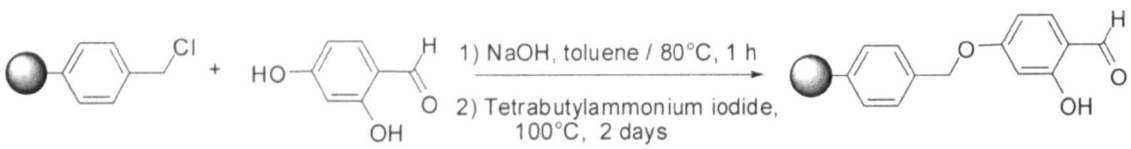

Scheme 2.13 *Functionalisation of poly(DVB-co-VBC) resin (11) with 2,4-dihydroxybenzaldehyde*

A 250 mL round-bottomed flask three necks containing chloromethylated polystyrene resin (**11**) (3 g, 14.6 mmol of $-CH_2Cl$), 2,4-dihydroxybenzaldehyde (6 g, 43.75 mmol), ground NaOH (1.75 g, 43.75 mmol) and dried toluene (100 ml) was heated and stirred at 80°C for 1 h. Then tetrabutylammonium iodide (5.4 g, 14.6 mmol) was added and temperature was raised to 100 °C for 48 h. Then beads were filtered off and washed successively with water, THF and then soxhlet overnight with THF and dried under vacuum 40°C.

Elemental microanalysis: 75.60% C, 5.94% H, 0% N, 1.96% Cl

FT-IR (ν_{max} [cm^{-1}]): 3443, 3024, 2924, 2853, 1678, 1629, 1600, 1577, 1505, 1446, 1371, 1335, 1290, 1258, 1225, 1166, 1133, 1115, 1013, 892, 793, 704, 650, 612, 545, 459.

2.2.9.1.2 Imination of functionalised poly(DVB-co-VBC)-2,4-dihydroxybenzaldehyde resin with (L)-phenylalanine methyl ester to yield Ps.Schiff Base (Ps.SB (23))

Synthesis of Ps.Schiff Base (Ps.SB (23))

The (L)-phenylalanine methyl ester (Phe) ligand was attached to functionalised poly(DVB-co-VBC)-2,4-dihydroxybenzaldehyde in order to produce an imine functionality bonded to the polymer. An excess of (L)-phenylalanine methyl ester was reacted with the polymer in mole ratio resin/ ligand 1/4 as shown in Scheme 2.14.

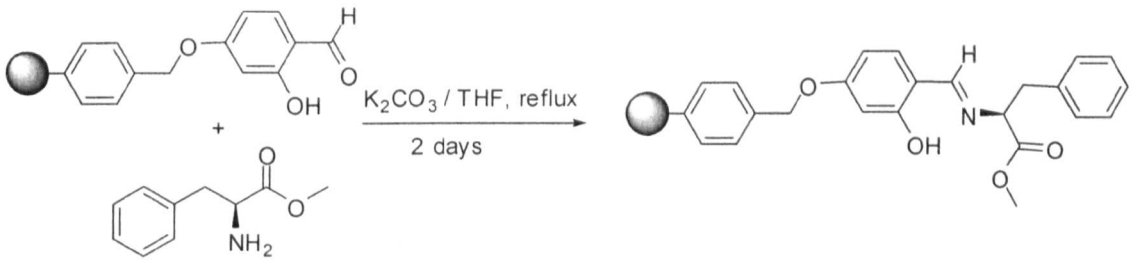

Scheme 2.14 *Imination of functionalised of poly(DVB-co-VBC)- 2,4-dihydroxybenzaldehyde*

A 250 mL round-bottomed three necked flask containing functionalised poly(DVB-co-VBC)-2,4-dihydroxylbenzaldehyde (2 g, 7.2 mmol), (L)-phenylalanine methyl ester (5.2 g, 28.8 mmol), potassium carbonate(1 g, 7.2 mmol) and dried THF (100 ml) was refluxed and stirred for 48 h. Then beads were filtered off and washed successively with water, THF and then extracted in a Soxhlet overnight with THF and dried under vacuum 40°C.
Elemental microanalysis: 76.42% C, 5.96% H, 1.74% N, 0.28% Cl
FT-IR (ν_{max} [cm^{-1}]): 3419, 3027, 2924, 1743, 1654, 1626, 1511, 1444, 1381, 1335, 1223, 1170, 1134, 1115, 1017, 892, 795, 703, 647, 548, 464.

Hydrolysis of Ps.Schiff Base (Ps.SB (23))

The basic hydrolysis of the methyl ester of polymer Ps.Schiff Base (Ps.SB) was carried out in the presence of NaOH and in a mixture of THF: H_2O in proportion 1: 2 according to Lawson's procedure[8].

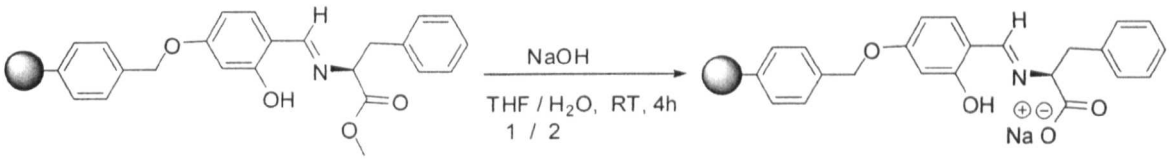

Scheme 2.15 *Hydrolysis of methyl ester of polymer Ps.SB* ***(23)***

Elemental microanalysis: 75.63% C, 6.3% H, 1.63% N, 0.28% Cl

FT-IR (ν_{max} [cm^{-1}]): 3027, 2933, 1741, 1678, 1626, 1602, 1509, 1444, 1288, 1225, 1169, 1134, 1116, 1016, 796, 703.

2.3 Synthesis of precursor inorganic MCM-41 supports

2.3.1 Synthesis of pure silica MCM-41

The MCM-41 inorganic support was supplied by our collaborator in Spain. However a typical synthesis of MCM-41 used in the synthesis was according to Lin's procedure[9] (Scheme 2.16).

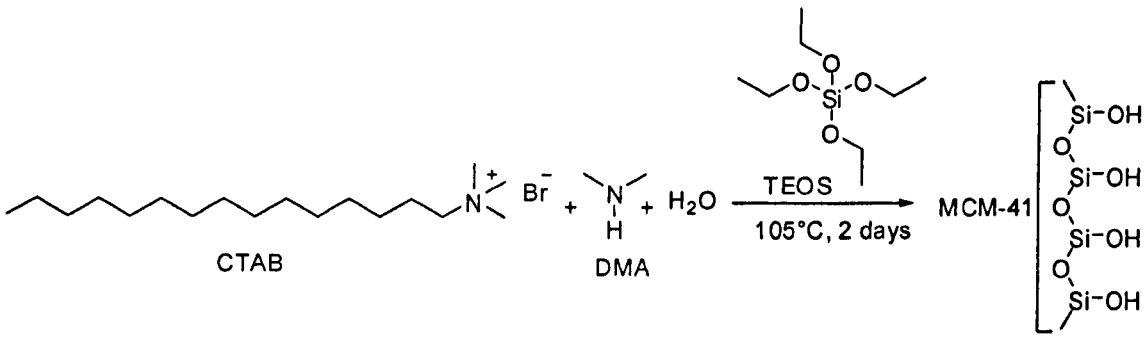

Scheme 2.16 Synthesis of MCM-41

Cetyltrimethylammonium bromide (CTAB) (2.4 g) was dissolved in distilled water (90.4 g) and dimethylamine (DMA) (7.4 g.) The mixture was stirred at room temperature until CTAB is completely dissolved (transparent solution). Then tetraethoxysilane (TEOS) (9.3 g) was added drop by drop. The resulting mixture was stirred for a further 4 h and was then loaded into an autoclave for 48 h at 105°C. After cooling down to room temperature, the product was recovered by filtration, washed with distilled water and dried at room temperature for 24h. The final product was calcined up to 550°C (heating rate = 1.8°C/min) in order to remove the surfactant hence yielding the mesoporous material.

Elemental microanalysis: 0.0% C, 0.45 % H, 0.0% N, 0.0 % S.

FT-IR (ν_{max} [cm^{-1}]): 3525, 3410, 1696, 1629, 1239, 1068, 1169, 806, 570, 453.

2.3.1.1 Synthesis of amine-functionalised MCM-41

3-Aminopropyl-trimethoxysilane (APTMS) was attached to calcined MCM-41 as shown in Scheme 2.17. Again this was carried out by our Spanish collaborator.

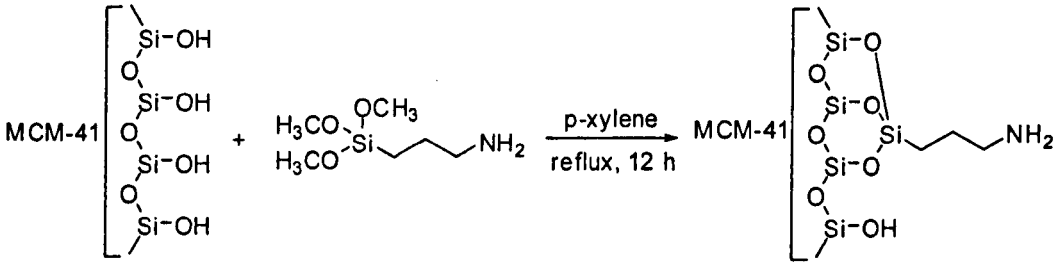

Scheme 2.17 Amine-functionalisation of MCM-41

The calcined MCM-41 support was further dried by azeotropic distillation in p-xylene for several hours. The suspension was cooled at room temperature, and 3-aminopropyl-trimethoxysilane (15% molar with regards to silica) was added and the mixture stirred for 1 h to allow the diffusion of ligand to the inside of the porous structure. Then the resulting mixture was refluxed overnight. The product was recovered by filtration and washed in a Soxhlet extraction with dried toluene for 2 h. The off-white solid was finally dried under high vacuum at 110°C overnight.

Elemental microanalysis: 13.66% C, 3.59 % H, 2.51% N, 0.0 % S

FT-IR (ν_{max} [cm^{-1}]): 3435, 2974, 1227, 1085, 1169, 797, 693, 551, 451.

2.3.1.2 Synthesis of Schiff base grafted MCM-41, (MCM-41-SB) (21)

The Schiff base grafted MCM-41-was synthesised at Strathclyde as shown in Scheme 2.18.

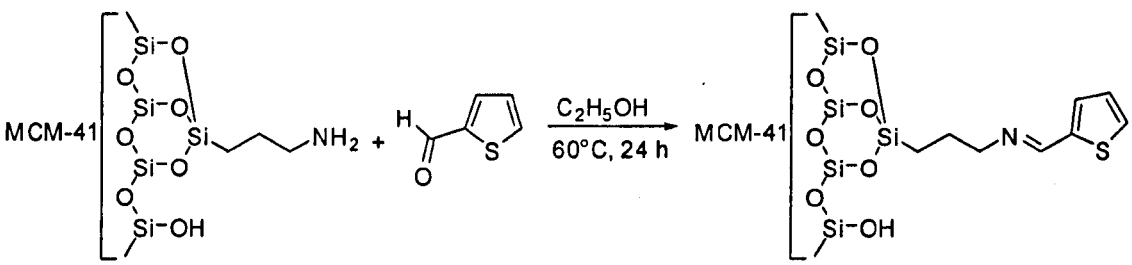

***Scheme 2.18** Synthesis of MCM-41.SB (21)*

A 250 mL round-bottomed three necked flask containing a solution of thiophene-2-carboxyaldehyde (0.56 g, 0.46 ml. 5 mmol) in absolute ethanol, functionalised amino-MCM-41 (2 g, 3.58 mmol of amine) was added and stirred at 60°C for 24 h. Then the brown light solid was filtered off and washed with ethanol and dried under vacuum oven 40°C.

Elemental microanalysis: 17.67% C, 2.58 % H, 2.82% N, 2.14 % S.

FT-IR (ν_{max} [cm^{-1}]): 2939, 2892, 1638, 1524, 1432, 1239, 1082, 858, 576, 460.

2.4 Preparation of Polymer-supported Mo Complexes

All supported Mo complexes were prepared using a ligand exchange procedure in which the resins were reacted with $MoO_2(acac)_2$ in the stoichiometric ratio 2 / 1 $MoO_2(acac)_2$: functional ligand as illustrated for PBI in Scheme 2.19.

Preparation of PBI.Mo

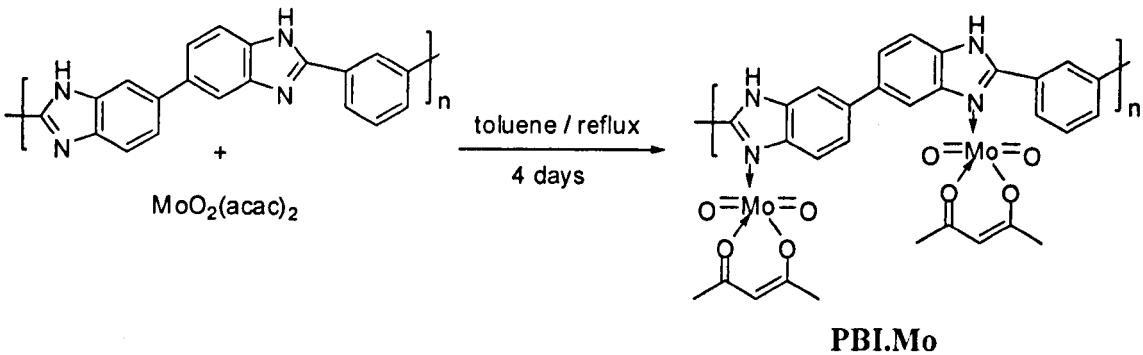

Scheme 2.19 Loading of Mo (VI) complex onto PBI resin.

A typical procedure for the synthesis of PBI.Mo metal complex was as follows: PBI resin (5.00g, 0.027 mol imidazole group) was refluxed with $MoO_2(acac)_2$ (17.68g, 0.054 mol Mo) in anhydrous toluene for a period of 4 days. Stirring was with an overhead mechanical device in order to prevent attrition of the resin beads. The resin changed colour from brown to green during this period, and then it was filtered off and extracted exhaustively with acetone in a Soxhlet apparatus for 48 h. During extraction a dark-blue colour was evident in the extracting solution. This disappeared eventually upon repeated introduction of fresh solvent. The supported complex was then dried under vacuum oven at 40°C.

Preparation of Ps.AMP.Mo

Using the same procedure again as described above, the resin changed colour from mauve to blue over 4 days, and the beads were dried under vacuum oven at 40°C (Scheme 2.20).

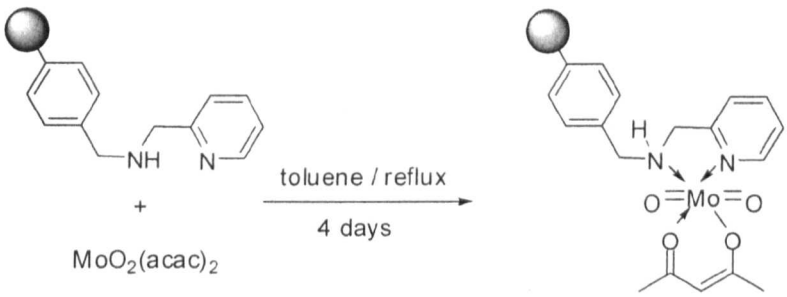

Ps.AMP.Mo

Scheme 2.20 *Loading of AMP loaded resins with Mo (VI) complex.*

Preparation of Ps.2-AMPH.Mo (28)

Using the same procedure again as described above, the resin changed colour from mauve to brown over 4 days, and the beads were dried under vacuum oven at 40°C (Scheme 2.21).

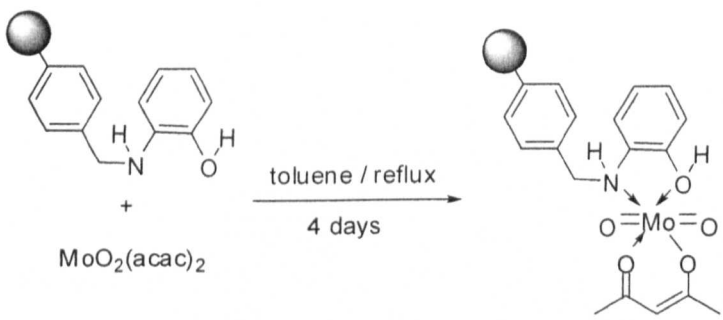

Ps.2-AMPH.Mo (28)

Scheme 2.21 *Loading of 2-AMPH loaded resins with Mo (VI) complex.*

Preparation of Ps.GLYC.Mo (29)

Using the same procedure again, the resin changed colour from mauve to green over 4 days, and the beads were dried under vacuum oven at 40°C (Scheme 2.22).

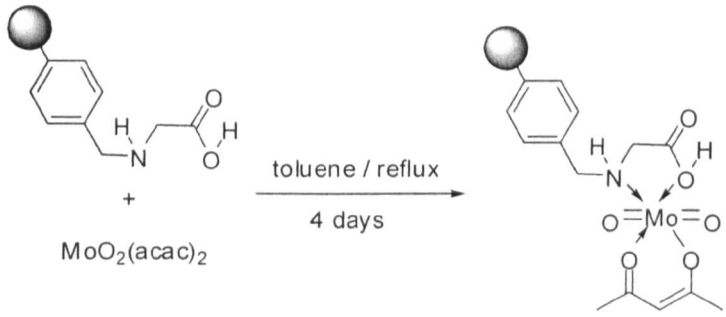

Ps.GLYC.Mo (29)

Scheme 2.22 *Loading of GLYC loaded resins with Mo (VI) complex.*

Preparation of Ps.IMDA.Mo (30)

Using the same procedure again, the resin changed colour from mauve to blue over 4 days, and the beads were dried under vacuum oven at 40°C (Scheme 2.23).

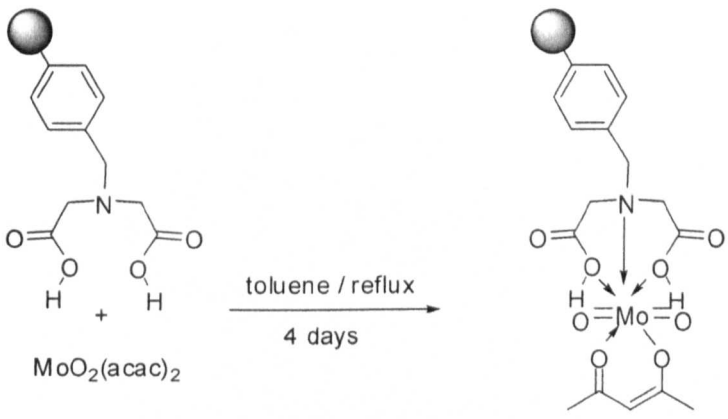

Ps.IMDA.Mo (30)

Scheme 2.23 *Loading of IMDA loaded resins with Mo (VI) complex.*

Preparation of Ps.EDTA.Mo (31)

Using the same procedure again, the resin changed colour from mauve to grey over 4 days, and the beads were dried under vacuum oven at 40°C (Scheme 2.24).

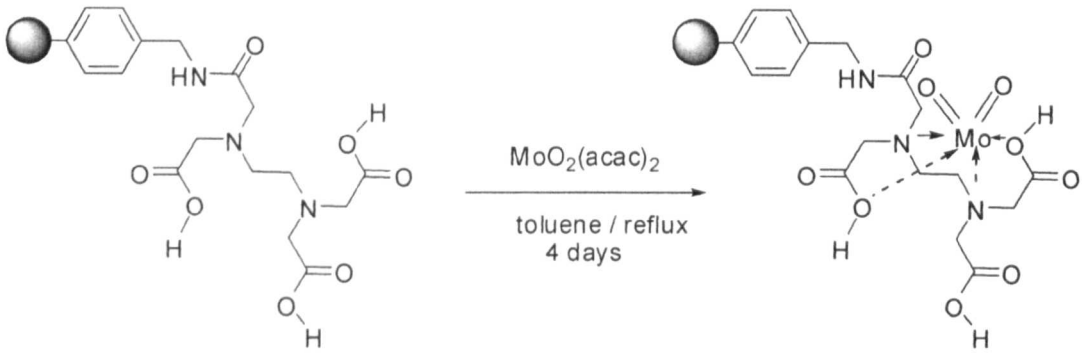

Ps.EDTA (20) **Ps.EDTA.Mo (31)**

Scheme 2.24 *Loading of EDTA loaded resins with Mo (VI) complex.*

Preparation of Ps.Phe.Mo (33)

Using the same procedure again, the resin changed colour from yellow to brown over 4 days, and the beads were dried under vacuum oven at 40°C (Scheme 2.25).

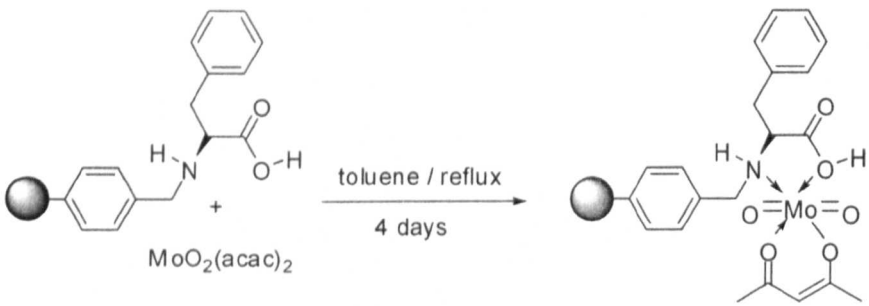

Ps.Phe.Mo (33)

Scheme 2.25 *Loading of Phe loaded resins with Mo (VI) complex.*

Preparation of Ps.SB.Mo (34)

Using the same procedure again, the resin changed colour from yellow to green over 4 days, and the beads were dried under vacuum oven at 40°C (Scheme 2.26).

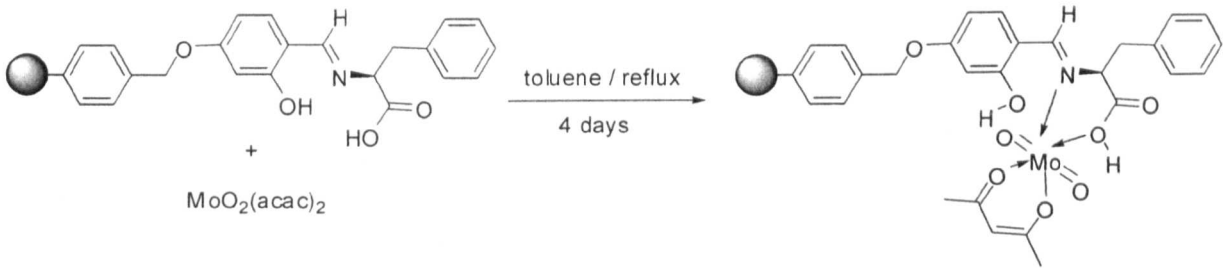

Ps.SB.Mo (34)

Scheme 2.26 *Loading of SB loaded resins with Mo (VI) complex*

2.5 Preparation of inorganic MCM-41.SB Supported Mo Complexes

Preparation of MCM-41.SB.Mo (32)

A typical synthesis of MCM-41.SB.Mo used here, was slightly different to the other complexes synthesised previously (Scheme 2.27).

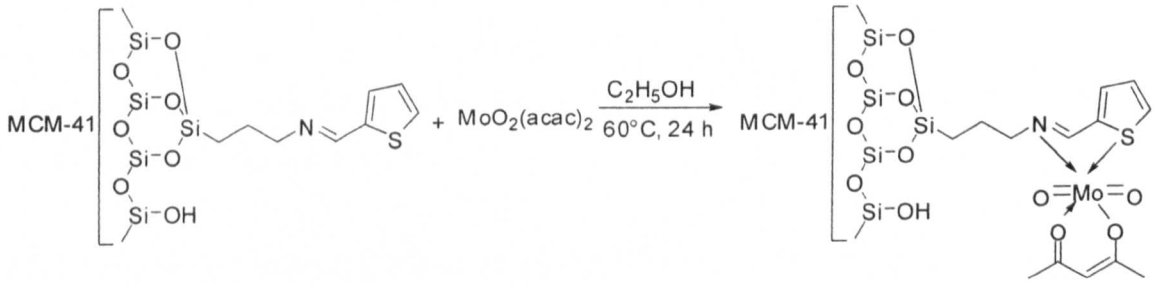

Scheme 2.27 *Loading of MCM-41.SB loaded resins with Mo (VI) complex*

A mixture of $MoO_2(acac)_2$ (2.25 g, 6,8 mmol)and MCM-41.SB (1.5 g, 3,44 mmol of imine) in absolute ethanol (100 ml) was heated at 60°C for 24 h. The supported complex was filtered, washed successively with ethanol and acetone, and the resulting green catalyst was dried under vacuum oven at 40°C.

2.6 Metal analysis of supported metal complexes

Each supported complex (~0.1 g) was ground to a fine powder, then digested for 3 days in aqua regia (15 ml). The resulting mixture was diluted to 100 ml with distilled water, and the metal content was assayed using standard atomic absorption spectrophotometric methods. The results obtained are shown in Table 3.

2.6.1 Atomic Absorption Spectrophotometry

From a standard molybdenum solution (1000 mg Mo. l^{-1}) supplied by Aldrich, the other standard solutions(0, 50, 100, 200 mg Mo.l^{-1}) were made by diluting an accurate amount of the standard (0 ml, 0.5 ml, 1 ml, 2 ml) with distilled water in an appropriate conical flask (10 ml). These standard solutions and the unknown samples solution were then introduced into the spectrometer and their absorbance readings were noted.

2.7 Oxygen atom source

An anhydrous solution of tert-butyl hydroperoxide (TBHP) in toluene was used exclusively in this work because its offers better thermal and storage stability than other varieties of organic oxygenations.

2.7.1 Anhydrous tert-Butyl hydroperoxide (TBHP)

Aqueous TBHP-70 (65 ml) and toluene (80 ml) were added to a 250 ml separating funnel and swirled for three minutes. The aqueous layer (15 ml) was removed and the organic

layer (130 ml) was drained into a 250 ml round bottomed flask equipped with a Dean-Stark trap and reflux condenser. Boiling stones were added and the solution was refluxed using a hot plate. After about 1 hour, 4 ml of water was collected in the side arm. A further 4 ml of distillate was removed through the side arm. The remaining solution (122 ml) of anhydrous TBHP was cooled down at the room temperature, and stored over 4 A° molecular sieves at room temperature.

2.7.2 Molarity of TBHP[10]

The accurate molarity of each TBHP solution was determined as follows: glacial acetic acid (2 ml) and isopropanol (25 ml) were placed in a 250 ml conical flask. The mixture was stirred and 10 ml of a freshly prepared solution of sodium iodide in isopropanol* (* NaI (22 g) in isopropanol (100 ml)-mixture was refluxed, cooled and filtered) was added followed by exactly 1 ml of the anhydrous TBHP solution. The mixture was then refluxed gently for 30 seconds. After dilution with distilled water (100 ml), the mixture was immediately titrated with 0.1 M sodium thiosulphate solution until the yellow iodine colour disappeared using starch indicator to enhance the end point in the usual way.

The molarity was calculated according to the following equation:

$M = (S \times M') / (2 \times \text{ml of sample})$ where

M = molarity of TBHP

S = ml of sodium thiosulphate solution

M' = molarity of sodium thiosulphate solution

2.8 Catalyst activation

When required, the polymer-supported Mo complex was activated before use in epoxidation reactions using the following procedure. An exact weight of each supported Mo complex (0.06 mmol Mo) was heated to reflux with anhydrous TBHP (1.4-1.5 ml, 5

mmol) in 1,2-dichloroethane (10-20 ml) for a given period. During this period of activation the colour of all the supported complexes changed to yellow. After completion the beads were filtered off, washed with 1,2-dichloroethane, and used immediately in a reaction or were stored in TBHP (1.4-1.5 ml, 5 mmol) and 1,2-dichloroethane (10 ml).

2.9 Catalytic epoxidation reactions

The reactions studied in this work, are the conversion of cyclohexene and styrene to cyclohexene oxide and styrene oxide respectively using homogenous or supported Mo complexes with TBHP as the oxygen source. The reactions were monitored by analysing the reaction mixtures for cyclohexene oxide product using ^{1}H NMR spectroscopy.

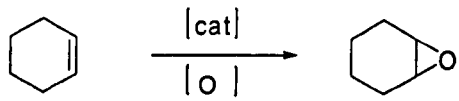

or

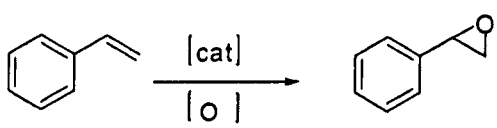

where [cat] is a homogenous or supported Mo catalyst, and [O] is an oxygen source exclusively the use of tert-butyl hydroperoxide (TBHP) for many reasons such as its selectivity, safety and stability.

Two different reaction conditions were employed in the case of cyclohexene epoxidation. The first was selected as fairly representative of large scale or commodity chemical epoxidations. This involves the use of the alkene in large excess over the oxidant, effectively acting as the solvent for the reaction, Such conditions tend to favour selective epoxidation, discourage over oxidation, minimise the risk of violent oxidation and are economically favourable when carried out on a 'large scale'. The second was chosen as

more representative of a 'small scale' or speciality alkene epoxidation. This involves use an alkene : oxidant mole ratio ~ 1: 1 and a diluting solvent. These conditions aim to achieve high conversion of the alkene to epoxide typical of that required in the synthesis of a pharmaceutical precursor or indeed of an epoxidation reaction in a multi-step synthesis of a pharmarceutical product. In the case of styrene epoxidations, the conditions employed were restricted to those of 'small scale' reactions.
Same investigations of the effect of microwave irradiation on epoxidations performed under both type of reaction conditions were also undertaken.

2.9.1 Catalytic epoxidations using an excess of cyclohexene relative to TBHP ('large scale' conditions)

The epoxidation reactions were carried out at 80°C in a three-necked 50 ml round-bottomed flask fitted with a reflux condenser, a mechanical stirrer and a septum cap for withdrawing samples.

A typical epoxidation reaction was carried out as follows: the activated polymer or MCM-41 supported Mo complex (weight corresponding to 0.06 mmol Mo), cyclohexene (8.4 ml, 0.083 mol), bromobenzene (0.5 ml, 5 mmol), and 1,2-dichloroethane (0.2 ml), were charged to a three-necked round-bottomed flask (50 ml) and the temperature was set at 80°C. The reaction was left to equilibrate thermally at 80°C for 20 min, then anhydrous TBHP (1.4-1.6 ml, 5 mmol) was added, and the reaction was heated for a period of 4 hours while the reaction mixture was monitored by ^{1}H NMR spectroscopy.

2.9.2 Catalytic epoxidations using a stoichiometric balance of alkene to TBHP in various solvents ('small scale' conditions)

The epoxidation reactions were also carried out at 80°C in a three-necked 50 ml round-bottomed flask fitted with a reflux condenser, a mechanical stirrer and a septum cap for withdrawing samples.

A typical epoxidation reaction was carried out as follows: the activated polymer or MCM-41 supported Mo complex (weight corresponding to 0.011 mmol Mo), cyclohexene (0.151 ml, 0.0015 mol), bromobenzene (0.16 ml, 0.0015 mol), and 1,2-dichloroethane (4 ml), were charged to a three-necked round-bottomed flask (50 ml) and the temperature was set at 80°C. The reaction was left to equilibrate thermally at 80°C for 20 min, then anhydrous TBHP (0.45-0.47 ml, 0.0015 mol) was added, and the reaction was heated for a period of 4 hours while the reaction mixture was monitored by ^{1}H NMR spectroscopy

2.9.3 Microwave assisted olefin epoxidations

As described in 2.9.1 and 2.9.2 similar investigations of the effect of microwave irradiation on epoxidations performed under both types of reaction conditions ('large scale' and 'small scale'olefin epoxidations) were also carried out.

2.9.4 Asymmetric epoxidation of styrene

Asymmetric styrene epoxidations under 'small scale' reaction conditions were also carried out at - 40°C, room temperature, 40°C and 80°C in a three-necked 50 ml round-bottomed flask fitted with a reflux condenser, a mechanical stirrer and a septum cap for withdrawing samples.

A typical epoxidation reaction was carried out as follows: the activated chiral polymer-supported Mo complex (weight corresponding to 0.011 mmol Mo), styrene (0.172 ml, 0.0015 mol), methoxybenzene (0.16 ml, 0.0015 mol), and 1,2-dichloroethane (4 ml), were charged to a three-necked round-bottomed flask (50 ml) and the temperature was set at 80°C. The reaction was left to equilibrate thermally at 80°C for 20 min, then anhydrous TBHP (0.45-0.47 ml, 0.0015 mol) was added, and the reaction was heated for a period of 4 hours while the reaction mixture was monitored by ^{1}H NMR spectroscopy

2.9.5 ^{1}H NMR spectroscopic analysis

Samples of each reaction mixture were withdrawn and the cyclohexene oxide product quantified from its ^{1}H NMR spectrum. The conversion of cyclohexene was deduced from the following relation between the integrated area of the two peaks due to two hydrogens (δ = 3.15 ppm) in the cyclohexene oxide product and the integrated area of the two peaks due to two hydrogens (δ = 7.59 ppm) in the standard bromobenzene as follows:

$$Conversion = \left[\frac{n_{bromobenzene} \left(\frac{2H\ (\delta = 3.15\ ppm)\ epoxide\ area}{2H\ (\delta = 7.59\ ppm)\ standard\ bromobenzene\ area} \right)}{n_{TBHP}} \right] \text{x } 100$$

2.10 Recycling of polymer-supported Mo catalysts

In order to evaluate the stability of each polymer-supported catalyst and in particular to assess the contribution to catalysis, and to determine the amount of Mo leaching, a given sample of each catalyst was employed in up to 10 consecutive reactions. Following isolation of the catalyst sample via filtration from each catalytic run, the corresponding supernatant solution, potentially containing leached Mo species, was evaporated to dryness. Epoxidation reaction components were added to any residue visible or not and the reaction run as before. This procedure was employed for all polymer-supported Mo catalysts.

2.11 Catalytic epoxidation in Reactive Distillation Column (RDC)

The epoxidation reactions were carried out in a packed RDC as shown in Scheme 2.28 at *Loughborough University*. The RDC consists of three distinct parts, a reactive section with catalytic packings containing PBI.Mo catalyst, enclosed in between a non-reactive

rectifying section and a non-reactive stripping section. The diameter of each section of the column is 0.030 m with length around 0.50 m for the reactive section and 1.5 m for each non-reactive section. The reboiler was heated by steam that was circulated through the boiler and all the sections of the column. The entire column was covered with heating tapes and insulation in the form of Superwool 607^{TM} MAX Blanket. The temperatures of different sections of the column were monitored by the use of a software LabVIEW^{TM} program connected to the columm via the thermocouples thermometers. The set-up of RDC also included a decanter, a time-controlled automatic reflux device and a water cooled condenser. The reactants were fed through Viton® tubing to the RDC through independent control valves. The flow rates of the feeds were monitored volumetrically with the help of calibrated pumps. The catalytic section of the column was filled with PBI.Mo catalyst, contained in a structured catalytic packing. These structured packings were designed to provide excellent heat and mass transfer between the liquid and vapour phases, which was achieved via its structure of ordered flow channels. The design of the structured packing allowed the use of high hydraulic capacity and low pressure drop. These characteristics of the packing materials gave a better separation of products from reactants for equilibrium limited reactions.

The reactants were introduced into the RDC at room temperature. In a typical experimental run, TBHP was fed at the top of the reactive section, and cyclohexene was introduced at the bottom of the reactive section. The temperature in each section of the column was noted after starting the reaction, and steady state was reached when the temperatures in various sections of the column were stabilised. The column was run for a total reflux for a period of 2 h and the 'bottom products' were continuously withdrawn and analysed for their composition.

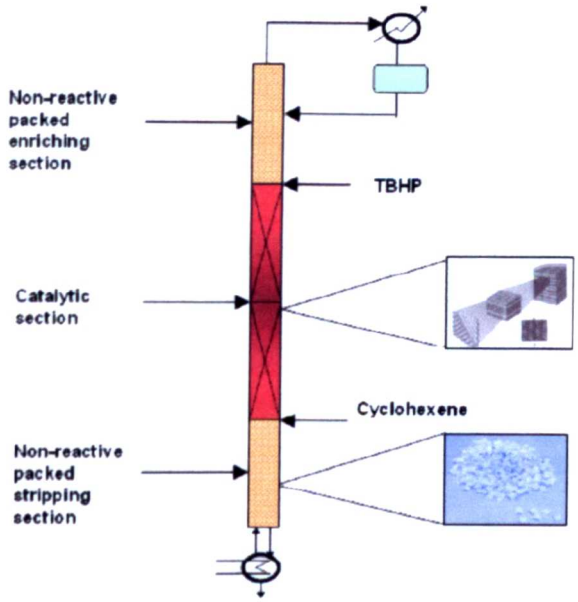

Scheme 2.28 *Schematic illustration of Reactive Distillation Column*

A typical epoxidation reaction was carried out as follows: a mixture of 200 ml of TBHP and 260 ml of cyclohexene was charged through Viton® tubing to the RDC at room temperature. The steam generator was set at pressure of 2 bar, and steady-state was reached when the temperatures stabilised in the entire column. The RDC was refluxed for 1 h and the conversions of TBHP checked at 4 positions of column. Then the feed to the column was started with the cyclohexene and TBHP in the ratio 3.5 : 1 respectively maintained with a calibrated pump for an additional 1 hour. TBHP was fed at the top of the reactive section for example, and cyclohexene was introduced at the bottom or the top of the reactive section or the top of the reboiler, and the 'bottom products' in the reboiler were continuously withdrawn and analysed for their composition by GC.

2.12 Analyses

^{1}H NMR spectra were recorded on a Bruker spectrometer 400 MHz. Chemicals shifts δ are given as ppm downfield from tetramethylsilane as the reference.

Infra-red spectra were recorded on a Perkin-Elmer spectrometer, and polymer resins and polymer-supported Mo complexes were recorded as KBr discs.

Elemental Microanalysis: Analysis of sample was carried out by the analytical staff in the Microanalytical laboratory, Department of Pure and Applied Chemistry.

Mo analyses of polymer-supported Mo complexes were made on a Perkin-Elmer spectrophotometer 200.

The optical rotation data were recorded on a Perkin-Elmer 341 polarimeter

Microwave chemical syntheses were performed on a CEM microwave equipped with a single mode cavity system for a batch system.

References

[1]D. C. Sherrington, *Chem. Commun.* **1998,** 2275.

[2]J. C. Sheehan, V. A. Bolhofer, *J. Am. Chem. Soc.* **1950,** 72, 2786.

[3]M. S. Motawia, J. Wengel, A. E. S. Abbel-Megid, E. B. Pedersen, *Synthesis.* **1989,** 384.

[4]A. Scozzafava, L. Menabuoni, F. Mincione, G. Mincione and C. T. Supuran, *Bioorg. Med. Chem. Lett.* **2002,** 11, 575.

[5]A. Scozzafava, L. Menabuoni, F. Mincione, and C. T. Supuran, *J. Med. Chem.* **2002,** 45, 1466.

[6]A. H. Blatt, *Organic Syntheses Collective 2.* **1943,** p397.

[7]C. Da, M. Ni, Z. Han, F. Yang, R. Wang. *J. Mol. Catal A: Chemical,* **2006,** 245, 1.

[8]E. C. Lawson, R. J. Santulli, A. B. Dyatkin, S. A. Ballentine, W. M. Abraham, S. Rudman, C. P. Page, L. Garavilla, B. P. Damiano, W. A. Kinney, and B. E. Maryanoff, *Bioorg. Med. Chem,* **2006,** 14, 4208.

[9]W. Lin, Q. Cai, W. Pang, Y. Yue, B. Zou, *Microporous and Mesoporous Matreials,* **1999,** 33, 187.

[10]K. B. Sharpless and T. R. Verhoeven, *Aldrichimica Acta,* **1979,** 12, 63.

Chapter 3

Results

3.1 Precursor polymer supports

The microanalytical data for the precursor resins, inorganic support MCM-41 and the corresponding supported chelating ligands are shown in Tables 3.1 and 3.2.

The ligand loadings of the resins were calculated from the nitrogen analyses by using the following expression:

$$\text{Ligand loading (mmol amine g}^{-1}) = \frac{\text{\% nitrogen in production / atomic mass nitrogen}}{\text{number of nitrogen atoms in ligand} \times 100}$$

Table 3.1 Elemental microanalytical data for precursor chloromethylated polystyrene resins

Precursor support	% found[a]				Surface Area
	C	H	N	Cl	($m^2 g^{-1}$)
PBI	**78.20**	**4.10**	**18.20**	-	
	68.60	4.40	15.10	-	700
Ps (8)	**90.85**	**7.55**	-	**1.40**	
DVB / VBC / St	89.60	7.80	-	0.95	552
75% / 5% / 20%					
Ps (9)	**90.60**	**7.55**	-	**1.65**	
DVB / VBC / St	84.10	7.00	-	1.15	55
12% / 5% / 83%					
Ps (10)	**85.35**	**7.10**	-	**7.40**	
DVB / VBC / St	86.50	7.40	-	4.70	43
12% / 25% / 63%					
Ps (11)	**73.05**	**6.05**	-	**20.80**	
DVB / VBC / St	73.75	6.02	-	16.45	26
12% / 88% / -					
Ps (12)	**82.05**	**8.15**	**9.20**	-	
Poly(4-amino methyl styrene)	78.25	6.79	5.17	0.68	26
	-	**1.3**	-	-	
MCM-41	-	0.45	-	-	1040

[a] Theoretical values for C, H, N, Cl are shown in bold type.

Table 3.2 Elemental microanalytical and ligand loading data for chelating polystyrene resins, PBI resins and MCM-41 resins

Precursor support	chelating resin	% found[a] C	H	N	Cl	S	ligand loading (mmol amine/g)	conversion[a] CH_2Cl(%)
PBI		68.60	4.40	15.10	-	-	2.70	-
Ps (8) DVB / VBC / St 75% / 5% / 20%	Ps.AMP (13)	90.10	8.20	0.55	0.55	-	0.20	53
Ps (9) DVB / VBC / St 12% / 5% / 83%	Ps.AMP (14)	90.15	7.66	1.07	-	-	0.38	100
Ps (10) DVB / VBC / St 12% / 25% / 63%	Ps.AMP (15)	89.00	7.80	2.25	0.50	-	0.80	89
Ps (11) DVB / VBC / St 12% / 88% / -	Ps.AMP (16)	81.40	5.80	6.45	1.80	-	2.30	89
Ps (11) DVB / VBC /St 12% / 88% / -	Ps.2-AMPH (17)	81.05	7.25	2.90	3.20	-	2.05	81
Ps (11) DVB / VBC / St 12% / 88% / -	Ps.GLYC (18)	72.25	7.20	2.85	0.20	-	2.05	98
Ps (11) DVB / VBC / St 12% / 88% / -	Ps.IMDA (19)	70.40	6.85	2.10	3.85	-	1.50	77
Ps (12) Poly(4-amino-methylstyrene)	Ps.EDTA (20)	73.05	7.15	6.75	0.15	-	1.60	99
MCM-41+amino		13.66	3.59	2.51	-	-	1.79	-
MCM-41.Schiff base (21)		17.67	2.58	2.82	-	5.14	2.10	-
Ps (11) DVB / VBC / St 12% / 88% / -	Ps.Phe (22)	77.84	6.56	4.20	2.57	-	3.00	77
Ps (11) DVB /VBC 12% / 88%	Ps.Schiff base (23)	75.63	6.35	1.63	1.32	-	1.16	92

[a]conversion of CH_2Cl was obtained according to the following formula:

$$\text{conversion of Cl (\%)} = \frac{(\text{mmol Cl in primary support} - \text{mmol Cl in chelating resin})}{(\text{mmol Cl in primary support})} \times 100$$

3.2 Synthesis of polymer-supported Mo (VI) complexes

Polymer-supported Mo (VI) complexes were prepared by refluxing each chelating resin with a 2: 1 molar excess of $MoO_2(acac)_2$.

During the synthesis of the polymer-supported Mo complexes, the initial green colour of the reaction mixture always changed to dark blue except for inorganic complex **MCM-41.SB.Mo (32)** in which the reaction mixture remained green. After filtration, extraction with acetone in a Soxhlet was carried out for two days or more and all polymer-supported Mo complexes were dried in a vacuum oven at 40°C.

The absorption bands in the infra-red spectra of all the polymer-supported Mo complexes are given in Tables 3.3, 3.4 and 3.5.

Table 3.3 Elemental microanalytical, infra-red and ligand loading data for polystyrene resin Mo complexes, **PBI.Mo** and **MCM-41.SB.Mo** complexes

Chelating resin	supported complex	% found C	H	N	Cl	S	ligand loading[a] (mmol g^{-1})	IR band (cm^{-1}) M=O str	M-O-M
PBI		68.60	4.40	15.10	-	-	2.70		
	PBI.Mo (batch 1)[b]	**53.34**	**3.74**	**12.01**	**-**	**-**	**2.15**	**950 988**	**-**
Ps.AMP (13)		90.10	8.20	0.55	0.55	-	0.20		
	Ps.AMP.Mo (24)	**87.20**	**7.25**	**0.41**	**0.53**	**-**	**0.15**	**902 960**	**-**
Ps.AMP (14)		90.15	7.66	1.07	-	-	0.38		
	Ps.AMP.Mo (25)	**86.55**	**7.58**	**0.45**	**-**	**-**	**0.16**	**906 963**	**-**
Ps.AMP (15)		89.00	7.80	2.25	0.50	-	0.80		
	Ps.AMP.Mo (26)	**80.57**	**6.77**	**2.01**	**-**	**-**	**0.72**	**905 958**	**-**
Ps.AMP (16)		81.40	5.80	6.45	1.80	-	2.30		
	Ps.AMP.Mo (27)	**64.53**	**4.79**	**4.68**	**-**	**-**	**1.67**	**906 958**	**-**
Ps.2-AMPH (17)		81.05	7.25	2.90	3.20	-	2.05		
	Ps.2-AMPH.Mo (28)	**68.25**	**5.85**	**2.42**	**2.56**		**1.72**	**906 956**	**-**
Ps.GLYC (18)		72.25	7.20	2.85	0.20	-	2.05		
	Ps.GLYC.Mo (29)	**62.45**	**5.60**	**2.35**	**0.29**		**1.67**	**910 960**	**-**
Ps.IMDA (19)		70.40	6.85	2.10	3.85	-	1.50		
	Ps.IMDA.Mo (30)	**63.61**	**5.94**	**1.94**	**2.94**		**1.38**	**909 960**	**-**
Ps.EDTA (20)		73.05	7.15	6.75	0.15	-	1.60		
	Ps.EDTA.Mo(31)	**66.95**	**6.23**	**5.35**	**0.18**	**-**	**1.27**	**903 956**	**-**
MCM-41.Schiff base (21)		17.67	2.58	2.82	-	5.14	2.10		
	MCM-41.SB.Mo (32)	**15.26**	**2.75**	**2.78**	**-**	**0.65**	**1.98**	**914 939**	**-**
Ps.Phe (22)		77.84	6.56	4.20	2.57	-	3.00		
	Ps.Phe.Mo (33)	**71.80**	**6.39**	**3.69**	**2.98**	**-**	**2.63**	**909 956**	**-**
Ps.Schiff base (23)		75.63	6.35	1.63	1.32		1.16		
	Ps.Schiff base.Mo (34)	**72.39**	**5.90**	**1.22**	**0.58**		**0.87**	**910 936**	**-**

[a]ligand loading was calculated according to the following expression:

$$\text{Ligand loading (mmol amine g}^{-1}) = \frac{\text{\% nitrogen in production / atomic mass nitrogen}}{\text{number of nitrogen atoms in ligand} \times 100}$$

Table 3.4. Microanalysis data and infra-red absorption bands of **PBI.Mo** complexes

Chelating resin	supported complex	% found[a] C	H	N	Cl	ligand loading[a] (mmol amine g^{-1})	IR band (cm^{-1}) M=O str		M-O-M
PBI		68.60	4.40	15.10	-	2.70	-	-	-
	PBI.Mo (batch 1)[b]	**53.34**	**3.74**	**12.01**	**-**	**2.15**	**950**	**988**	**-**
	PBI.Mo (batch 2)[b]	**60.82**	**3.45**	**12.41**	**-**	**2.20**	**905**	**944**	**-**
	PBI.Mo (batch 3)[c]	**66.54**	**3.64**	**12.53**	**-**	**2.23**	**955**	**989**	**-**
	PBI.Mo (batch 4)[d]	**66.56**	**4.05**	**15.05**	**-**	**2.68**	**955**	**980**	**-**
	PBI.Mo (batch 5)[e]	**66.22**	**4.11**	**15.01**	**-**	**2.68**	**902**	**955**	**-**

[a]ligand loading was calculated according to the following formula:

$$\text{Ligand loading (mmol amine g}^{-1}) = \frac{\text{\% nitrogen in production / atomic mass nitrogen}}{\text{number of nitrogen atoms in ligand} \times 100}$$

[b]**PBI.Mo** batch 1 was performed on a small scale with ligand and $MoO_2(acac)_2$ in the stoichiometric ratio 2 : 1.whereas **PBI.Mo** batch 2 was performed on a large scale with ligand and $MoO_2(acac)_2$ in the stoichiometric ratio 1 : 2.

[c]**PBI.Mo** batch 3 was performed on a small scale with ligand and $MoO_2(acac)_2$ in the stoichiometric ratio 1 : 1.

[d]**PBI.Mo** batch 3 was performed on a small scale with ligand and $MoO_2(acac)_2$ in the stoichiometric ratio 1 : 0.5.

[e]**PBI.Mo** batch 3 was performed on a small scale with ligand and $MoO_2(acac)_2$ in the stoichiometric ratio 1 : 0.1.

Table 3.5 Microanalysis data Infra-red absorption bands of **Ps.AMP.Mo** complexes

Chelating resin	supported complex	% found[a] C	H	N	Cl	ligand loading[a] (mmol amine g^{-1})	IR band (cm^{-1}) M=O str	M-O-M	
Ps.AMP (16)		81.40	5.80	6.45	1.80	2.30	-	-	-
Ps.AMP.Mo (27)[b]		**64.53**	**4.79**	**4.68**	**-**	**1.67**	**906**	**958**	**-**
Ps.AMP.Mo (35)[c]		**70.23**	**4.97**	**5.02**	**-**	**1.80**	**901**	**959**	**-**
Ps.AMP.Mo (36)[d]		**71.03**	**6.06**	**5.20**	**-**	**1.85**	**906**	**948**	**-**
Ps.AMP.Mo (37)[e]		**77.15**	**6.42**	**5.32**	**-**	**1.90**	**902**	**978**	**-**

[a]ligand loading was calculated according to the following formula:

$$\text{Ligand loading (mmol amine g}^{-1}) = \frac{\text{\% nitrogen in production / atomic mass nitrogen}}{\text{number of nitrogen atoms in ligand} \times 100}$$

[b]**Ps.AMP.Mo (27)** was performed on a small scale with ligand and $MoO_2(acac)_2$ in the stoichiometric ratio 1 : 2.

[c]**Ps.AMP.Mo (35)** was performed on a small scale with ligand and $MoO_2(acac)_2$ in the stoichiometric ratio 1 : 1.

[d]**Ps.AMP.Mo (36)** was performed on a small scale with ligand and $MoO_2(acac)_2$ in the stoichiometric ratio 1 : 0.5.

[e]**Ps.AMP.Mo (37)** was performed on a small scale with ligand and $MoO_2(acac)_2$ in the stoichiometric ratio 1 : 0.1.

3.3 Metal analyses of polymer-supported Mo (VI) complexes

The standard Mo solutions and the solution of each dissolved complex were introduced into the spectrometer and their corresponding absorbance readings were obtained. From the standard Mo solutions, the calibration graph was plotted and this graph was used to ascertain the metal loading of each Mo complex. A sample solution calculation for the **PBI.Mo** complex is given as example:

Standard molybdenum solutions (mg Mo / L)	Absorbance
0	0.000
50	0.051
100	0.093
200	0.173
Unknown solution	0.120

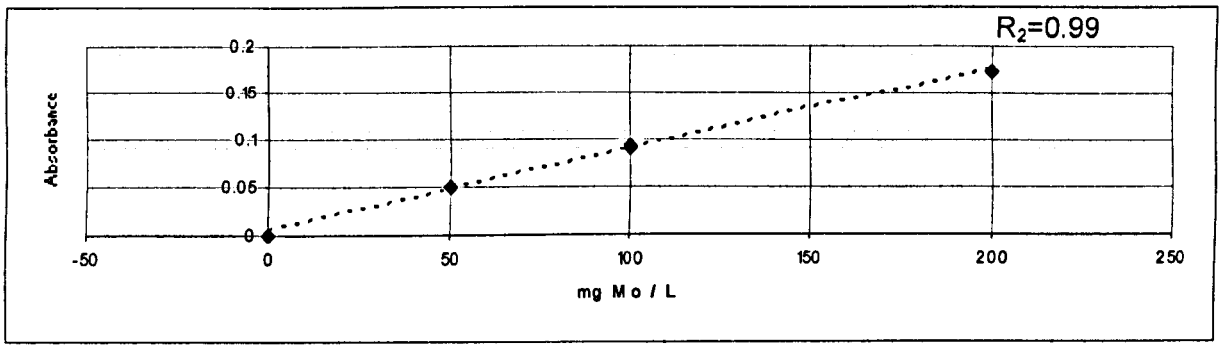

Figure 3.1 Atomic absorption spectrometer calibration curve for molybdenum.

From the calibration graph (Figure 3.1 above), the unknown solution has a molybdenum concentration of 135.299 mg Mo / L.

Then 13. 5299 mg Mo per 100 ml of solution prepared.

Weight of **PBI.Mo** originally used analysis was 0.1009 g

0.01352 g Mo is present in 0.1009 g of **PBI.Mo**

0.01352 / 0.1009 = 0.1339 g Mo per g of resin

0.1339 / 96 = 1. 40 mmol Mo g^{-1} of resin

Metal loading of all polymer-supported Mo complexes were calculated in the same manner. The results are summarised in Tables 3.6, 3.7, 3.8 and 3.9

Table 3.6 Metal loading data, ligand loading and ligand : metal ion ratio of polymer-supported molybdenum complexes

Supported complex	Metal loading (mmol g^{-1})	(g g^{-1})	Ligand loading[a] (mmol g^{-1})	Ligand : metal ratio
PBI.Mo (batch 1)[b]	1.43	0.137	1.84	1.30 : 1
Ps.AMP.Mo (24)	0.20	0.018	0.15	0.75 : 1
Ps.AMP.Mo (25)	0.22	0.020	0.16	0.73 : 1
Ps.AMP.Mo (26)	0.50	0.048	0.67	1.35 : 1
Ps.AMP.Mo (27)	1.33	0.128	1.45	1.10 : 1
Ps.2-AMPH.Mo (28)	0.98	0.095	1.55	1.58 : 1
Ps.GLYC.Mo (29)	1.30	0.125	1.46	1.12 : 1
Ps.IMDA.Mo (30)	1.05	0.102	1.24	1.20 : 1
Ps.EDTA.Mo(31)	0.32	0.030	1.23	3.84 : 1
MCM-41.SB.Mo (32)	0.62	0.058	1.85	2.98 : 1
Ps.Phe.Mo (33)	0.67	0.065	2.45	3.60 : 1
Ps.Schiff base.Mo (34)	0.36	0.034	0.84	2.36 : 1

[a](1-weight of Mo per gram of supported complex) *(loading of supported complex)

Table 3.7 Metal loading data, ligand loading and ligand : metal ion ratio of **PBI.Mo** complexes

Supported complex	Metal loading (mmol g^{-1})	($g\ g^{-1}$)	Ligand loading[a] (mmol g^{-1})	Ligand : metal ratio
PBI.Mo (batch 1)[b]	1.43	0.137	1.84	1.30 : 1
PBI.Mo (batch 2)[b]	1.02	0.098	1.95	1.90 : 1
PBI.Mo (batch 3)[c]	0.45	0.044	2.23	4.95 : 1
PBI.Mo (batch 4)[d]	0.35	0.034	2.50	7.15 : 1
PBI.Mo (batch 5)[e]	0.23	0.022	2.60	11.30 : 1

[a]**(1-weight of Mo per gram of supported complex) *(loading of supported complex)**

[b]**PBI.Mo** batch 1 was performed on a small scale with ligand and $MoO_2(acac)_2$ in the stoichiometric ratio 1 : 2.whereas **PBI.Mo** batch 2 was performed on a large scale with ligand and $MoO_2(acac)_2$ in the stoichiometric ratio 1 : 2.

[c]**PBI.Mo** batch 3 was performed on a small scale with ligand and $MoO_2(acac)_2$ in the stoichiometric ratio 1 : 1.

[d]**PBI.Mo** batch 4 was performed on a small scale with ligand and $MoO_2(acac)_2$ in the stoichiometric ratio 1 : 0.5.

[e]**PBI.Mo** batch 5 was performed on a small scale with ligand and $MoO_2(acac)_2$ in the stoichiometric ratio 1 : 0.1.

Table 3.8 Metal loading data, ligand loading and ligand : metal ion ratio of **PBI.Mo** (scale up) complexes

Supported complex	Metal loading (mmol g^{-1})	(g g^{-1})	Ligand loading[a] (mmol g^{-1})	Ligand : metal ratio
PBI.Mo (scale up) 1	0.92	0.088	1.95	2.10 : 1
PBI.Mo (scale up) 2	0.98	0.094	1.93	1.95 : 1
PBI.Mo (scale up) 3	0.90	0.086	1.95	2.15 : 1
PBI.Mo (scale up) 4	0.98	0.094	1.93	1.95 : 1
PBI.Mo (scale up) 5	1.39	0.133	1.85	1.33 : 1
PBI.Mo (batch 2)	1.02	0.098	1.95	1.90 : 1

[a]**(1-weight of Mo per gram of supported complex) *(loading of supported complex)**

[b]**PBI.Mo** (scale up) and **PBI.Mo** batch 2 were performed on a large scale with ligand and $MoO_2(acac)_2$ in the stoichiometric ratio 1 : 2.

Table 3.9 Metal loading data, ligand loading and ligand : metal ion ratio of **Ps.AMP.Mo** complexes

Supported complex	Metal loading (mmol g^{-1})	(g g^{-1})	Ligand loading[a] (mmol g^{-1})	Ligand : metal ratio
Ps.AMP.Mo (27)[b]	1.33	0.128	1.45	1.10 : 1
Ps.AMP.Mo (35)[c]	0.85	0.082	1.65	1.95 : 1
Ps.AMP.Mo (36)[d]	0.65	0.062	1.75	2.70 : 1
Ps.AMP.Mo (37)[e]	0.23	0.021	1.85	8.05 : 1

[a]**(1-weight of Mo per gram of supported complex) *(loading of supported complex)**

[b]**Ps.AMP.Mo (27)** was performed on a small scale with ligand and $MoO_2(acac)_2$ in the stoichiometric ratio 1 : 2.

[c]**Ps.AMP.Mo (35)** was performed on a small scale with ligand and $MoO_2(acac)_2$ in the stoichiometric ratio 1 : 1.

[d]**Ps.AMP.Mo (36)** was performed on a small scale with ligand and $MoO_2(acac)_2$ in the stoichiometric ratio 1 : 0.5.

[e]**Ps.AMP.Mo (37)** was performed on a small scale with ligand and $MoO_2(acac)_2$ in the stoichiometric ratio 1 : 0.1.

3.4 Catalyst activation

Catalyst activation was carried out for all polymer-supported and the MCM-41 supported Mo complexes and during this process all supported complexes turned yellow colour. Each sample of supported complex was accurately weighed and then activated for a period of from 4h, 24h, 48h to 1 month under the same conditions using a molar ratio Mo : THBP =0.06 : 5 and 20 ml of 1,2-dichloroethane at reflux. When the activation catalysts were completed, the activated resins were filtered off and washed with 10 ml of 1,2-dichloroethane . The resulting activated supported Mo were used as catalysts for cyclohexene and styrene epoxidations

3.5 Catalytic epoxidation of cyclohexene and styrene

3.5.1 ^{1}H NMR spectroscopy

The epoxidation reactions were monitored by ^{1}H NMR spectroscopy as previously stated in 2.9.1. Bromobenzene was used as the internal standard for all the epoxidation reactions of cyclohexene whereas methoxybenzene was used as internal standard for all the epoxidation reactions of styrene.

3.5.2 Homogeneous $MoO_2(acac)_2$ catalyst experiments

In order to optimize the results of the epoxidation reactions, homogeneous epoxidations were carried out at different temperatures with excess of cyclohexene ('large scale' conditions) and with styrene in different solvents ('small scale'conditions) at 80°C. The results obtained with the homogenous catalyst are summarised in Tables 3.10 and 3.11

Table 3.10 Effect of reaction temperature with homogeneous $MoO_2(acac)_2$ catalyst in the case of epoxidation of cyclohexene under 'large scale' conditions.

Catalyst		Conversion to epoxide (%)[a]				
	T/°C	2 min	6min	20 min	60 min	120 min
$MoO_2(acac)_2$	80	90	90	90	94	94
$MoO_2(acac)_2$	40	76	82	85	85	85
$MoO_2(acac)_2$	RT	74	77	78	78	78

[a]Conversion to epoxide based on conversion of TBHP, i.e. 5 mmol TBHP= 5 mmol cyclohexene oxide = 100% yield

Reaction conditions: [TBHP] = 5 mmol, [Cyclohexene] = 83 mmol, [Catalyst] = 0.06 mmol.

Cyclohexene oxide conversion was monitored by 1H NMR.

Table 3.11 Catalytic epoxidation of styrene using homogeneous $MoO_2(acac)_2$ complex in various organic solvents under 'small scale' conditions.

$MoO_2(acac)_2$	TBHP	Styrene	TBHP:styrene	Solvent	Conversion of styrene (%)[a]					
(mmol,mol%)	(ml,mmol)	(ml,mmol)	(molar: ratio)	(ml)	20 min	40 min	60 min	120 min	180 min	240 min
0.011, 0.7	0.45, 1.5	0.172, 1.5	1 : 1	CH_3CN (4)	-	-	-	3	3	3
0.011, 0.7	0.45, 1.5	0.172, 1.5	1 : 1	$CH_3CO_2CH_2CH_3$(4)	-	2	3	3	3	3
0.011, 0.7	0.45, 1.5	0.172, 1.5	1 : 1	THF (4)	-	-	-	-	-	-
0.011, 0.7	0.45, 1.5	0.172, 1.5	1 : 1	toluene (4)	19	21	25	25	27	27
0.011, 0.7	0.45, 1.5	0.172, 1.5	1 : 1	1,2-DCE (4)	15	18	18	18	19	19.

[a]Based on conversion of TBHP i.e. 1.5mmol of TBHP = 100% yield

$$\text{Conversion} = \left[\frac{n_{methoxybenzene}\left(\frac{1H(\delta = 2.82\,ppm)\text{styrene oxide area}}{1H(\delta = 3.80\,ppm)\text{standard methoxybenzene area}} \right)}{n_{TBHP}} \right] \times 100$$

3.5.2.1 Effect of wet TBHP on epoxidation of cyclohexene with $MoO_2(acac)_2$ used as catalyst

The use of wet TBHP as oxidant was also carried out in order to assess the activity and the selectivity of homogeneous $MoO_2(acac)_2$ catalyst in the case of epoxidation of cyclohexene using'large scale' conditions as shown in Figure 3.2.

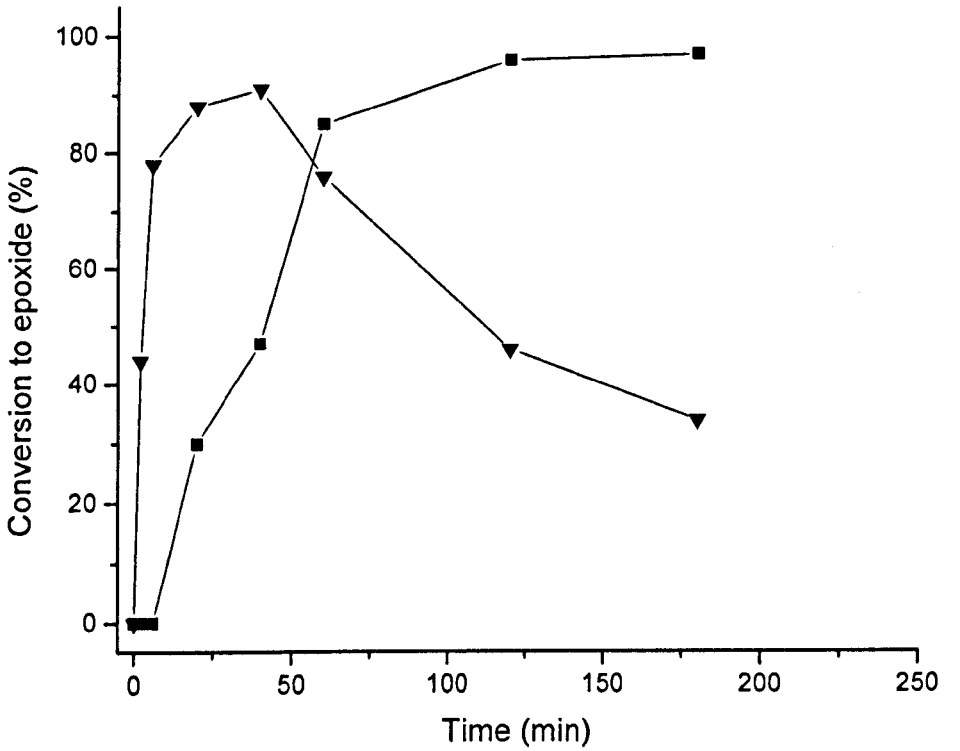

*Figure 3.2 Conversion curves for epoxidation of cyclohexene under 'large scale' conditions using wet-TBHP catalysed by: ▼, $MoO_2(acac)_2$ and ■, **PBI.Mo** activated for 4 h.*

3.5.3 Epoxidation of cyclohexene and styrene using PBI.Mo as catalyst

Similar studies to that previously described for the homogeneous catalyst were also carried out with the **PBI.Mo** complex and the **PBI.Mo** activated complex using excess of cyclohexene and in different solvents at 80°C under a nitrogen atmosphere, and in different solvents with styrene. The results of epoxidations of cyclohexene and styrene are shown in Table 3.12, 3.13 and 3.14

Table 3.12 Effect of reaction temperature and comparison with **PBI.Mo** (batch 1) catalyst in the case of epoxidation of cyclohexene under 'large scale' conditions.

Catalyst		Conversion to epoxide (%)[a]					
	T/°C	20min	40min	60 min	120 min	180min	240 min
$MoO_2(acac)_2$	80	90	90	92	94	94	94
PBI.Mo(activated 4h)	80	91	100	100	100	100	100
PBI.Mo non-activated	80	74	98	100	100	100	100
PBI.Mo(activated RT)[b]	80	10	36	79	94	100	100

[a]Conversion to epoxide based on conversion of TBHP, i.e. 5 mmol TBHP = 5 mmol cyclohexene oxide = 100% yield

Reaction conditions: [TBHP] = 5 mmol, [Cyclohexene] = 83 mmol, [Catalyst] = 0.06 mmol.

Cyclohexene oxide conversion was monitored by 1H NMR.

[b]**PBI.Mo** activated at room temperature for a period of one momth

Table 3.13 Catalytic epoxidation of styrene using **PBI.Mo** (batch 1) complex activated 4h in various organic solvents under 'small scale' conditions.

PBI.Mo 1 activated 4h (mmol,mol%)	TBHP (ml,mmol)	Styrene (ml,mmol)	TBHP:styrene (molar: ratio)	Solvent (ml)	Conversion of styrene (%)[a] 20 min	40 min	60 min	120 min	180 min	240 min
0.011, 0.7	0.45, 1.5	0.172, 1.5	1 : 1	CH_3CN (4)	-	-	-	2	2	2
0.011, 0.7	0.45, 1.5	0.172, 1.5	1 : 1	$CH_3CO_2CH_2CH_3$(4)	-	-	-	2	4	8
0.011, 0.7	0.45, 1.5	0.172, 1.5	1 : 1	THF (4)	-	-	-	-	3	5
0.011, 0.7	0.45, 1.5	0.172, 1.5	1 : 1	toluene (4)	2	5	10	18	27	33
0.011, 0.7	0.45, 1.5	0.172, 1.5	1 : 1	1,2-DCE (4)	5	11	16	33	38	42

[a]Based on conversion of TBHP i.e. 1.5mmol of TBHP = 100% yield

$$\text{Conversion} = \left[\frac{n_{methoxybenzene}\left(\frac{1H(\delta = 2.82ppm)\text{styrene oxide area}}{1H(\delta = 3.80ppm)\text{standard methoxybenzene area}} \right)}{n_{TBHP}} \right] \times 100$$

Table 3.14 Catalytic epoxidation of cyclohexene using **PBI.Mo** (batch 1) complex activated 4h in various organic solvents under 'small scale'conditions.

PBI.Mo 1 activated 4h (mmol,mol%)	TBHP (ml,mmol)	cyclohexene (ml,mmol)	TBHP:cyclohexene (molar: ratio)	Solvent (ml)	Conversion of cyclohexene (%)[a] 20 min	40 min	60 min	120 min	180 min	240 min
No.catalyst	0.47, 1.5	0.051, 0.5	3 : 1	CCl_4 (4)	-	-	-	-	-	-
0.011, 2.2[b]	0.47, 1.5	0.051, 0.5	3 : 1	CCl_4 (4)	49	87	100			
0.011, 0.7	0.47, 1.5	0.151, 1.5	1 : 1	CCl_4 (4)	22	53	68	82	87	89
No catalyst	0.47, 1.5	0.051, 0.5	3 : 1	toluene (4)	-	-	-	-	-	-
0.011, 2.2[b]	0.47, 1.5	0.151, 0.5	3 : 1	toluene (4)	-	21	35			
0.011, 0.7	0.47, 1.5	0.151, 1.5	1 : 1	toluene (4)	9	37	40	65	79	84
0.060, 1.2[c]	1.45, 5.0	8.400, 83	1 : 16.5	-	87	100	100	100	100	100
0.011, 0.7[a]	0.47, 1.5	0.151, 1.5	1 : 1	1,2-DCE (4)	48	82	96	97	99	99
0.011, 2.2[a]	0.30, 1.0	0.051, 0.5	1 : 0.5	1,2-DCE (4)	59	92	100	100	100	100

[a]Based on conversion of TBHP i.e. 1.5mmol of TBHP = 100% yield

$$\text{Conversion} = \left[\frac{n_{bromobenzene}\left(\frac{2H(\delta = 3.15ppm)\text{ cyclohexene oxide area}}{2H(\delta = 7.59ppm)\text{ standard bromobenzene area}} \right)}{n_{TBHP}} \right] \times 100$$

[b]Reaction was performed for one hour

Table 3.15 Catalytic conversion of cyclohexene ***oxide*** using **PBI.Mo** (batch 1) activated 4 h complex in various organic solvents using 'small scale' conditions.

PBI.Mo 1 activated 4h (mmol,mol%)	TBHP (ml,mmol)	Cyclohexene oxide (ml,mmol)	TBHP/cyclohexene oxide (molar: ratio)	Solvent (ml)	Conversion of cyclohexene oxide (%)[a] 40 min	60 min	120 min	180 min	240 min
No.catalyst	0.47, 1.5	0.051, 0.5	3 : 1	CCl_4 (4)	-	-	-	-	-
0.011, 2.2[b]	0.47, 1.5	0.051, 0.5	3 : 1	CCl_4 (4)	-	-	-	-	-
0.011, 0.7	0.47, 1.5	0.151, 1.5	1 : 1	CCl_4 (4)	-	-	-	-	-

[a]Based on conversion of cyclohexene oxide, temperature =77°C

3.5.4 Effect of wet TBHP on epoxidation of cyclohexene using PBI.Mo as catalyst

A similar study to that described in 3.5.2.1 was also carried out with wet TBHP as oxidant and **PBI.Mo** complex used as catalyst in the case of epoxidation of cyclohexene under 'large scale' conditions as shown in Figure 3.3.

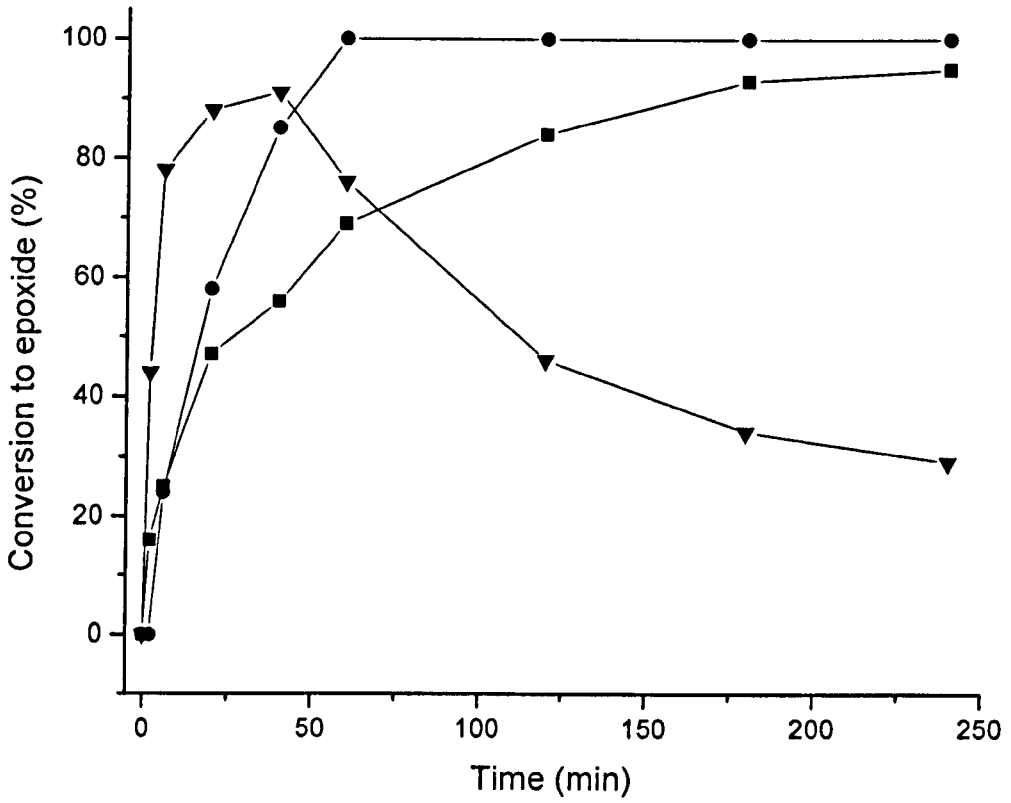

Figure 3.3 Conversion curves for epoxidation of cyclohexene under 'large scale' conditions using wet-TBHP catalysed by: ▼, $MoO_2(acac)_2$; ■, ***PBI.Mo*** *(batch 1) activated for 4 h; and* ●, *using anhydrous TBHP with* ***PBI.Mo*** *(batch 1) activated for 4h.*

3.5.5 Epoxidation of cyclohexene and styrene using inorganic support MCM-41.SB.Mo (32) as catalyst

The epoxidation of styrene in different solvents and cyclohexene in 1,2-DCE were also carried out with inorganic support **MCM-41.SB.Mo (32)** used as catalyst and TBHP as oxidant as shown in Tables 3.16 and 3.17.

Table 3.16 Catalytic epoxidation of styrene using **MCM-41.SB.Mo (32)** complex activated 4 h in various organic solvents under 'small scale' conditions.

MCM-41.SB.Mo activated 4 h (mmol,mol%)	TBHP (ml,mmol)	Styrene (ml,mmol)	TBHP:styrene (molar: ratio)	Solvent (ml)	Conversion of styrene (%)[a] 20 min	40 min	60 min	120 min	180 min	240 min
0.011, 0.7	0.45, 1.5	0.172, 1.5	1 : 1	CH_3CN (4)	-	-	3	4	4.5	5.5
0.011, 0.7	0.45, 1.5	0.172, 1.5	1 : 1	$CH_3CO_2CH_2CH_3$(4)	-	-	-	6	12	17
0.011, 0.7	0.45, 1.5	0.172, 1.5	1 : 1	THF (4)	-	-	-	-	-	2
0.011, 0.7	0.45, 1.5	0.172, 1.5	1 : 1	toluene (4)	5	6.5	18.5	18	30	34
0.011, 0.7	0.45, 1.5	0.172, 1.5	1 : 1	1,2-DCE (4)	4	9.5	15	29	31.5	32

[a]Based on conversion of TBHP i.e. 1.5mmol of TBHP = 100% yield

$$\text{Conversion} = \left[\frac{n_{methoxybenzene}\left(\frac{1H(\delta = 2.82ppm)\text{styrene oxide area}}{1H(\delta = 3.80ppm)\text{standard methoxybenzene area}} \right)}{n_{TBHP}} \right] \times 100$$

Table 3.17 Catalytic epoxidation of cyclohexene using **MCM-41.SB.Mo (32)** complex activated 4 h in 1,2-DCE using 'small scale' conditions.

MCM41.SB.Mo activated 4h (mmol,mol%)	TBHP (ml,mmol)	cyclohexene (ml,mmol)	TBHP:cyclohexene (molar: ratio)	Solvent (ml)	Conversion of cyclohexene (%)[a] 20 min	40 min	60 min	120 min	180 min	240 min
0.011, 0.7[a]	0.47, 1.5	0.151, 1.5	1 : 1	1,2-DCE (4)	30	58	74	92	98	99
0.011, 2.2[a]	0.30, 1.0	0.051, 0.5	1 : 0.5	1,2-DCE (4)	16	42	58	88	96	99

[a]Based on conversion of TBHP i.e. 1.5mmol of TBHP = 100% yield

$$\text{Conversion} = \left[\frac{n_{bromobenzene}\left(\frac{2H(\delta = 3.15ppm)\text{ cyclohexene oxide area}}{2H(\delta = 7.59ppm)\text{ standard bromobenzene area}} \right)}{n_{TBHP}} \right] \times 100$$

3.5.6 Epoxidation styrene using chiral Ps.Phe.Mo (33) and Ps.SB.Mo (34) as catalysts

The epoxidation of styrene in 1,2-DCE were also carried out with **Ps.Phe.Mo (33)** **Ps.SB.Mo (34)** used as catalysts and TBHP as oxidant as shown in Tables 3.18 and 3.19 respectively.

Table 3.18 Catalytic epoxidation of styrene using **Ps.Phe.Mo (33)** complex activated 4 h in 1,2-DCE using 'small scale' conditions.

Ps.Phe.Mo (33) activated 4 h (mmol,mol%)	TBHP (ml,mmol)	Styrene (ml,mmol)	TBHP : styrene (molar ratio)	Solvent (ml)	Temp (°C)	Time (min)	conversion of styrene (%)[a]
0.011, 0.7	1.3, 4.5	0.172, 1.5	3 : 1	1,2-DCE (4)	- 40	240	-
0.011, 0.7	1.3, 4.5	0.172, 1.5	3 : 1	1,2-DCE (4)	RT	240	-
0.011, 0.7	1.3, 1.5	0.172, 1.5	3 : 1	1,2-DCE (4)	RT	24 h	12
0.011, 0.7	1.3, 4.5	0.172, 1.5	3 : 1	1,2-DCE (4)	30	120	-
0.011, 0.7	1.3, 4.5	0.172, 1.5	3 : 1	1,2-DCE (4)	40	120	-
0.011, 0.7	1.3, 1.5	0.172, 1.5	3 : 1	1,2-DCE (4)	80	240	87

[a]Based on conversion of styrene

Table 3.19 Catalytic epoxidation of styrene using **Ps.SB.Mo (34)** complex activated 4 h in 1,2-DCE or no solvent using 'small scale'conditions.

Ps.SB.Mo (34) activated 4 h (mmol,mol%)	TBHP (ml,mmol)	Styrene (ml,mmol)	TBHP : styrene (molar ratio)	Solvent (ml)	Temp (°C)	Time (min)	conversion of styrene (%)[a]
0.011, 0.7	1.3, 4.5	0.172, 1.5	1 : 1	1,2-DCE (4)	80	120	16
0.011, 0.7	1.3, 4.5	0.172, 1.5	1 : 1	1,2-DCE (4)	80	240	33
0.011, 0.7	1.3, 4.5	0.172, 1.5	3 : 1	1,2-DCE (4)	80	240	82
0.011, 0.7	1.3, 1.5	0.172, 1.5	1 : 1	no solvent	80	120	54

[a]Based on conversion of styrene

3.5.7 Microwave assisted epoxidation reactions

3.5.7.1 Microwave catalytic epoxidation of cyclohexene using $MoO_2(acac)_2$, PBI.Mo and inorganic support MCM-41.SB.Mo (32) as catalysts with no solvent

Microwave epoxidation of cyclohexene without solvent was also carried out using homogeneous $MoO_2(acac)_2$, **PBI.Mo** and **MCM-41.SB.Mo (32)** as catalysts and data from these reactions are shown in Tables 3.20, 3.21 and 3.22.

Table 3.20 Microwave catalytic epoxidation of cyclohexene using homogeneous $MoO_2(acac)_2$ complex with no solvent.

$MoO_2(acac)_2$ activated 4h (mmol, mol%)	TBHP (ml, mmol)	Cyclohexene (ml, mmol)	TBHP / cylohexene (molar ratio)	Solvent (ml)	Temp (°C)	Time (min)	conversion to epoxide (%)[a],
0.011, 0.7	0.47, 1.5	0.151, 1.5	1 / 1	No solvent	40	15	56
0.011, 0.7	0.47, 1 .5	0.151, 1.5	1 / 1	No solvent	80	15	75
0.011, 0.7	0.47, 1.5	0.151, 1.5	1 / 1	No solvent	80	60	94

[a]Based on conversion of cyclohexene

Table 3.21 Microwave catalytic epoxidation of cyclohexene using **PBI.Mo** (batch 1) activated for 4 h with no solvent.

PBI.Mo 1 activated 4h (mmol, mol%)	TBHP (ml, mmol)	Cyclohexene (ml, mmol)	TBHP / cylohexene (molar ratio)	Solvent (ml)	Temp (°C)	Time (min)	conversion to epoxide (%)[a],
0.011, 0.7	0.47, 1.5	0.151, 1.5	1 / 1	No solvent	40	15	35
0.011, 0.7	0.47, 1 .5	0.151, 1.5	1 / 1	No solvent	80	15	42
0.011, 0.7	0.47, 1.5	0.151, 1.5	1 / 1	No solvent	80	60	82

[a]Based on conversion of cyclohexene

Table 3.22 Microwave catalytic epoxidation of cyclohexene using **MCM-41.SB.Mo (32)** activated for 4 h with no solvent.

MCM-41.SB.Mo activated 4h (mmol, mol%)	TBHP (ml, mmol)	Cyclohexene (ml, mmol)	TBHP : cylohexene (molar ratio)	Solvent (ml)	Temp (°C)	Time (min)	conversion to epoxide (%)[a],
0.011, 0.7	0.47, 1.5	0.151, 1.5	1 : 1	No solvent	40	15	-
0.011, 0.7	0.47, 1 .5	0.151, 1.5	1 : 1	No solvent	80	15	-
0.011, 0.7	0.47, 1.5	0.151, 1.5	1 : 1	No solvent	80	120	69

[a]Based on conversion of cyclohexene

3.5.7.2 Microwave catalytic epoxidation of styrene using chiral Ps.Phe.Mo (33) and Ps.SB.Mo (34) as catalysts with 1,2-dichloroethane as solvent or in the absence of solvent

Table 3.23 Microwave catalytic epoxidation of styrene in 1,2-dichloroethane or no solvent using chiral **Ps.Phe.Mo (33)** activated for 4 h

Ps.Phe.Mo (33) activated 4 h (mmol,mol%)	TBHP (ml,mmol)	Styrene (ml,mmol)	TBHP : styrene (molar ratio)	Solvent (ml)	Temp (°C)	Time (min)	conversion of styrene (%)[a]
0.011, 0.7	1.3, 4.5	0.172, 1.5	3 : 1	1,2-DCE (4)	30	120	-
0.011, 0.7	1.3, 4.5	0.172, 1.5	3 : 1	1,2-DCE (4)	40	120	-
0.011, 0.7	1.3, 1.5	0.172, 1.5	3 : 1	1,2-DCE (4)	80	60	66
0.011, 0.7	1.3, 4.5	0.172, 1.5	3 : 1	1,2-DCE (4)	80	120	92
0.011, 0.7	1.3, 1.5	0.172, 1.5	3 : 1	no solvent	80	15	99

[a]Based on conversion of styrene

Table 3.24 Microwave catalytic epoxidation of styrene using no solvent and chiral **Ps.SB.Mo (34)** activated for 4 h.

Ps.SB.Mo (34) activated 4 h (mmol,mol%)	TBHP (ml,mmol)	Styrene (ml,mmol)	TBHP : styrene (molar ratio)	Solvent (ml)	Temp (°C)	Time (min)	conversion of styrene (%)[a]
0.011, 0.7	1.3, 4.5	0.172, 1.5	3 : 1	no solvent	80	15	40
0.011, 0.7	1.3, 4.5	0.172, 1.5	3 : 1	no solvent	80	40	72
0.011, 0.7	1.3, 4.5	0.172, 1.5	3 : 1	no solvent	80	60	98

[a]Based on conversion of styrene

$$\text{Conversion} = \left[\frac{(1\,\text{H styrene oxide area})}{1\,\text{H styrene oxide area} + 1\,\text{H styrene area}}\right] \times 100$$

3.5.8 Continuous epoxidation of cyclohexene in a Reactive Distillation Column with PBI.Mo as catalyst

Table 3.25 Catalytic epoxidation of cyclohexene using **PBI.Mo** (batch 1) activated for 4h complex in a Reactive Distillation Column

Run	Cyclohexene:TBHP mole ratio			Flow rate [ml/min]		Temperature of the catalytic section [°C]				TBHP conversion [%]	
	Re-boiler	Pumps	Total	Cyclohexene	TBHP	Bottom part		Top part		60 minutes	120 minutes
						vapour	liquid	vapour	liquid		
1	3.5:1	3.4:1	3.45:1	1.3	1.1	74	71	74	71	90	92
2	3.5:1	3.75:1	3.62:1	1.3	1.0	71	70	74	71	97	97
3	3.5:1	3.6:1	3.55:1	1.3	1.0	74	71	74	71	97	97
4	3.5:1	3.5:1	3.5:1	1.3	1.0	74	71	74	72	98	98

Note. The yellow results highlighted, are the yields usually obtained using a RDC with these reaction conditions after 1 h and 2 h.

Feed location of Reactive Distillation Column

Run 1: TBHP was fed into the top of reaction section

Cyclohexene was fed in the bottom of reaction section

Run 2: TBHP was fed under condenser

Cyclohexene was fed in the bottom of reaction section

Run 3: TBHP was fed into the top of reaction section

Cyclohexene was fed above rebolier

Run 4: TBHP was fed under condenser

Cyclohexene was fed above rebolier

3.5.9 Catalyst recycling experiments

Extensive catalyst recycling reactions were carried out as described in 2.10 and using the 'large scale' reaction conditions reported in 2.9.1. This was to evaluate the stability of each polymer-supported Mo catalyst and in particular to assess Mo leaching during each epoxidation reaction, and its potential contribution to catalysts.

3.5.9.1 Long-term activity of polymer-supported Mo catalysts experiments

Also in order to assess the long-term activity of each polymer catalyst, a sample of each polymer catalyst was re-used in up to 10 consecutive reactions. Data from several consecutive runs using these polymer-supported Mo catalysts are shown in Figures 3.4 to 3.14.

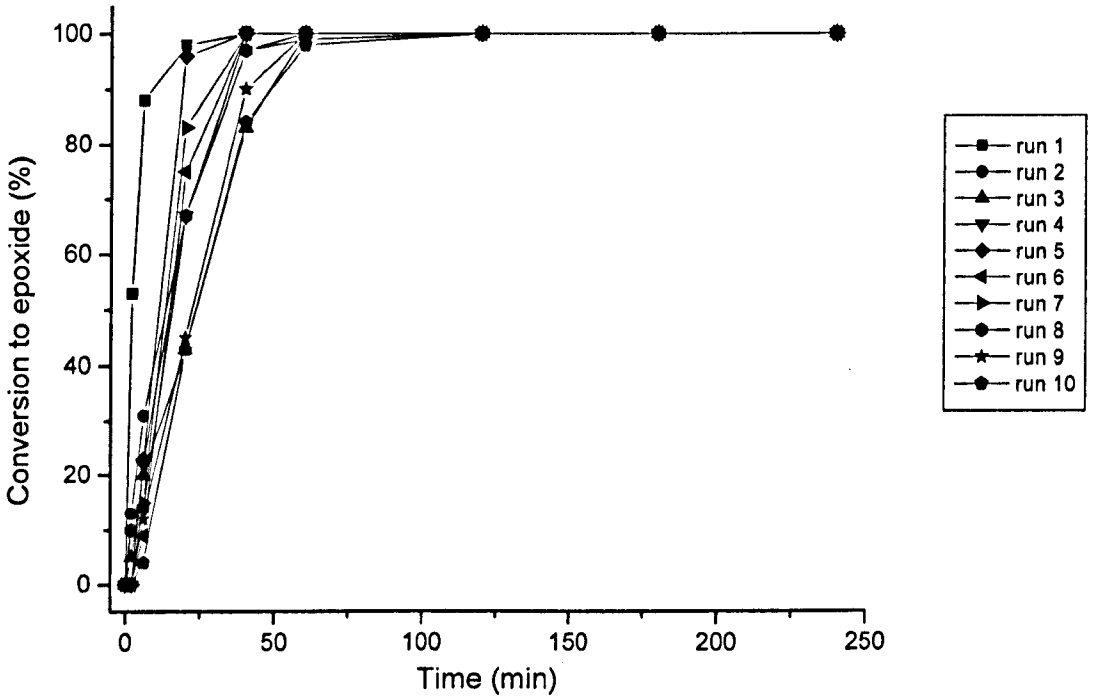

Figure 3.4 Conversion curves for the epoxidation of cyclohexene using anhydrous TBHP at 80°C catalysed by ***PBI.Mo batch 1*** *activated for 4 hours and recycled in 10 consecutive reactions ('large scale' reaction conditions).*

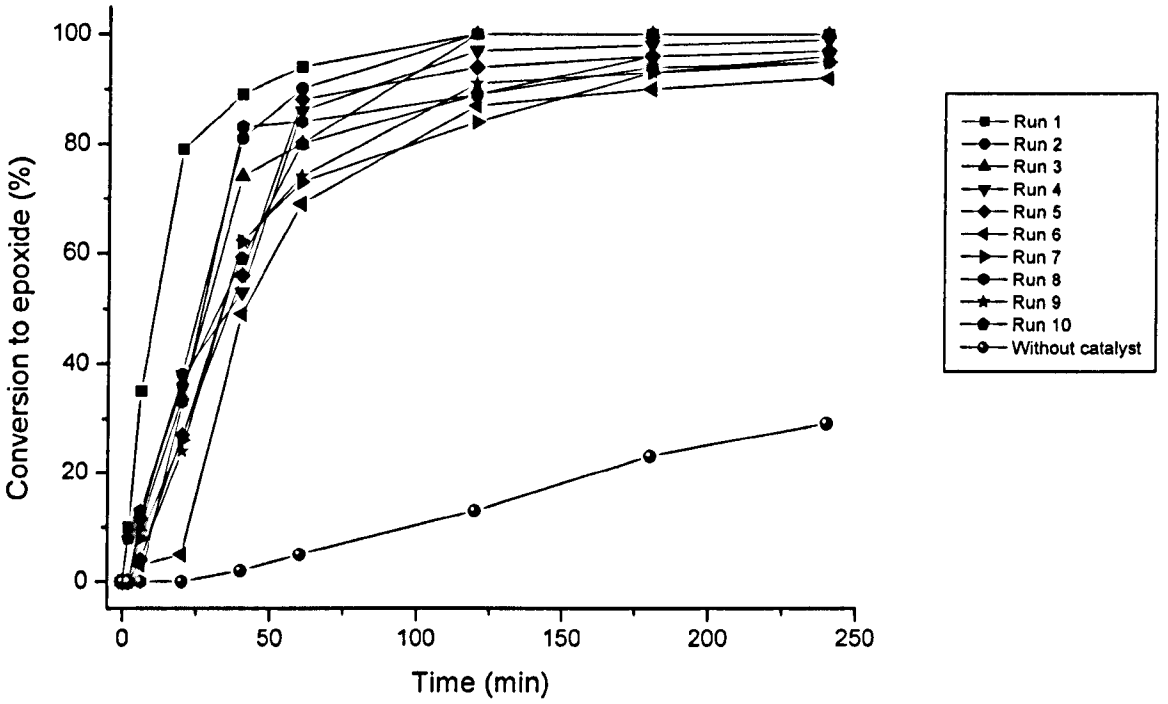

Figure 3.5 Conversion curves for the epoxidation of cyclohexene using anhydrous TBHP at 80°C catalysed by ***PBI.Mo batch 2*** *activated for 1 month at room temperature and recycled in 10 consecutive reactions ('large scale' reaction conditions).*

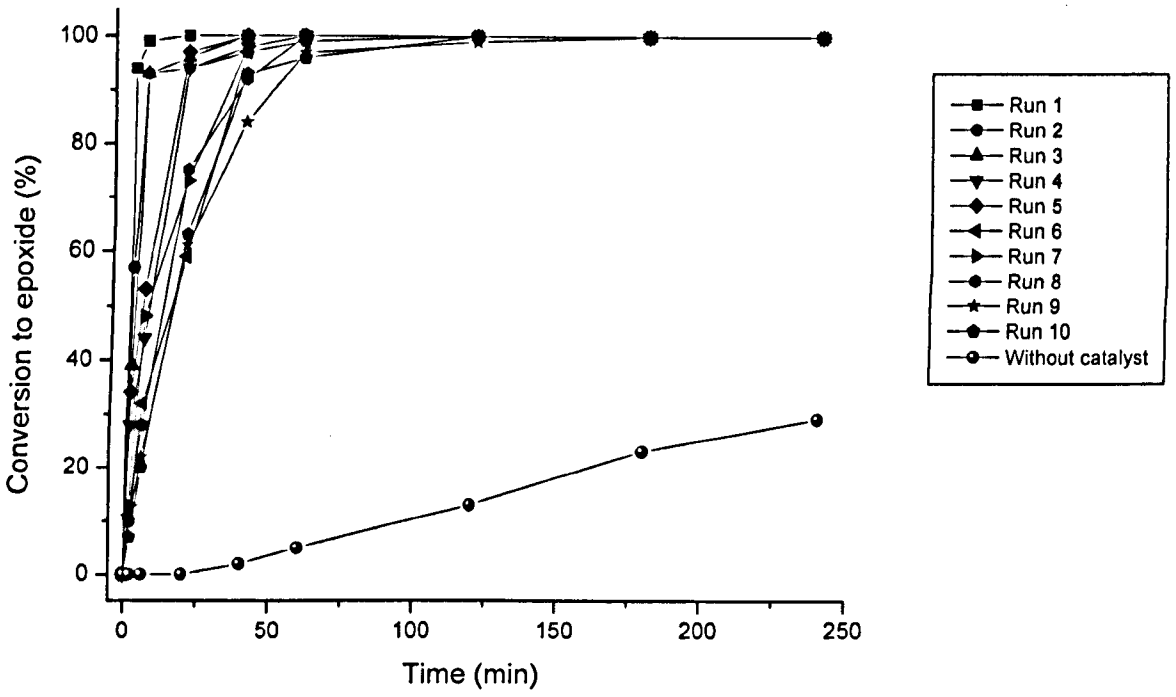

Figure 3.6 *Conversion curves for the epoxidation of cyclohexene using anhydrous TBHP at 80°C catalysed by* ***Ps.AMP.Mo (5%VBC)*** *(25) activated for 4 hours and recycled in 10 consecutive reactions ('large scale' reaction conditions).*

Ps.AMP.Mo (5%VBC) *(25) was prepared on a small scale with a ligand : $MoO_2(acac)_2$ mole ratio of 1 : 2.*

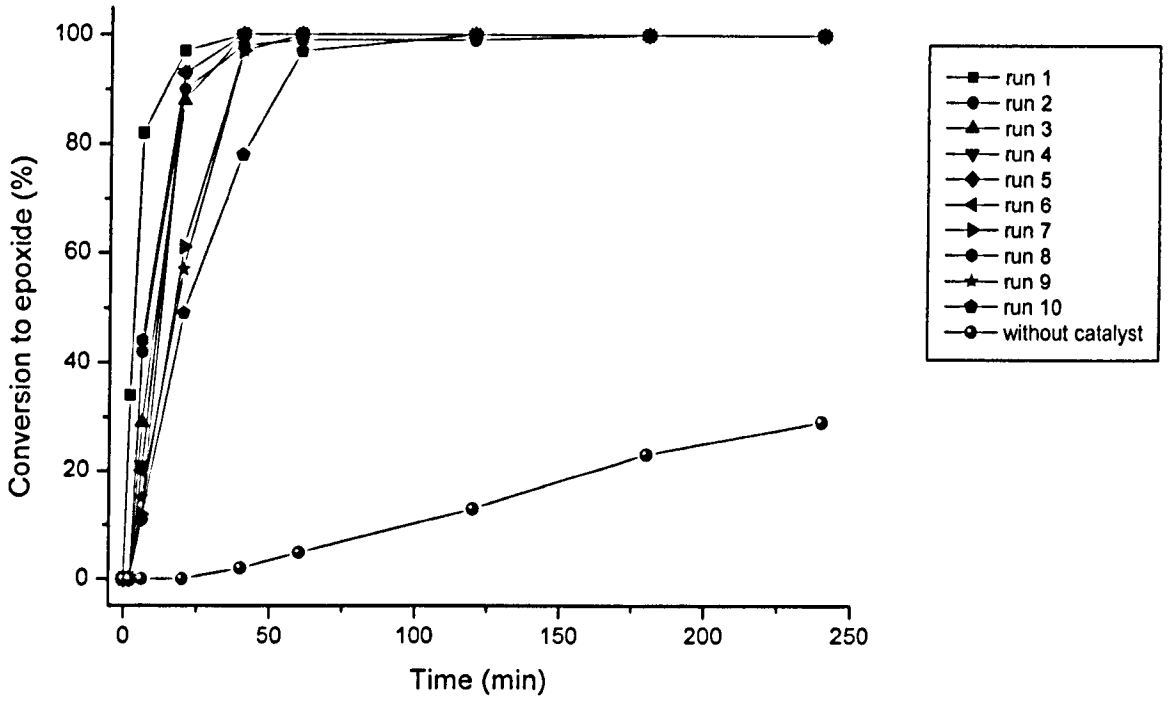

Figure 3.7 *Conversion curves for the epoxidation of cyclohexene using anhydrous TBHP at 80°C catalysed by* ***Ps.AMP.Mo (25%VBC)*** *(26) activated for 4 hours and recycled in 10 consecutive reactions ('large scale' reaction conditions).*

Ps.AMP.Mo (25%VBC) *(26) was prepared on a small scale with a ligand : $MoO_2(acac)_2$ mole ratio of 1 : 2.*

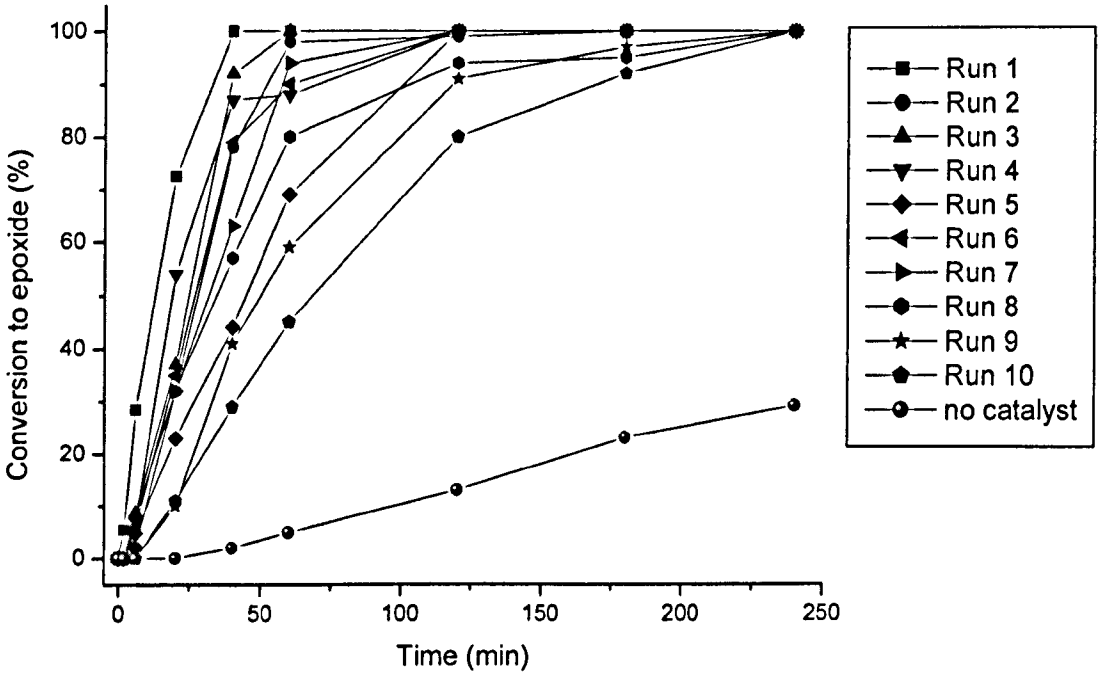

Figure 3.8 Conversion curves for recycling of ***Ps.AMP.Mo (88 % VBC)*** *(27) in epoxidation of cyclohexene by TBHP in 10 consecutive runs.* ***Ps.AMP.Mo (88%VBC)*** *(27) activated for 4 hours at 80°C ('large scale' reaction conditions).*

Ps.AMP.Mo (88%VBC) *(27) was prepared on a small scale with a ligand :$MoO_2(acac)_2$ mole ratio of 1 : 2.*

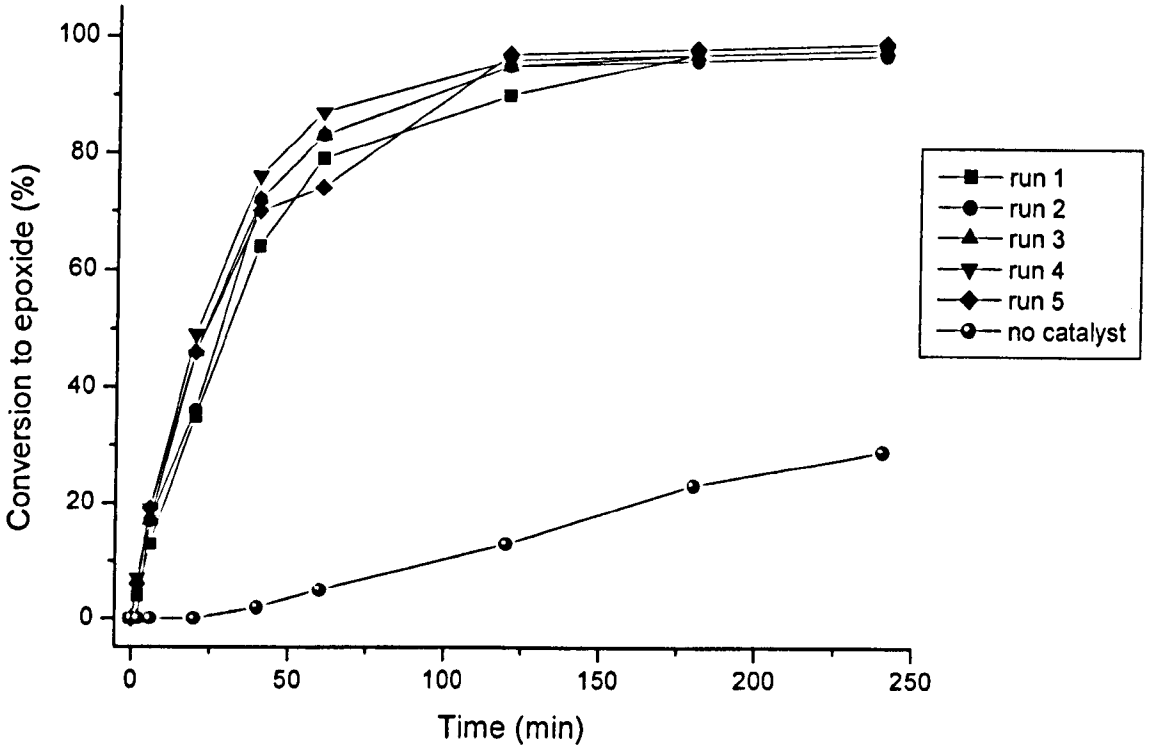

Figure 3.9 *Conversion curves for recycling of* ***Ps.AMP.Mo (88 % VBC) (36)*** *in epoxidation of cyclohexene by TBHP in 5 consecutive runs.* ***Ps.AMP.Mo (36)*** *activated for 4 hours at 80°C ('large scale' reaction conditions).*

Ps.AMP.Mo (36) *was prepared on a small scale with a ligand : $MoO_2(acac)_2$ mole ratio of 1 : 0.5.*

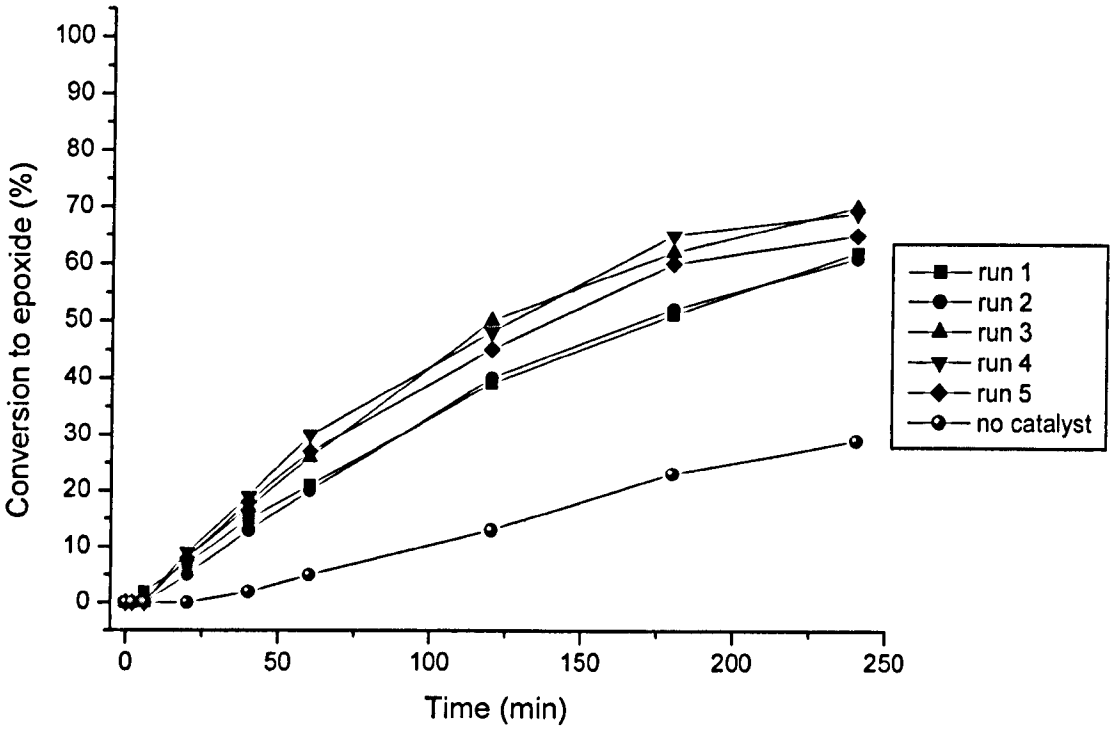

Figure 3.10 Conversion curves for recycling of ***Ps.AMP.Mo (88 % VBC) (37)*** *in epoxidation of cyclohexene by TBHP in 5 consecutive runs.* ***Ps.AMP.Mo (37)*** *activated for 4 hours at 80°C ('large scale' reaction conditions).*

Ps.AMP.Mo (37) *was prepared on a small scale with a ligand : $MoO_2(acac)_2$ mole ratio of 1 : 0.1.*

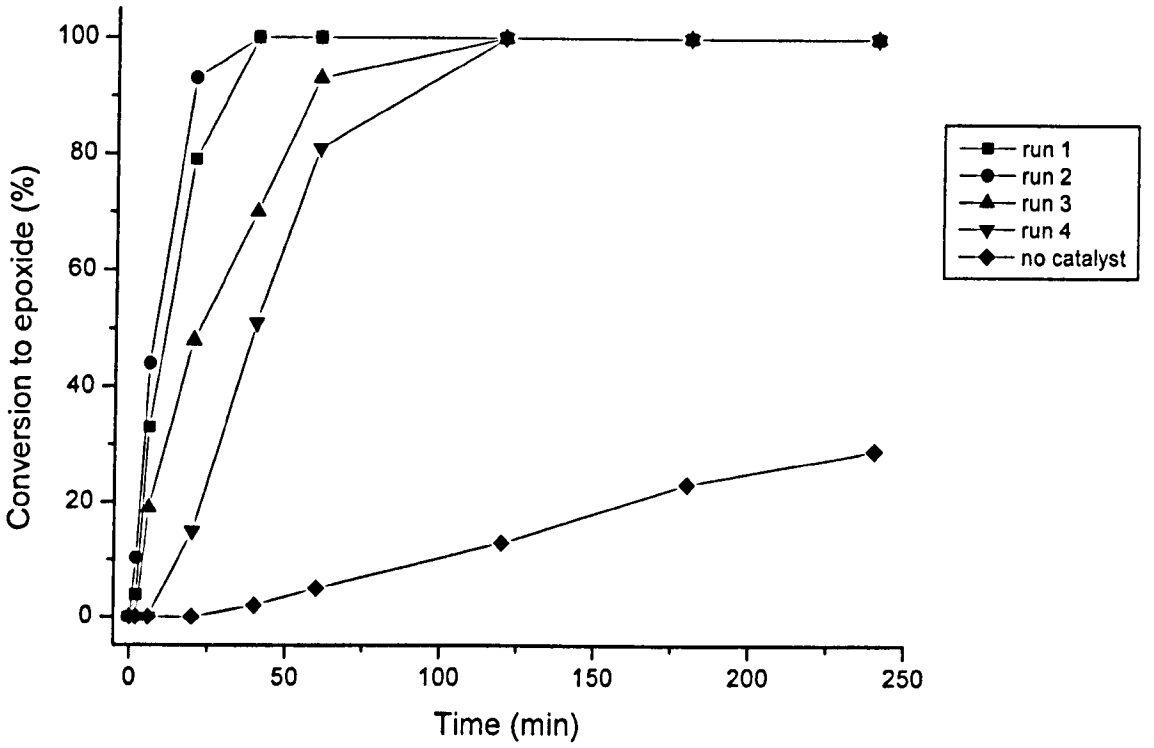

Figure 3.11 *Conversion curves for recycling of* ***Ps.AMP.Mo (88% VBC) (27)*** *in epoxidation of cyclohexene by TBHP in 4 consecutive runs.* ***Ps.AMP.Mo (27)*** *activated for 8 hours each day at 80°C for a period of 1 week ('large scale' reaction conditions).* ***Ps.AMP.Mo (27)*** *was prepared on a small scale with a ligand : $MoO_2(acac)_2$ mole ratio of 1 : 2.*

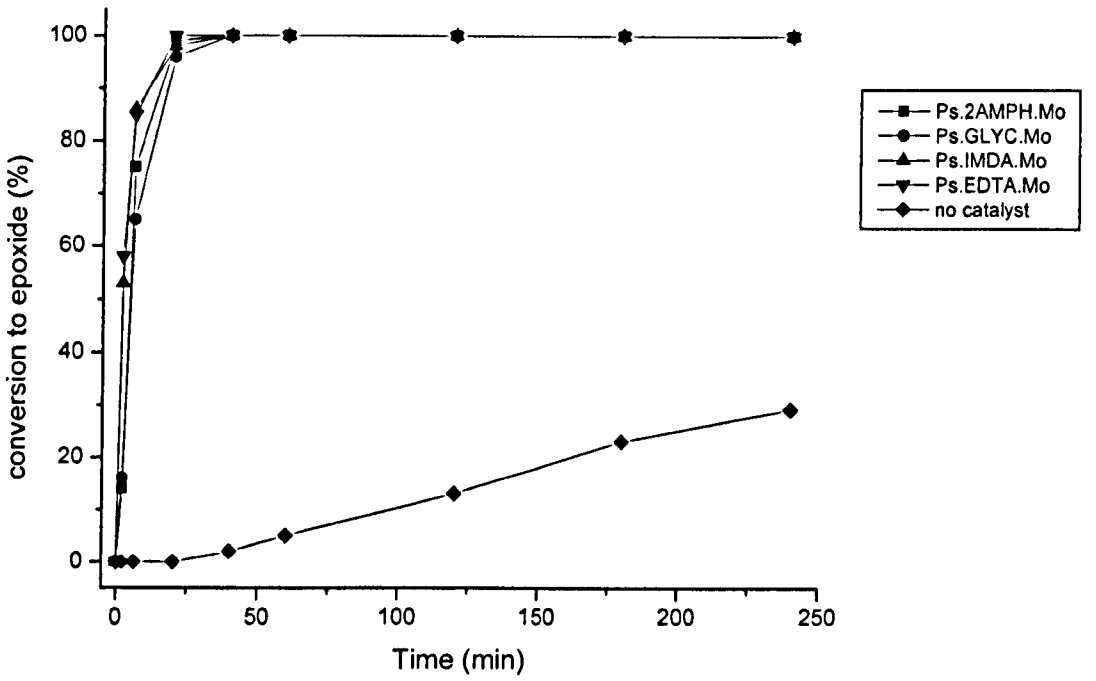

Figure 3.12 *Conversion curves for the epoxidation of cyclohexene at 80°C catalysed by* ■, ***Ps.2-AMPH.Mo*** (28); ♦, ***Ps.GLYC.Mo*** (29); ▲, ***Ps.IMDA.Mo*** (30); ▼, ***Ps.EDTA.Mo*** (31) *with TBHP. All catalysts activated for 4 hours at 80°C ('large scale' reaction conditions).*

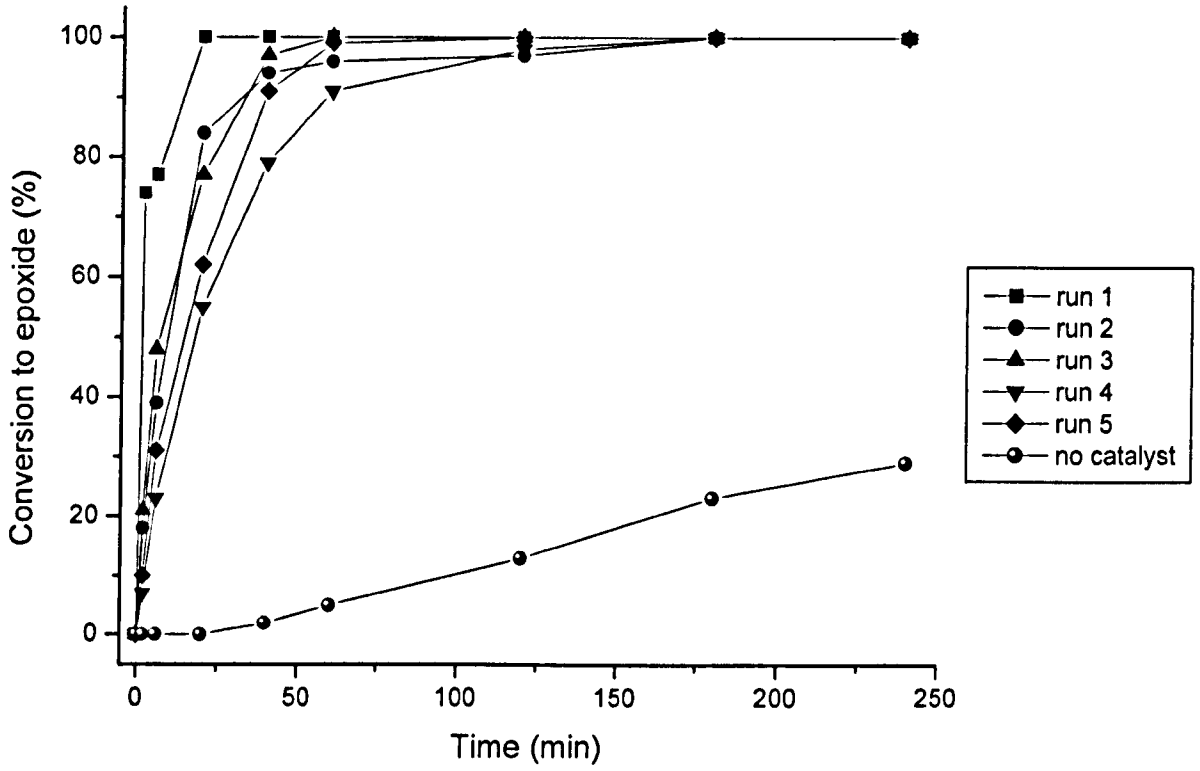

Figure 3.13 *Conversion curves for the epoxidation of cyclohexene using anhydrous TBHP at 80°C catalysed by* ***Ps.IMDA.Mo*** *(30) activated for 4 hours and recycled in 5 consecutive reactions ('large scale' reaction conditions).*

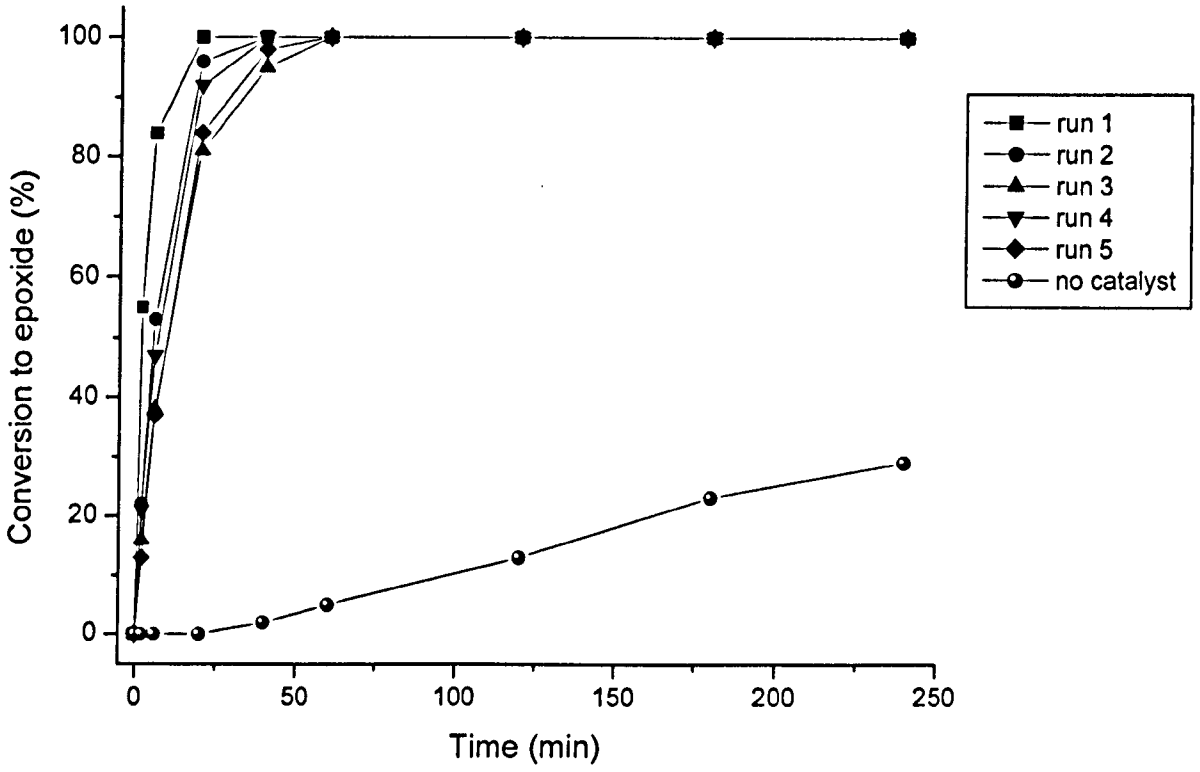

Figure 3.14 Conversion curves for the epoxidation of cyclohexene using anhydrous TBHP at 80°C catalysed by ***Ps.EDTA.Mo*** **(31)** *activated for 4 hours and recycled in 5 consecutive reactions ('large scale' reaction conditions).*

3.5.9.2 Mo leaching from polymer-supported Mo catalysts

In order to determine whether significant leaching of catalytically active Mo species occurs during reactions in the several consecutive cycles, each catalyst sample was filtered off after each run, and the corresponding supernatant solution, potentially containing leached Mo species, was evaporated to dryness. The resulting residue visible or not was used as a potential catalyst for cyclohexene epoxidation. All polymer-supported Mo catalysed reactions were carried out using the ('large scale' reaction conditions and examined using the same procedure. Data for the reactions using the residues from the corresponding supernatant solutions of all polymer-supported Mo catalysts are shown Figures 3.15-3.24. In the case of **PBI.Mo** batch 1 attempts were also made to quantify the leached Mo using AAS. These data are shown in Table 3.26.

Table 3.26 Supernatant liquids from **PBI.Mo batch 1**

Supernatant liquids from PBI.Mo batch 1 activated 4h	Absorbance	Metal loading (mmol g^{-1})	(g g^{-1})	% Mo leached
Run 1	0.003	0.00	0.00	0.00
Run 2	0.001	0.00	0.00	0.00
Run 3	0.002	0.00	0.00	0.00
Run 4	-0.003	0.00	0.00	0.00
Run 5	-0.003	0.00	0.00	0.00
Run 6	-0.005	0.00	0.00	0.00

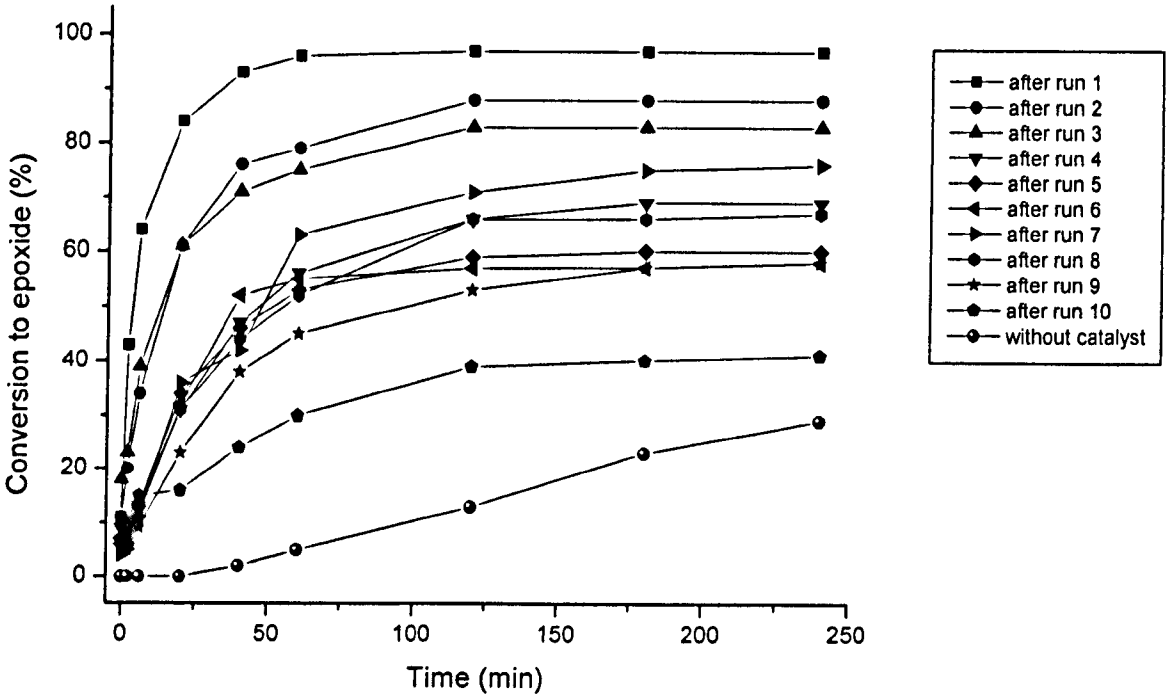

Figure 3.15 Conversion curves for the epoxidation of cyclohexene at 80°C using the residues from reaction supernatant liquids from ***PBI.Mo*** *batch 1 catalysed reactions as potential catalysts ('large scale' reaction conditions).*

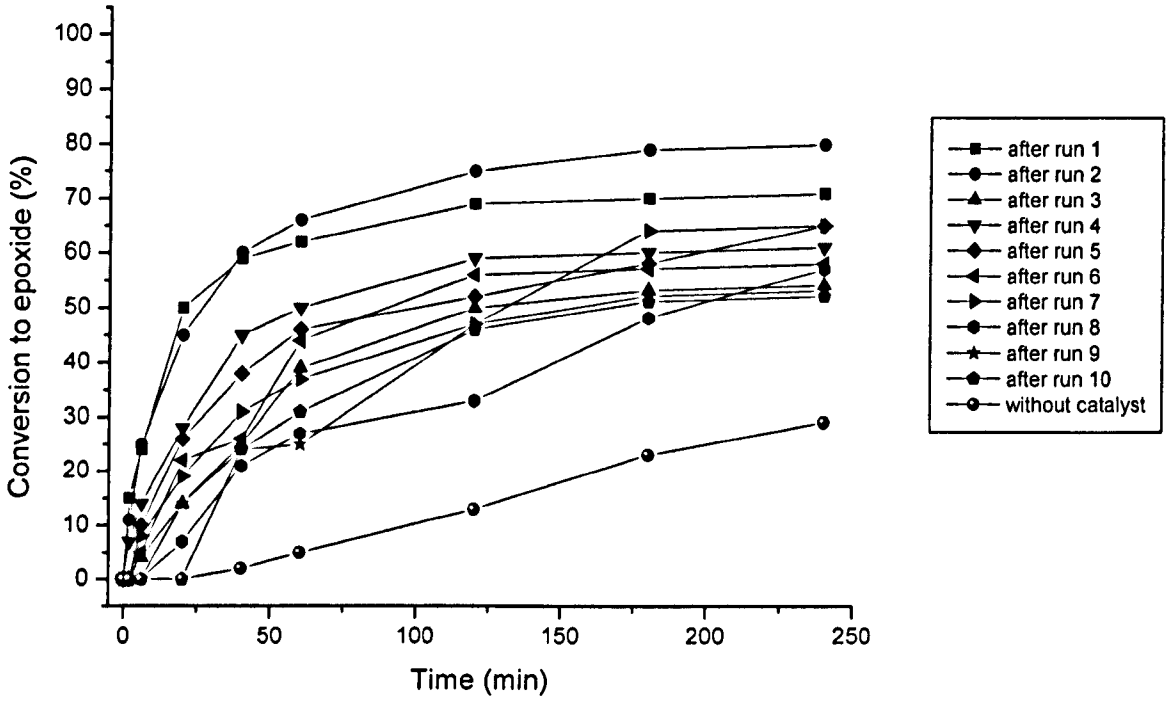

Figure 3.16 Conversion curves for the epoxidation of cyclohexene at 80°C using the residues from reaction supernatant liquids from ***PBI.Mo*** *batch 2 catalysed reactions as potential catalysts ('large scale' reaction conditions).*

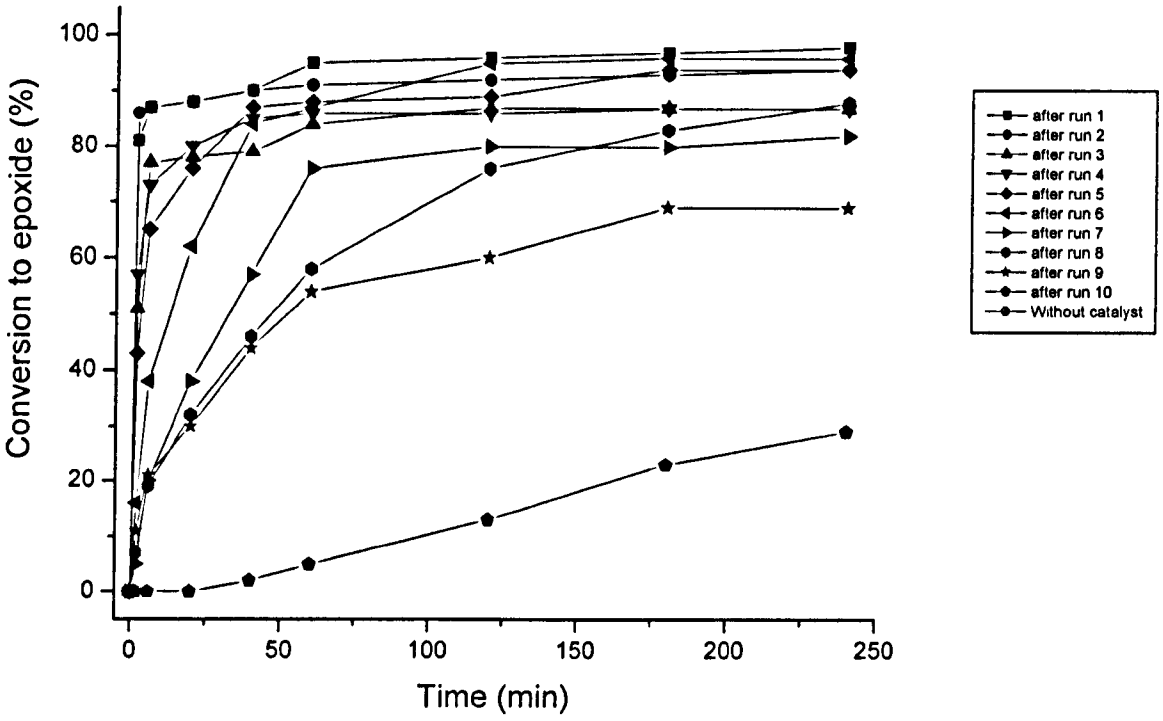

Figure 3.17 *Conversion curves for the epoxidation of cyclohexene at 80°C using the residues from the reaction supernatant liquids from* ***Ps.AMP.Mo (5% VBC)*** *(25) catalysed reactions as potential catalysts ('large scale' reaction conditions).*

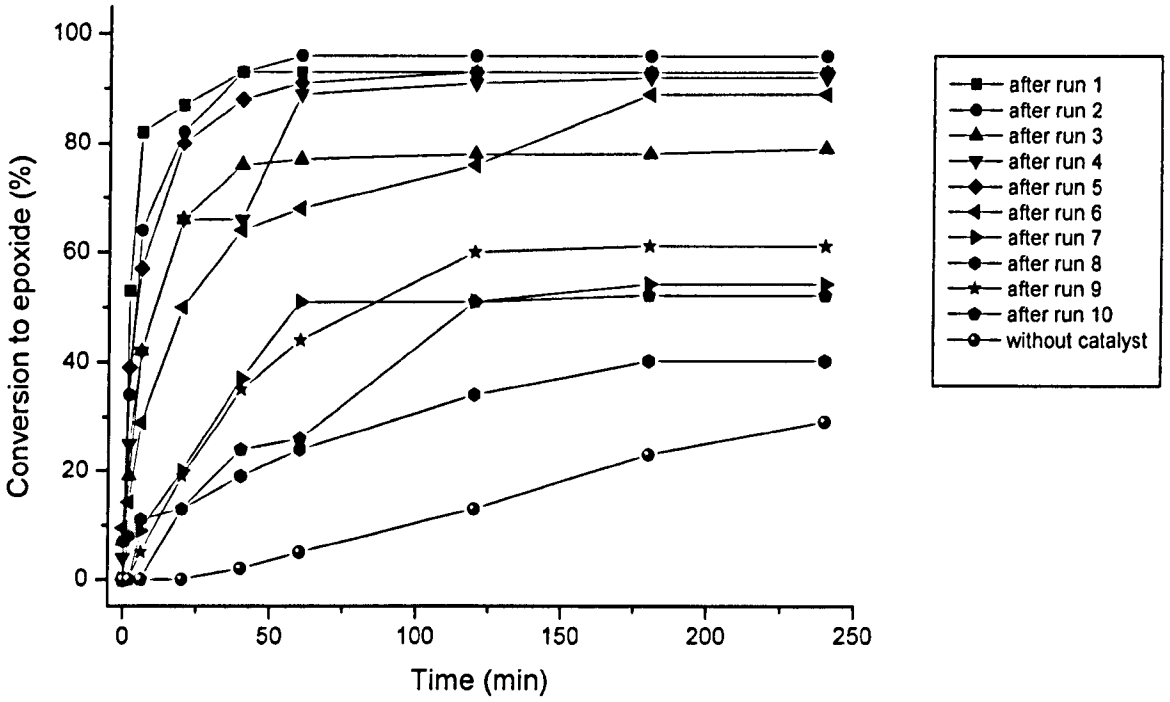

Figure 3.18 Conversion curves for the epoxidation of cyclohexene at 80°C using the residues from the reaction supernatant liquids from ***Ps.AMP.Mo (25% VBC) (26)*** *catalysed reactions as potential catalysts ('large scale' reaction conditions).*

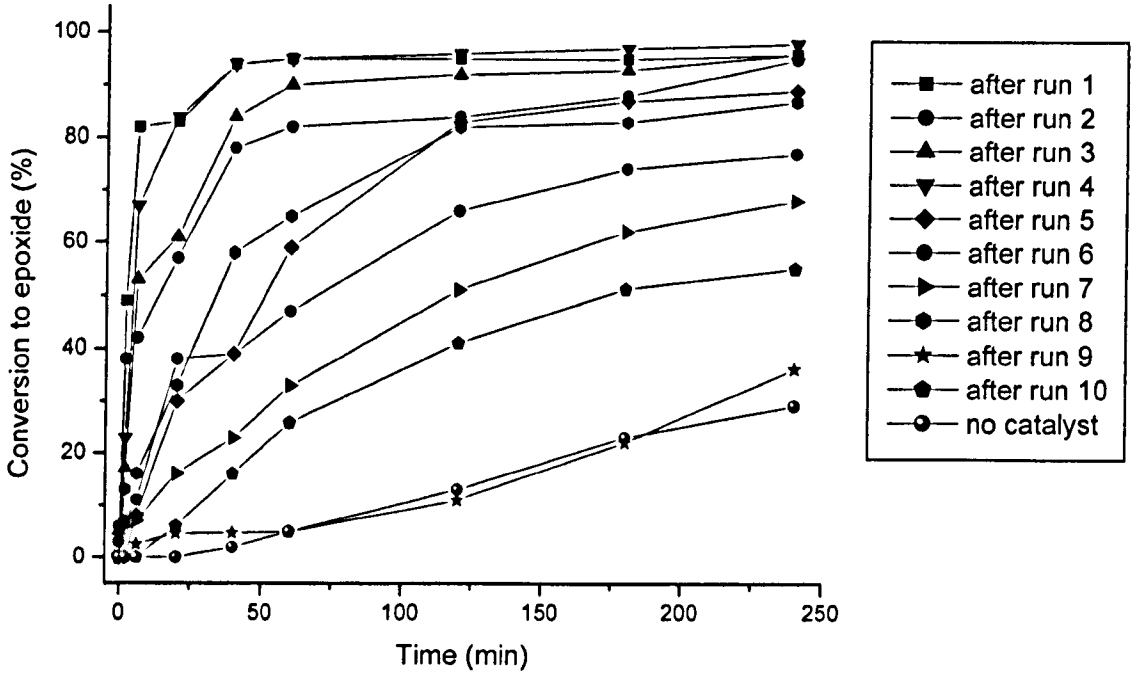

*Figure 3.19 Conversion curves for the epoxidation of cyclohexene at 80°C using the residues from the reaction supernatant liquids (**Ps.AMP.Mo (88% VBC)** (27) activated 4h) as potential catalysts ('large scale' reaction conditions).*

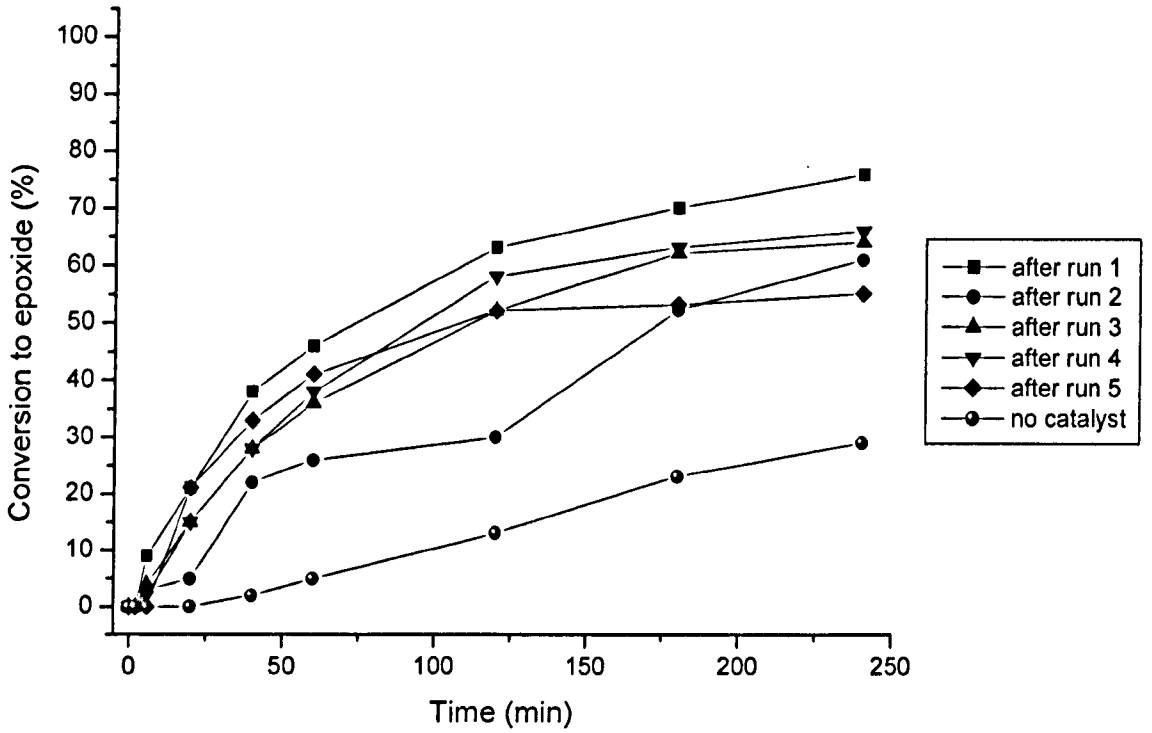

Figure 3.20 *Conversion curves for the epoxidation of cyclohexene at 80°C using the residues from the reaction supernatant liquids (**Ps.AMP.Mo (36) (88% VBC)** activated 4h) as potential catalysts ('large scale' reaction conditions).*

Ps.AMP.Mo (36) *was prepared on a small scale with a ligand : $MoO_2(acac)_2$ mole ratio of 1 : 0.5.*

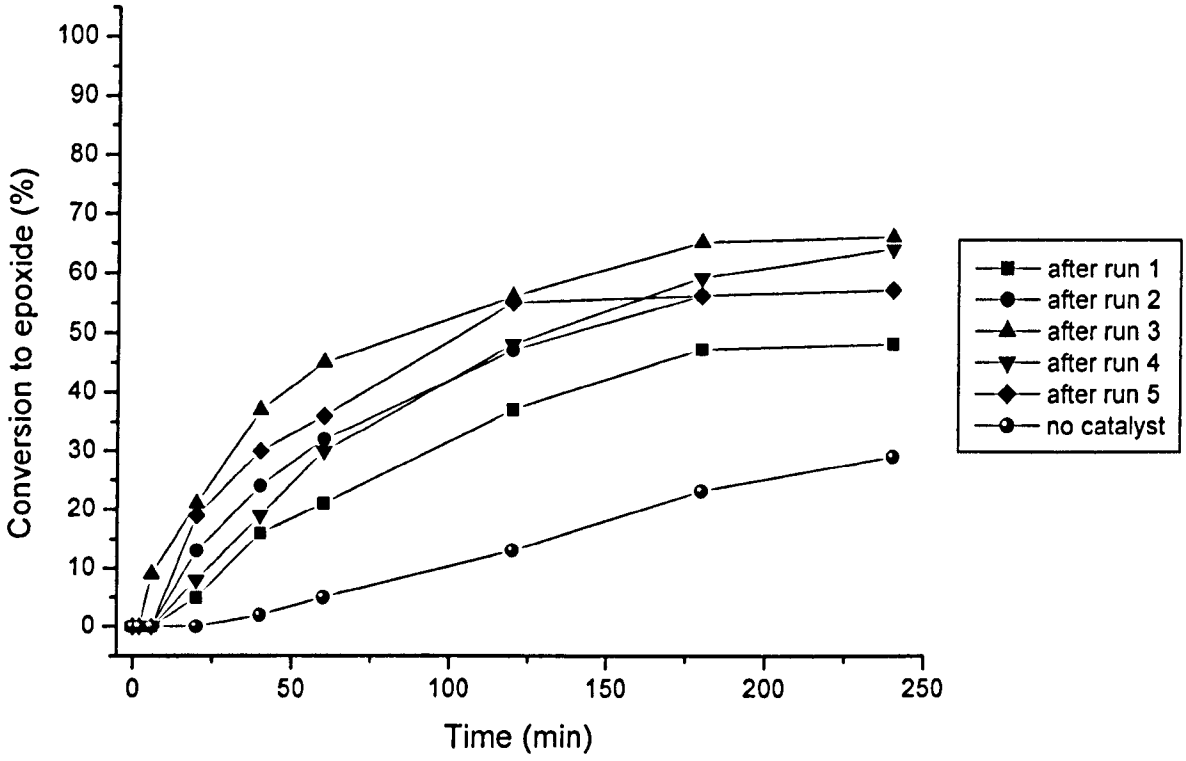

Figure 3.21 *Conversion curves for the epoxidation of cyclohexene at 80°C using the residues from the reaction supernatant liquids (**Ps.AMP.Mo (37) (88% VBC)** activated 4h) as potential catalysts ('large scale' reaction conditions).*

Ps.AMP.Mo (37) *was prepared on a small scale with a ligand : $MoO_2(acac)_2$ mole ratio of 1 : 0.1.*

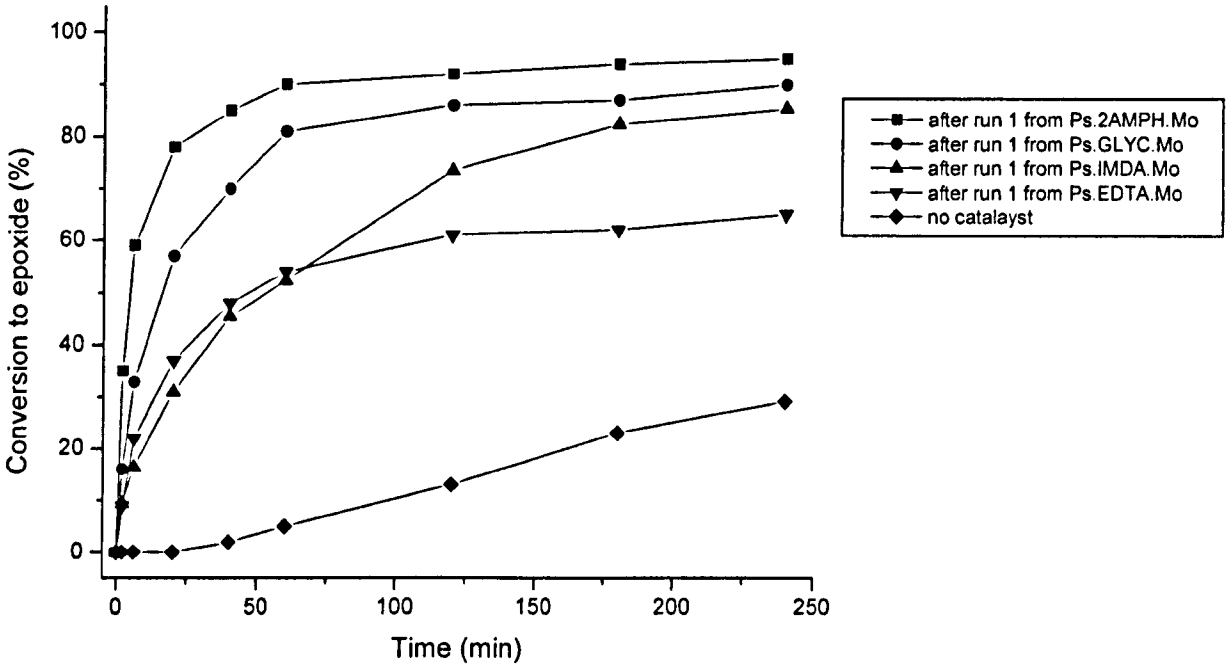

Figure 3.22 *Conversion curves for the epoxidation of cyclohexene at 80°C using the residues from reaction supernatant liquids from* ■, ***Ps.2-AMPH.Mo*** *(28);* ●, ***Ps.GLYC.Mo*** *(29);* ▲, ***Ps.IMDA.Mo*** *(30);* ▼, ***Ps.EDTA.Mo*** *(31) catalysed reactions as potential catalysts ('large scale' reaction conditions).*

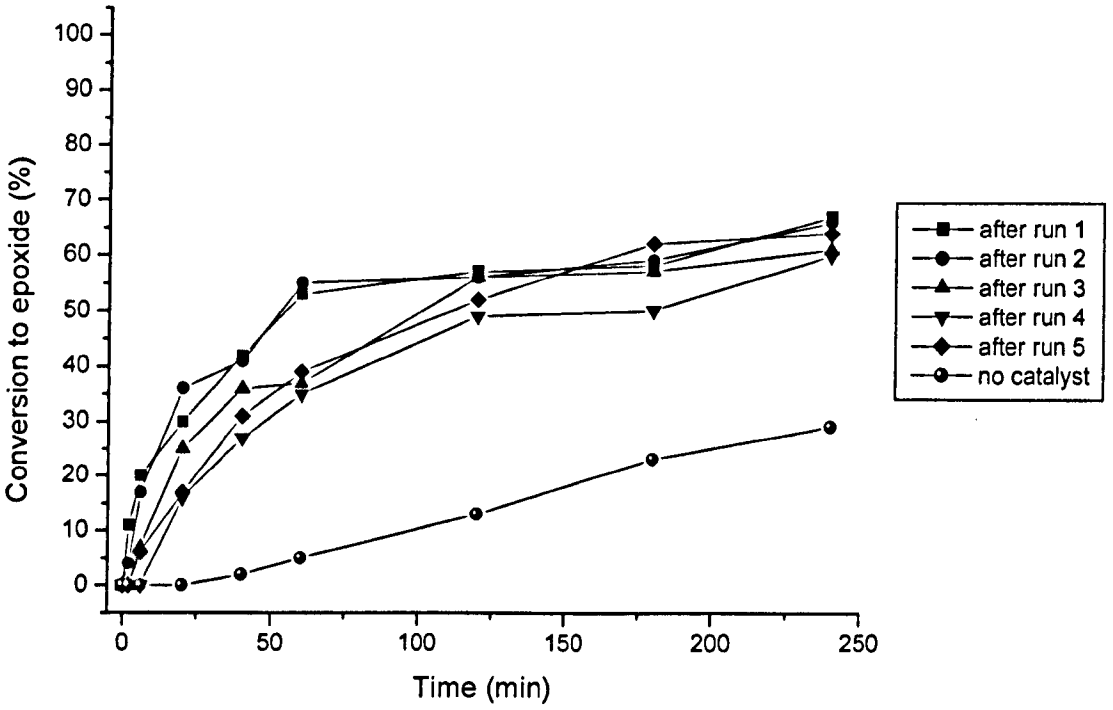

Figure 3.23 *Conversion curves for the epoxidation of cyclohexene at 80°C using the residues from the reaction supernatant liquids (**Ps.IMDA.Mo (30) (88% VBC)** activated 4h) as potential catalysts ('large scale' reaction conditions).*

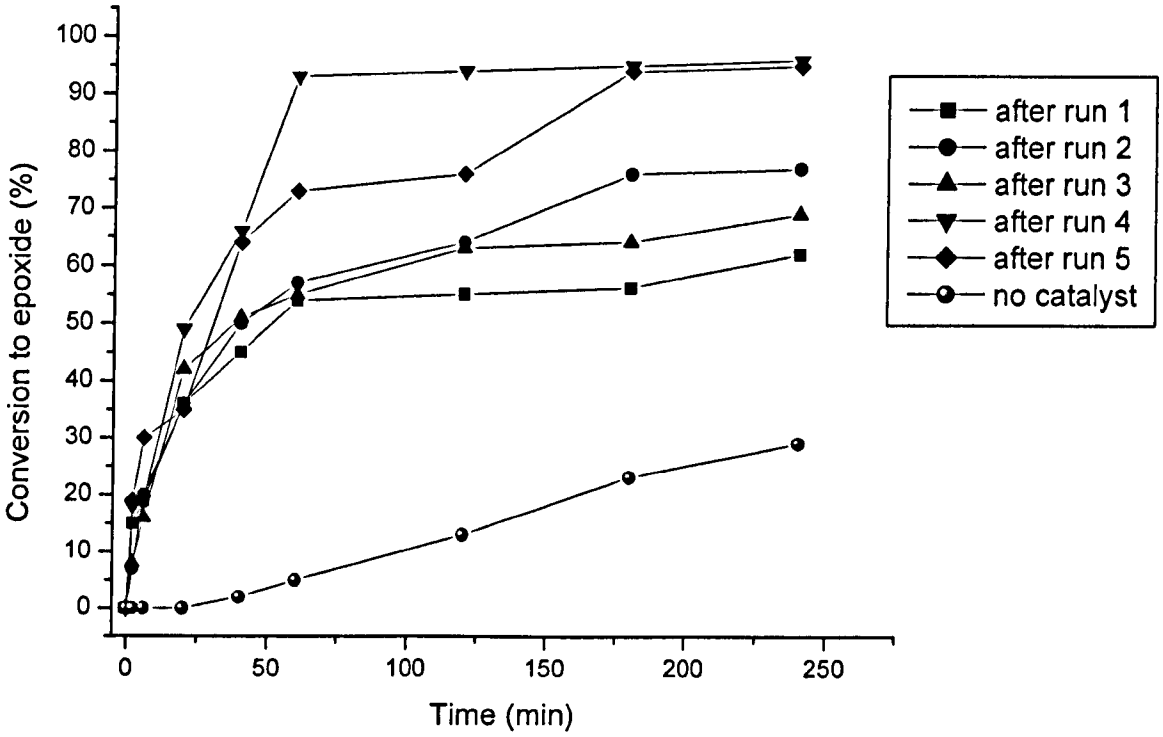

Figure 3.24 *Conversion curves for the epoxidation of cyclohexene at 80°C using the residues from the reaction supernatant liquids (**Ps.EDTA.Mo (31) (88% VBC)** activated 4h) as potential catalysts ('large scale' reaction conditions).*

3.5.9.3 Long-term activity of inorganic support MCM-41.SB.Mo (32) catalyst experiments

In order to assess the long-term activity of inorganic **MCM-41.SB.Mo (32)** catalyst, a sample of **MCM-41.SB.Mo (32)** catalyst was re-used in 5 consecutive reactions. Data from 5 consecutive runs using this inorganic Mo catalyst are shown in Figure 3.25.

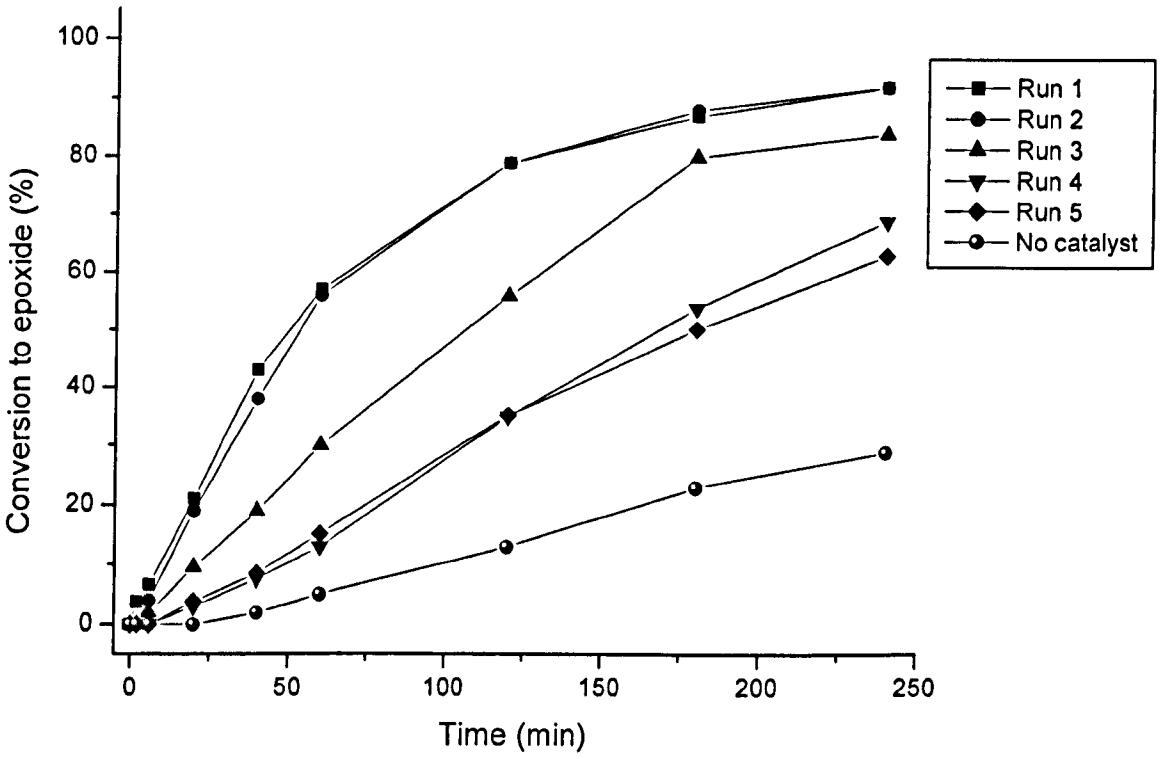

*Figure 3.25 Conversion curves for the epoxidation of cyclohexene using anhydrous TBHP at 80°C catalysed by **MCM-41.SB.Mo (32)** activated for 4 hours and recycled in 5 consecutive reactions ('large scale' reaction conditions).*

3.5.9.4 Mo leaching from inorganic support MCM-41.SB.Mo (32) catalyst experiments

In order to determine whether significant leaching of catalytically active Mo species occurs during reactions in the 5 consecutive cycles, a catalyst sample was filtered off after each run, and as with the polymer-supported Mo catalysts, the corresponding supernatant solution potentially containing leached Mo species, was evaporated to dryness. The resulting yellow residue was used as potential catalyst for cyclohexene epoxidation. Data for the reactions using these residues from inorganic Mo catalyst corresponding supernatant solutions are shown in Figure 3.25.

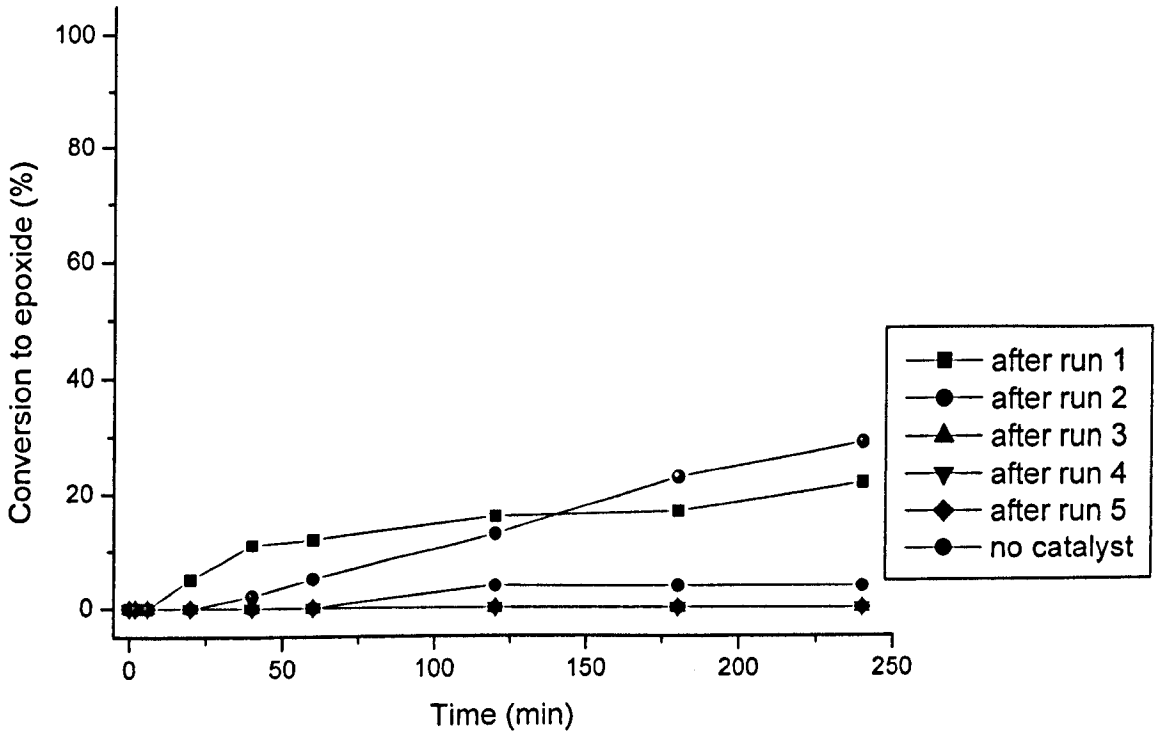

*Figure 3.26 Conversion curves for the epoxidation of cyclohexene at 80°C using the residues from the reaction supernatant liquids **MCM-41.SB.Mo** (32) activated 4h as potential catalysts ('large scale' reaction conditions).*

Chapter 4

Discussion

4.1 Synthesis of polymer supports.

4.1.1 Synthesis of the precursor chloromethylated polystyrene resins

All of the copolymerisations performed via free radical addition suspension polymerisation, were successful. For example the copolymerisations of DVB, VBC and styrene and the copolymerisation of DVB and VBC (Ps (VBC 88%) (11)) yield macroporous beads with surface area > 26 m^2 g^{-1} and good mechanical properties. The infra-red spectrum in 3.1 show a strong band at 1260 cm^{-1} characteristic of the CH_2Cl functional group, and elemental microanalytical data (Table 3.1) confirm the presence of the chlorine as expected.

The polystyrene resins (Ps (VBC 5%) (8)), (Ps (VBC 5%) (9)), (Ps (VBC 25%) (10)) were used as the precursor support for preparing the polymer complexes **Ps.AMP.Mo** (24 to 26) whereas (Ps (VBC 88%) (11)) was used as the precursor support for preparing the polymer complexes **Ps.AMP.Mo** (27), **Ps.AMPH.Mo** (28), **Ps.GLYC.Mo** (29), **Ps.IMDA.Mo** (30), **Ps.EDTA.Mo** (31), **Ps.Phe.Mo** (33) and **Ps.Schiff,base.Mo** (34).

4.1.2 Synthesis of AMP chelating polystyrene resins (Ps.AMP) (16)

Synthesis of AMP chelating polystyrene resins involved a nucleophilic substitution of the CH_2Cl functional groups by the primary amino group of AMP. The amination reactions of the chloromethylated polystyrene resins were all satisfactory. Elemental microanalytical data in 3.1 (Table 3.2) reveal that the conversion of the CH_2Cl groups lies between 53% and 100%, and the infra-red absorption band at 1260 cm^{-1} characteristic of the CH_2Cl functional group become considerably weaker. This observation confirms the successful amination of the chloromethylated polystyrene resins (see Scheme 2.1). The ligand loading data are shown in Table 3.2.

4.1.3 Synthesis of 2-AMPH, GLYC, IMDA and EDTA chelating polystyrene resins

Two types of functionalised polystyrene resins have been used as the precursor support resins in this present work. The chloromethylated polystyrene resin (**11**) was reacted directly with the different ligands aminomethylpyridine, 2-aminophenol, glycine or iminodiacetic acid (AMP, 2-AMPH, GLYC and IMDA). The poly (4-aminomethyl styrene) resin (**12**) was obtained using Gabriel's procedure, by transforming the chloride functional groups of the chloromethylated polystyrene resin (**11**) to the primary amine functional groups. Thus the resulting poly(4-aminomethyl styrene) resin (**12**) was reacted with the ligand ethylenediaminetetraacetic acid (EDTA) according to Supuran's procedure[1,2].

Attachment of the ligands AMP, 2-AMPH, GLYC and IMDA to chloromethylated polystyrene resin (**11**) also involved a nucleophilic substitution of the CH_2Cl functional group by the primary or secondary amino group of the different ligands (see Schemes 2.1, 2.2, 2.3 and 2.4). These amination reactions were all satisfactory. Elemental microanalytical data (Table 3.2) reveal that the conversion of CH_2Cl lies between 77% and 100%, and the infra-red absorption band at 1260 cm^{-1} characteristic of the CH_2Cl functional group become considerably weaker. This observation confirms the successful amination of the chloromethylated polystyrene resins (see Schemes 2.1 to 2.4). The ligand loadings are shown in Tables 3.2 and 3.3.

4.1.4 Synthesis of EDTA chelating polystyrene resin from resin (12).

Synthesis of resin Ps.EDTA (**20**) involved a selective monoamidation of one of the tetraacetic acid functional groups of the ETDA by the primary amino groups of resin (**12**). The amidation reaction resin was satisfactory. Elemental microanalytical data (Table 3.2) reveal that the amount of nitrogen content of resin (**20**) increases in comparison with the initial poly(4-aminomethyl styrene) (**12**) and the infra-red absorption

spectrum also reveals the appearance of a weak band at 1771 cm^{-1} characteristic of the amide functional group (see Scheme 2.6). These observations confirm the successful amidation of the polymer resin as illustrated by the ligand loadings in Table 3.2 and 3.3.

4.1.5 Synthesis of Phe chelating polystyrene resin Ps.Phe (22)

Synthesis of Ps.Phe (22) involved the functionalisation of the chloromethylated polystyrene resin (11) by (L)-phenylalanine methyl ester ligand (Phe). The amination reaction was satisfactory. Elemental microanalytical data (Table 3.2) reveal the appearance of a significant amount of nitrogen (4.20 % N) in the resulting resin (22) and the infra-red absorption spectrum also shows the appearance of a strong band at 1676 cm^{-1} characteristic of the carbonyl functional group of (L)-phenylalanine methyl ester ligand (Phe) (see Scheme 2.11). These observations confirm the successful amination of the polymer resin as illustrated by the ligand loadings in Table 3.2 and 3.3.

4.1.6 Synthesis of Schiff base chelating polystyrene resin Ps.SB (23)

Synthesis of resin Ps.SB (23) was carried out in two steps reactions. The 2,4-dihydroxybenzaldehyde ligand was first attached to the polystyrene resin (11) via a nucleophilic substitution of the CH_2Cl functional group by the 4-phenolic group of the 2,4-dihydroxybenzaldehyde ligand. This etherification reaction was also satisfactory (see Scheme 2.13). Elemental microanalytical data (Table 3.1) reveal that the conversion of CH_2Cl lies around 92% and the infra-red absorption spectra bands at 1260 cm^{-1} characteristic of the CH_2Cl functional group become considerably weaker. Thus the resulting functionalised polystyrene-2,4-dihydroxybenzaldehyde resin was reacted with (L)-phenylalanine methyl ester ligand to yield chelating polystyrene resin Ps.SB (23). This imination reaction was also satisfactory. Elemental microanalytical data (Table 3.2) reveal a significant of nitrogen content (1.74 % N) in the resulting resin (23) and the

infra-red absorption spectrum also shows the appearance of a strong band at 1626 cm^{-1} characteristic of the imine functional group (see Scheme 2.14). These observations confirm the successful imination of the polymer resin as illustrated by the ligand loadings in Table 3.2 and 3.3.

4.2 Synthesis of inorganic support.

As stated earlier in 1.2.4.4 immobilisation of catalysts on inorganic supports has also several potential advantages over the use of organic polymer supports. The chemical stability of the inorganic supports allows their use in harsh and high temperature oxidizing conditions. In addition, their mechanical stability is often excellent and often superior than organic polymer supports counterparts.

The discovery of mesoporous MCM-41 materials has given an enormous stimulus to research in heterogeneous catalysis[3-6]. This is due to their outstanding advantages such as their hexagonal arrays of one dimensional channels of uniform mesoporous with pore diameter in the range 15-100 Å, depending on the nature of the template and synthesis conditions.

The main drawback of MCM-41 support materials for practical applications is their rather low hydrothermal stability. The structure hexagonal of MCM-41 arranged with silica framework is only stable when surfactant template molecules are present. To overcome this scope many research groups reported new improved hydrothermal stability synthesis of MCM-41 materials.

Chen et al[7] reported that the calcined MCM-41 samples, which have no template molecules are present in their pores, have very poor structural stability, especially in hot water. By contrast, the crystalline structure of pure silica MCM-41 was found to be retained up to 850 °C and even in a 100% steam flow under atmospheric pressure at 500 °C. However the structure of MCM-41 collapses if it is placed in hot water or aqueous solutions for an extended period of time. Partial substitution of Si by other atoms like Ti or Al are reported to improve the thermal and hydrothermal stability to some extent[8]. It

has been also reported that improved hydrothermal stability can be achieved by adjusting the gel pH several times during the thermal crystallization process[9]. However this pH adjustment is a tedious process and limits this method. Das et al[10] reported that the hydrothermal stability of MCM-41 material can be improve significantly by simply adding different cations such as tetraalkylammonium (TAA^+) or sodium (Na^+) ions to the synthesis medium gel and without the necessity of multiple pH adjustment steps. They also claimed that highly ordered MCM-41 materials were obtained only at cation surfactant molar ratios between 0.6-1.4. It seems that the presence of cations in the synthesis medium gel could facilitate and increase condensation of the silanol groups during the formation of the mesostructure of the MCM-41 material. The resulting MCM-41 crystalline detemplated structure has been proved to remain stable after impregnation with hot water at 100°C for 4 days. However Lin et al[11] reported a simple and effective strategy for the preparation of pure silica MCM-41 with high order and high hydrothermal stability by using in place of NaOH, small organic weak bases such as methylamine (MA), dimethylamine (DMA), ethylamine (EA)and diethylamine (DEA). These act as a buffer in the synthesis medium gel. MCM-41 samples synthesized with organic bases display excellent thermal stability up to 1373 K in air after removal of the templates and also prove to be very hydrothermally stable when the calcined structure of MCM-41 samples are impregnated with hot water at 100°C for 24 h and 48 h, the structure of MCM-41 remains intact. The authors believe that the high thermal and high hydrothermal stability of MCM-41 materials are related exclusively to the use of organic bases since the condensation between silicate species depend significantly on the geometry, charge density and polymerization of the silicate polyanions present in the synthesis medium. These three factors are closely related to the pH value of the solution. When tetraethoxysilane (TEOS) is used as the silica source and NaOH is used as the mineralizing agent, HO^- is consumed as the reaction (1) proceeds.

$$n\ Si(OC_2H_5)_4 + OH^- + n\ H_2O \longrightarrow [Si_nO_{4n}H_{4n-1}]^{-1} + 4n\ C_2H_5OH$$

$$[Si_nO_{4n}H_{4n-1}]^{-1} + CTA^+ \longrightarrow MCM\text{-}41. \qquad (1)$$

Thus, the pH of the synthesis medium decreases because the mineralizing agent NaOH is consumed during the formation of MCM-41. In contrast, when amines are used as mineralizing agents, they can replenish the consumed HO^- via their hydrolysis, and therefore offer a fixed pH value for the formation of MCM-41 as shown in reaction (2) illustrated with the ethylamine used as mineralizing agent.

$$\begin{aligned} &C_2H_5NH_2 + H_2O \longrightarrow C_2H_5NH_3^+ + OH^- \\ &n\ Si(OC_2H_5)_4 + OH^- \longrightarrow [Si_nO_{4n}H_{4n-1}]^{-1} + 4n\ C_2H_5OH \\ &[Si_nO_{4n}H_{4n-1}]^{-1} + CTA^+ \longrightarrow MCM\text{-}41. \end{aligned} \qquad (2)$$

Thus, under these conditions, the building blocks (the silicate anions) of the silica wall of MCM-41 can be produced with uniform and excellent degree of polymerization and charge density. As a result, a well-condensed structure of MCM-41 material with high order and high stability is synthesised. Therefore, the organic mineralization agents in effect act as buffer in the synthesis media. This synthetic method was used in our present work for the synthesis of our MCM-41 material as emphasized in 2.3.1.

4.2.1 Synthesis of MCM-41 inorganic resin

The calcined MCM-41 material used as the precursor support in this present work, has been synthesised successfully by our Spanish collaborator according to Lin's procedure in which cetyltrimethylammonium bromide (CTAB) is used as surfactant, dimethylamine (DMA) is used as mineralizing agent and in presence of tetraethoxysilane (TEOS) which is used as the silica source. The chemical compositions and structural characteristics such as surface area and pore diameter of our detemplated MCM-41 sample are in agreement with the earlier findings[11, 12, 13].

4.2.2 Synthesis of the amine functionalised MCM-41 inorganic resin

The modification of the MCM-41 channel wall with 3-aminopropyl-trimethoxysilane (APTMS) was again carried out successfully by our Spanish collaborator. Elemental analysis of the final product shows the appearance of nitrogen (2.51% N) and the infra-red absorption spectrum also displays a strong band at 3435 cm^{-1} characteristic of amine functionality group. These observations confirm that the successful grafting of 3-aminopropyl-trimethoxysilane to the MCM-41 material.

4.2.3 Synthesis of the Schiff Base MCM-41 (21)

Direct reaction of the modified MCM-41 and thiophene-2-carboxyaldehyde in ethanol at 60°C generated the functionalised imine-MCM-41 material referred to as Schiff Base MCM-41. Elemental microanalysis of this shows the appearance of sulfur (2.18% N) and the infra-red absorption spectrum also exhibits the disappearance of the amine peak at 3435 cm^{-1} and the appearance of new strong band at 1638 cm^{-1} characteristic of imine functionality group. All these observations confirm the successful synthesis of the Schiff Base MCM-41 material.

4.3 Synthesis of supported Mo (VI) complexes

4.3.1 Synthesis of polymer-supported Mo (VI) complexes

PBI.Mo and all the corresponding polystyrene Mo complexes were prepared using a ligand exchange procedure in which the PBI and the Ps.AMP resins were reacted with an excess of $MoO_2(acac)_2$ under reflux in toluene for 4 days. The unreacted $MoO_2(acac)_2$ was removed by filtration and by washing the beads for several hours with acetone. The resins changed colour during this period from mauve to green for **PBI.Mo**, to blue for

the **Ps.AMP.Mo** complexes, and to a brown coloured complex for **Ps.2-AMPH.Mo**, to a green coloured complex for **Ps.GLYC.Mo**, to a blue coloured complex for **Ps.IMDA.Mo** and to a grey coloured complex for **Ps.EDTA.Mo**. The Mo loading data in 3.3.1 (Table 3.6 to 3.9) were determined on a standard atomic absorption spectrophotometer, and the results of all the analyses of the polymer-supported Mo species are very satisfactory and the polymeric complexes are suitable for catalytic applications. The metal loading in all polymer resins varies from 0.2-1.4 mmol of Mo per gram of resin, with ligand : metal ratios > 1, suggesting that each metal centre is complexed by at least one ligand.
The IR spectra (Table 3.3-3.5) also show for all complexes the presence of two strong bands at 900-910 and 930-988 cm^{-1} which can be assigned to the asymmetric and symmetric stretches of the MoO_2 group. There are however no clear bands at 720-740 cm^{-1} characteristic of a bridged Mo-O-Mo species[14, 15].

4.3.2 Synthesis of inorganic-supported Mo (VI) complex

The inorganic Mo complex was synthesised using a ligand exchange procedure in which the Schiff base MCM-41 material was reacted with an excess of $MoO_2(acac)_2$ under reflux in ethanol for 24 hours. The unreacted $MoO_2(acac)_2$ was removed by filtration and by washing the beads for several hours with ethanol. The material changed colour during this period from brown light to green. The Mo loading data (Table 3.6) was determined on a standard atomic absorption spectrophotometer, and the result of the analysis of the inorganic-supported Mo species was very satisfactory and suitable for catalytic applications. The metal loading in inorganic material was 0.62 mmol of Mo per gram of material, with ligand : metal ratio > 1, also suggesting that each metal centre is complexed by at least one ligand. The IR absorption spectrum (Table 3.3) also shows again the presence of two strong bands at 900-910 and 930-988 cm^{-1} which can be assigned to the asymmetric and symmetric stretches of the MoO_2 group. There are however no clear bands at 720-740 cm^{-1} characteristic of a bridged Mo-O-Mo species[15].

4.4 Cyclohexene epoxidations catalysed by supported Mo complexes under typical reactions conditions of 'large scale' synthesis

4.4.1 Effect of reaction temperature with $MoO_2(acac)_2$ and PBI.Mo as catalysts

The effect of temperature on TBHP conversion was studied in order to optimize the epoxidation of cyclohexene The preliminary results using homogeneous $MoO_2(acac)_2$ and heterogeneous **PBI.Mo** are shown in 3.5.2. and 3.5.3 respectively (Tables 3.10 and 3.12). The homogeneous $MoO_2(acac)_2$ catalyst yields 78% conversion of TBHP after 20 min of reaction at room temperature and this conversion remains the same after 240 min of reaction at room temperature. Increasing the temperature to 40°C increases the yield of TBHP to 85% after 20 min of reaction and again the reaction yield stays identical after 240 min of reaction at 40°C. It seems that the reaction has reached a plateau after a short period of time. The highest conversion of TBHP obtained with $MoO_2(acac)_2$ as catalyst, is 94% after 20 min of reaction at 80 °C and this yield stays the same after 240 min of reaction. It is clear that the higher temperature (80°C) gives the better conversion of TBHP with homogeneous $MoO_2(acac)_2$ as catalyst despite the fact that the epoxidation is incomplete even for a long reaction time. It is also apparent as shown in Tables 3.10 and 3.12 that the reaction rate catalysed by homogeneous $MoO_2(acac)_2$ is faster than with the heterogeneous **PBI.Mo** species, e.g. after 2 min of the reaction, nearly 90% conversion of TBHP was achieved at 80°C with $MoO_2(acac)_2$ whereas 73% conversion of TBHP was achieved with **PBI.Mo**. However, a significant result is that the heterogeneous **PBI.Mo** species gives the highest conversion of TBHP ~100 % after 40 min of reaction and the best selectivity of epoxide (~100%). The latter observation confirms that **PBI.Mo** is very potent and a better catalyst than the homogeneous $MoO_2(acac)_2$ counterpart (Table 3.12) in the case of the epoxidation of cyclohexene.

4.4.2 Effect of water on homogeneous $MoO_2(acac)_2$ and PBI.Mo as catalysts

On the basis of the results of experiments which are shown in 3.5.2 (Table 3.10), it is clear that the homogeneous species $MoO_2(acac)_2$ is a good catalyst for the epoxidation of cyclohexene because it gives high yields of cyclohexene oxide with high selectivity and good reaction rates. Indeed, with homogeneous $MoO_2(acac)_2$ as catalyst, the reaction rate is very fast with high yield (>78%) of cyclohexene epoxide even at room temperature. Using homogeneous $MoO_2(acac)_2$ as catalyst, in the presence of wet-TBHP (as supplied directly from the Aldrich Chemical Co.) as oxidant and with a high cyclohexene concentration, the reaction rate is still high with initially a good yield (>80%) of epoxide. However further reaction occurs to yield primarily 1,2-cyclohexanediol as shown in 3.5.2.1 (Figure 3.2). Clearly the initially formed cyclohexene oxide is rapidly and efficiently hydrolysed to 1,2-cyclohexanediol. Interestingly however the reaction catalysed by **PBI.Mo batch 1** as illustrated in 3.5.4 (Figure 3.3) using wet-TBHP as oxidant, is slower than when the TBHP is anhydrous but it does not show the same hydrolysis observed with the use of homogeneous $MoO_2(acac)_2$ as catalyst, and in effect the resin provides some protection to the epoxide. Why this is so remains unclear at the moment. Possibly the resin acts as a water scavenger.

4.4.3 Catalyst activation

All polymer catalysts and an inorganic support catalyst were activated under reflux or at room temperature in an excess of TBHP in dichloroethane for periods from 4h, 24h, 48h to 1 month. During this activation process, all catalysts changed their initial colours to yellow complexes. These observations confirm earlier findings[15-18] and suggest that during the activation process, each polymer-supported complex generates a high level of Mo in oxidation state +VI, which seems to be responsible for the immediate high activity and selectivity of the polymer-supported Mo complexes. However a significant result is that for **PBI.Mo** a non-activated sample is also extremely active (Table 12) at 80°C. It

seems evident in this case that the pre-activation (oxidation) of the **PBI.Mo** complex is not necessary for producing an active catalyst (Table 12) presumably any oxidation to the highest oxidation state occurs very rapidly in the reaction or the complex is already in the +VI state. Again this result is in agreement with earlier findings[15-18].

4.4.4 Long-term activity of supported Mo catalysts

4.4.4.1 Long-term activity of PBI.Mo and Ps.AMP.Mo catalysts

In order to assess the long-term activity of each polymer catalyst a sample of each polymer catalyst was re-used in 10 consecutive reactions.

Data for 10 consecutive runs using as catalysts **PBI.Mo batch 1** activated 4h or **PBI.Mo batch 2** activated for 1 month at room temperature curves are shown in Figures 3.4 and 3.5. These demonstrate that the catalysts are still extremely active even over 10 runs. The high and sustained activity and selectivity of the catalysts suggests that **PBI.Mo** is a very stable species. Interestingly the control reaction without any catalyst also shows a low but measurable conversion to epoxide. It is difficult to directly compare the performance of **PBI.Mo batch 1** with **PBI.Mo batch 2** because the Mo loadings differ a little but it does seem that the longer activation period for **PBI.Mo batch 2** results in a catalyst with marginally lower activity.

Similar data for **Ps.AMP.Mo (5% VBC)** (25) activated 4 h, **Ps.AMP.Mo (25% VBC)** (26) activated 4 h and **Ps.AMP.Mo (88% VBC)** (27) activated 4 h are shown in Figures 3.6-3.8. At 80°C it is clear that all **Ps.AMP.Mo** (25) to (27) species are extremely active catalysts over 10 consecutive runs. However it is appears that **Ps.AMP.Mo (25% VBC)** (26) shows a little better reaction rate and stability than **Ps.AMP.Mo (5% VBC)** (25). This latter observation suggests that perhaps, the loading level of the ligand and Mo (VI)

on the polymer support plays an important role in the stability of these types of complexes. However the results of recycling **Ps.AMP.Mo (88% VBC)** (27) (Figure 3.8) demonstrate that the reaction rate using (27) is lower than that using the similar resins (25) and (26) (Figures 3.6 and 3.7). In fact these recycling data of (27) are surprising and disappointing in the view of the higher loading of (27). Furthermore despite the fact that this catalyst is less active in the first place in comparison to its analogues, it appears to be more stable than (25) and (26) in term of Mo loss during the catalytic process (see discussion later in Mo loss from polymer catalysts).

One way to improve the activity of the catalyst might be to increase the pre-activation period of the catalyst. Severe pre-activation of **Ps.AMP.Mo (88% VBC)** (27) was carried out for 8 h per day at 80°C for a period of 5 days. The results of recycling data of **Ps.AMP.Mo (88% VBC)** (27) activated 8 h per day at 80°C for a period of 5 days has shown in Figure 3. 11. It is clear that more severe activation of (27) does not improve the catalytic activity. It seems that (27) activated for 4 h at 80°C is the best pre-activation condition for this catalyst to achieve optimum activity and selectivity. It does seem that perhaps the morphology of polystyrene resin for example surface area and pore size distribution of resin also play a significant role in the activity and stability of these polystyrene resin Mo (VI).complexes.

4.4.4.2 Long-term activity of Ps.2-AMPH.Mo, Ps.GLYC.Mo, Ps.IMDA.Mo, Ps.EDTA.Mo catalysts

Similar studies to the above were carried out in order to examine the activity of four additional catalysts employing different ligands. However, one run of the epoxidation of cyclohexene was carried out first with each new catalyst at 80°C in order to investigate a relative activity between these 4 additional catalysts. Data for the epoxidation of cyclohexene using **Ps.2-AMPH.Mo** (28), **Ps.GLYC.Mo** (29), **Ps.IMDA.Mo** (30) **and Ps.EDTA.Mo** (31) as catalysts at 80°C are shown in Figure 3.12. It is clear that all four

catalysts seem very active. However , in the case of two of these 4 catalysts (30) and (31) further recycling experiments were carried out in order to evaluate their long term activity and their stability (see later in 4.4.5.2).

Thus in order to assess the long-term activity, a sample of each polymer catalyst was re-used in 5 consecutive reactions. Data for these 5 consecutive runs using (30) and (31) each activated for 4 h are shown in Figures 3.13 and 3.14 respectively. Superficially these data indicate that catalysts (30) and (31) remain very active over 5 cycles and seem comparable to e.g. **PBIMo** (Figure 3.4) and **Ps.AMP.Mo (25% VBC)** (26) (Figure 3.7). In addition both (30) and (31) are also selective since no side products were observed during the catalytic reactions. However, the Mo leaching evaluation is important in terms of the long term activity of (30) and (31) (see 4.4.5.2).

4.4.4.3 Long-term activity of MCM-41-SB.Mo (32) catalyst

In order to examine the long-term activity of the inorganic catalyst (32) in the epoxidation of cyclohexene at 80°C, a smple of catalyst was recycled 5 times. The conversion data on recycling (Figure 3.25) show that this catalyst is still active over 5 consecutive runs. in the case of the epoxidation of cyclohexene. The better conversion of TBHP was 92% after 4 h for run 1 and run 2. The lowest conversion of TBHP obtained, was 63% after 4 h for run 5. Nevertheless the initial activity is lower than that e.g. with **PBI.Mo** or (26) and it is clear that its activity decreases significantly and progressively with each run. This could imply that **MCM-41-SB.Mo** (32) is less active than the polymer-supported Mo catalysts highlighted in 4.4.4.1 and 4.4.4.2. However it could be that the reduction of the activity of (32) after each run is related to its morphology since (32) has a hexagonal arrangement of cylindrical micropores with the active sites located within its channels. It is may be possible that some channels in this catalyst become blocked during the catalytic process causing accessibility problems and hence reduction

of the activity. Overall however, it appears that **MCM-41-SB.Mo (32)** is less active than all polymer-supported Mo catalysts described previously in the case of the epoxidation of cyclohexene under typical industrial 'large scale' reaction conditions.

4.4.5 Mo loss from supported Mo catalysts

A very important issue is whether any of these supported Mo catalysts show any tendency to leach Mo. Previous work with **PBI.Mo** in the epoxidation of propene suggested that leaching was almost totally absent. However this conclusion was derived from the analysis of reaction mixture for Mo residues and the method of analysis had rather limited sensitivity[16,17]. In addition preliminary results of Mo residues from **PBI.Mo** used as a catalyst in this work are shown in 3.5.9.2 (Table 3.26). Evaluation of these data from supernatant liquids from **PBI.Mo** catalysed epoxidation of cyclohexene in 6 consecutive runs was assessed by the atomic absorption spectrometry. These also suggests that leaching does not occur during the catalytic process. This latter observation at least suggests that the amount of Mo species lost during the catalytic process is very small and below the detection limit of the standard atomic absorption spectrometer. The best way to detect any trace of active leached Mo species from all supported Mo catalysts, is to assess the residues from reaction supernatant liquids as potential catalysts for the epoxidation reaction and to compare the conversion curves with the control reaction using no catalyst. Accordingly during recycling of these supported Mo catalysts, each sample was filtered off after each run, and the corresponding supernatant solution, potentially containing leached Mo species, was evaporated to dryness. The resulting yellow residue was used as a potential catalyst for cyclohexene epoxidation. All supported Mo catalysed reactions were examined using the same procedure.

4.4.5.1 Mo loss from PBI.Mo and Ps.AMP.Mo catalysts

Data for the reactions using the residues from corresponding supernatant solutions are shown in Figures 3.15-3.19. From these data it is clear that the **PBI.Mo** and **Ps.AMP.Mo** (**24**-**27**) complexes used in the epoxidation of cyclohexene undergo loss of catalytically active Mo species during the catalytic process. The amount of Mo lost during the catalytic process is however very small because it was impossible to detect this when the supernatant liquids were assessed with the standard atomic absorption spectrometer (see Table 3.26). Nevertheless, our very sensitive study exploiting the catalytic reaction itself confirms that there are small but significant amounts of active Mo species lost from the **PBI.Mo** and **Ps.AMP.Mo** (**24**-**27**) complexes assessed. The data from use of the residues from the corresponding supernatant solutions from recycling of **PBI.Mo (batch 1)** activated 4h with TBHP are shown in Figure 3.15. It is evident from these that the amount of leached Mo species decreases progressively in the supernatant liquids from run 1 to run 10. It seems that in the latter case leaching of Mo species is almost complete after run 10 because the gap between the data from these of the residue of the supernatant liquid from run 10 and the curve for the control reaction with no added catalyst is very small. The data from the use of the residues from corresponding supernatant solutions from the recycling of **PBI.Mo (batch 2)** activated for one month at room temperature are shown in Figure 3.16. It is also clear from these that the amount of Mo species lost again decrease from run 1 to run 10. In addition from the limited conversion (~75%) achieved, it seems that the loss of Mo species from **PBI.Mo (batch 2)** activated with TBHP for one month at room temperature is less pronounced than that from the **PBI.Mo (batch 1)** activated 4h. It is tempting to suggest therefore that the pre-treatment of Mo complexes plays a role in determining the leaching behaviour of Mo species, but it is too early to draw any firm conclusions and further work is needed to deal with this issue. Data from the use of residues from the supernatant liquid from the recycling of the polystyrene resin supported catalysts **Ps.AMP.Mo** (**25**) activated 4h with TBHP, **Ps.AMP.Mo** (**26**) activated 4h and **Ps.AMP.Mo** (**27**) activated 4h are shown in Figures 3.17 and 3.18. On

the basis of the results of these experiments, it is clear that the loss of Mo species from (25) is more severe than from **PBI.Mo** species, with the loss from the (26) catalyst being similar to that from the **PBI.Mo** species. The results for **Ps.AMP.Mo** (27) (Figure 3.19) are less clear cut, but leaching of Mo from (27) may be least of all between (25)-(27). Overall these observations tend to confirm that the **PBI.Mo** catalyst is more stable than the polymer-supported polystyrene Mo (VI) catalysts where leaching varies a little and suggests that the different leaching behaviour from the latter may be due to the different morphology of these polymer-supports or due to the different ligand and Mo loadings. There is a possible trend that leaching of Mo dercreases from (25) to (26) and to (27) and the ligand content may be a key factor in the ability to retain Mo effectively. Further results using the **Ps.AMP.Mo** (36) and **Ps.AMP.Mo** (37) catalysts prepared using the same precursor resin (88% VBC) but with low Mo loading relative to ligand achieved by preparing these using ligand and $MoO_2(acac)_2$ in the stoichiometric ratios 1 : 0.5 and 1: 0.1 respectively are shown in Figures 3.9 and 3.10. Both catalysts remain active over 5 cycles but less so than e.g. **PBI.Mo**. The corresponding data for testing of the supernatants from these reactions are shown in Figures 3.20 and 3.21. The results are not particularly conclusive, but it is worth noting that the Mo contents of (36) and (37) are 0.65 mol Mo g^{-1} and 0.23 mol Mo g^{-1} respectively which are both higher than that of (25) (0.22 mol Mo g^{-1}). However the Mo leaching from the (25) is more severe than from (36) and (37). This observation suggests that the ligand content does indeed play an important role in the capacity to retain Mo effectively. However there are many other factors which can also contribute to Mo loss from polymer-supported catalysts. For example physical properties such as particle size distribution, surface area and pore size of these polystyrene supports could also be responsible of the different Mo losses observed. Very importantly as well the procedure used for evaluation of Mo loss does not distinguish between Mo species which are leached by solubilisation and those perhaps contained in traces of polymer microgel released as a result of mechanical attrition of the beads. Further work is required to shed light on these possibilities.

4.4.5.2 Mo loss from Ps.2-AMPH.Mo (28), Ps.GLYC.Mo (29), Ps.IMDA.Mo (30) and Ps.EDTA.Mo (31) catalysts

A similar study to the above was carried out to check if any of the four polymer-supported catalysts (28)-(31) undergo any tendency to leach Mo species. We examined first the corresponding supernatant liquids from one run of each these four polymer-supported Mo complexes to have an idea of their relative stability. The conversion data obtained using the residues from the corresponding supernatant solutions are shown in Figure 3.22. The experimental curves using the residues especially those from (28)-(31) show high conversions of TBHP similar to those observed with the catalysts (28)-(31) themselves (Figure 3.12). It is clear therefore that there are active Mo species leached from each of these polymer-supported catalysts. The level of Mo species lost from (28) seems more pronounced than that from (29) and (30). Furthermore the Mo residue from (31) seems to be the lowest. Indeed the activity of this residue from run 1 is lower than any previous residue from a first run. This holds out the promise that the level of Mo leaching from (31) and potentially from (30) after extensive use of each in say 5 or 10 consecutive reactions may well be negligible. Thus a more extensive study was carried out with the corresponding supernatant liquids from epoxidations using these two catalysts to check if this is indeed the case.

Data for the reactions using the residues after each run from corresponding reactions supernatant solutions involving (30) and (31) are shown respectively in Figures 3.23 and 3.24. It is clear that these two polymer catalysts leach Mo during five cycles but the pattern differs with each. Leaching from (30) is less pronounced than from (31) but remais more or less constant over 5 cycles. On the other hand leaching from (31) appears to fall on recycling. This suggests that anionic iminodiacetic acid ligand (IMDA) binds Mo more strongly than the anionic ethylene diamine tetraacetic acid ligand (EDTA) the fact that the first preliminary results suggested the contrary outcome. A further indicator

is that the Mo loading of **Ps.IMDA.Mo (30)** is 1.05 mmol Mo g^{-1} and for **Ps.EDTA.Mo (31)** is only 0.32 mmol Mo g^{-1} using the identical preparation procedure for complexation. This also suggests that the binding of the IMDA ligand to Mo is much stronger than the binding of the EDTA ligand. Leaching of Mo may be controlled by the strength of the ligand-Mo bonding or may be associated with mechanical degradation of the polymer support. Since **Ps.2-AMPH.Mo (28)**, **Ps.GLYC.Mo (29)**, **Ps.IMDA.Mo (30)** and **Ps.EDTA.Mo (31)** were all synthesised from the same precursor resin Ps (**11**) it is unlikely that the difference activity and leaching behaviour of these catalysts is attributable to any physical properties of the common support. It is much more likely to be associated with the ligand-Mo bonding. It was hoped that the anionic ligands, GLYC, IMDA and EDTA with respectively 1-3 carboxylate ligands in addition to nitrogen donor atoms might provide tighter coordination of Mo than for example the earlier neutral AMP ligand, or the neutral AMPH ligand. In fact overall it seems that the opposite is the case, and that the original AMP ligand is more effective in this respect, and that the structurally related AMPH is the best of the latter group investigated.

4.4.5.3 Mo loss from MCM-41-SB.Mo (32) catalyst

The recycling data for the inorganic catalyst (**32**) are shown in Figure 3.25 and the corresponding data for the reactions residues are shown in Figure 3.26. From these data it is clear that this (**32**) does not undergo any loss of Mo species during the catalytic process. All curves exhibit similar or lower conversion of TBHP than the conversion curve for the control reaction with no catalyst in this case. This observation suggests that the inorganic species is a very stable catalyst, and even more stable than all the previous polymer-supported Mo catalysts described in 4.4.5.1 and 4.4.5.2. However it is important to note that the activity of the catalyst itself (Figure 3.25) is somewhat poorer than the better polymer-supported species e.g. **PBI.Mo**. Strong binding between the ligand and

the Mo metal may not be the only factor responsible of the stability of this inorganic catalyst. It is possible that the porous morphology of the (32) in form of cylindrical channels, and the presence of excess OH functionality inside its channels may allow complementary interactions which could help to retain the Mo strongly and offer overall better stability. Despite this lack of leaching of active Mo, (32) does show a decay in its activity (Figure 3.25) and this may indicate that Mo is lost, but is so in an inactive form.

4.5 Cyclohexene and styrene epoxidations catalysed by supported Mo complexes under typical reaction conditions of 'small scale' synthesis

Multi-step organic syntheses commonly use dilute solution conditions. Thus it was necessary for us to assess our supported Mo complexes in various organic solvents under'small scale' synthesis conditions in order to evaluate their potential catalytic effect and their usability in typical fine organic syntheses. $MoO_2(acac)_2$, **PBI.Mo** and **MCM-41-SB.Mo** (32) complexes were tested as catalysts in the case of cyclohexene and styrene epoxidations in these dilute organic solution: 'small scale' syntheses. An essential feature of these is that the alkene is not present in excess though the oxidant nay well be.

4.5.1 Cyclohexene and styrene epoxidations using PBI.Mo complex under typical reactions conditions of 'small scale' synthesis

The epoxidation of cyclohexene and styrene in various solvents were carried out with **PBI.Mo** complex activated for 4 h used as catalyst and TBHP as oxidant are shown in Tables 3.14 and 3.13 respectively. The effect of the TBHP/alkene molar ratio on the reaction rate and conversion of cyclohexene to cyclohexene oxide at 77°C was investigated. When the cyclohexene to TBHP molar ratio was 1: 3, 100% conversion to cyclohexene oxide was achieved after 1 h in carbon tetrachloride, whereas only 35% conversion was observed after 1 h in toluene. It seems that the reaction rate in carbon

tetrachloride is significantly faster than in toluene. However when the cyclohexene to TBHP molar ratio was 1:1 using the same catalytic procedure, 89% conversion to cyclohexene oxide was observed after 4 h in carbon tetrachloride, whilst 84% conversion was obtained after 4 h in toluene. The latter observation suggests that the rates of epoxidation of cyclohexene in carbon tetrachloride and toluene are similar on the one hand, and on the other hand it may be that with a long reaction time some of the epoxide formed undergoes ring opening reactions in carbon tetrachloride. Thus in order to investigate this suggestion, cyclohexene oxide itself was reacted with TBHP in a molar ratio 1:3 and 1:1 using the same catalytic procedure. On the basis of the results of these experiments shown in Table 3.15 it is clear that no epoxide ring opening occurs in carbon tetrachloride with **PBI.Mo** as catalyst. The best result overall was obtained with 1,2-dichloroethane used as solvent. When the cyclohexene to TBHP molar ratio was 1:1, 99% of conversion of cyclohexene was completed after 3 h. In addition it also seems that chloronated organic solvents give better conversion to epoxides than other organic solvents. It is clear therefore that the reaction rate and conversion of cyclohexene to epoxide are solvent dependent. Since carbon tetrachloride is highly non-polar, and 1,2-dichloroethane is reasonably polar it is difficult to rationalise these results on polarity grounds alone. Other solvation factors may be involved.

Further studies were carried out with styrene and the homogeneous $MoO_2(acac)_2$ used as catalyst as shown in Table 3.11 to investigate solvent effects. Again it appears that solvents such as acetonitrile or ethyl acetate give poor conversion of styrene. Whereas very modest conversions of styrene are obtained in solvents such as toluene or 1,2-dichloroethane. A similar study was also carried out with styrene and the **PBI.Mo** complex activated for 4 h as shown in Table 3.13. Again poor conversion of styrene was observed in acetonitrile and ethyl acetate whereas modest conversions of styrene were completed in toluene and 1,2-dichloroethane. However a significant result is again that the supported **PBI.Mo** complex is a more potent catalyst than its homogeneous counterpart in the case of the epoxidation of cyclohexene and styrene. It is also clear that

cyclohexene and styrene epoxidations catalysed by **PBI.Mo** can be efficient and selective in dilute solutions under 'small scale' syntheses conditions, indeed these compare well with the standard reactions in bulk cyclohexene and styrene. A mole ratio cyclohexene /TBHP of 1:1 provides sufficient oxidant to achieve essentially complete epoxidation of the alkene (note the conversions in these reactions are based on NMR analysis at the alkene and its oxide) and so the procedure has potential for use in multi-step organic syntheses.

4.5.2 Cyclohexene and styrene epoxidations using MCM-41-SB.Mo (32) complex under typical reaction conditions of 'small scale' synthesis

The study of **MCM-41.SB.Mo (32)** as catalyst in typical fine chemical synthesis conditions was also carried out in the case of the epoxidation of cyclohexene and styrene. Data of the epoxidation of styrene in various organic solvents and cyclohexene in 1,2-DCE with **(32)** as catalyst and TBHP as oxidant are shown in Tables 3.16 and 3.17 respectively. Again it is apparent that the use of solvents such as acetonitrile, tetrahydrofuran and ethyl acetate in the case of the epoxidation of styrene give low conversions. However the use of solvents such as toluene and 1,2-dichloroethane in presence of the same molar ratio of TBHP and styrene give modest yields of styrene oxide. The poorer solvents that retard the epoxidation of styrene may be interacting adversely with the catalytic Mo species during the epoxidation process. Overall 1,2-dichloroethane appears to be the best solvent in the case of the epoxidation of cyclohexene with **(32)** as catalyst yielding 99 % cyclohexene oxide after 4 h with the cyclohexene to TBHP molar ratio 1: 1 (Table 3.17). **(32)** is therefore a selective and potent catalyst under 'small scale' conditions since no side products were found during the epoxidations.

4.6 Microwave assisted cyclohexene epoxidation using $MoO_2(acac)_2$, PBI.Mo and MCM-41.SB.Mo (32) catalysts

In order to further improve the rate of conversion of cyclohexene to its with the use of aTBHP : cyclohexene molar ratio 1: 1, microwave asssitance with no solvent was investigated using homogeneous $MoO_2(acac)_2$, **PBI.Mo** and **MCM-41.SB.Mo (32)** as catalysts. Data from these reactions are shown in Tables 3.20, 3.21 and 3.22 respectively. These indicate that the microwave assisted epoxidation using a TBHP: cyclohexene molar ratio 1: 1 with homogeneous $MoO_2(acac)_2$ with no solvent is a fast reaction. For example at 40°C, 56% cyclohexene oxide is formed after 15 min, and at 80°C, 75% and 94% cyclohexene oxide were obtained after 15 min and 60 min respectively. 94% cyclohexene oxide seems to be the maximum conversion possible when homogeneous $MoO_2(acac)_2$ is used (Table 3.20). Comparative studies with **PBI.Mo (batch 1)** as catalyst show again that the reaction is fast but the reaction is faster with $MoO_2(acac)_2$ than with **PBI.Mo (batch 1)** (Table 3.21). Use of **MCM-41.SB.Mo (32)** activated for 4 h gives 69% of cyclohexene oxide after 120 min at 80°C and no conversion to cyclohexene oxide was observed after 15 min at 40°C and 80°C respectively (Table 3.22). Overall, it appears that microwave assisted catalytic epoxidation in the case of a TBHP: cyclohexene molar ratio 1: 1 with homogeneous $MoO_2(acac)_2$ or **PBI.Mo** with no solvent is a useful and convenient way to obtain cyclohexene oxide under these fine chemicals synthesis conditions.

4.7 Asymmetric styrene epoxidation

For asymmetric styrene epoxidation, two polymer-supported chiral Mo complexes have been synthesised: **Ps.Phe.Mo (33)** and **Ps.SB.Mo (34)**. These complexes were pre-activated for a period of 4 h before use as catalysts in the asymmetric epoxidation of

styrene under non-microwave (Tables 3.18 and 3.19) and in microwave assisted in 'small scale' conditions and in microwave assisted 'small scale'conditions with no solvent as shown in Tables 3.23 and 3.24 respectively.

4.7.1 Asymmetric styrene epoxidation non-microwave reactions

The asymmetric styrene epoxidations were carried out under non-microwave conditions with **Ps.Phe.Mo (33)** and **Ps.SB.Mo (34)** catalysts and with a molar ratio of TBHP : styrene 1 : 1, gave poor yields and very poor enantiomeric excess. For example only 33% of styrene oxide was obtained after 4 h at 80°C with an enantiomeric excess around 4% with (34) as catalyst and 1,2-DCE as solvent. However it is often possible to increase the enantiomeric excess by lowering the temperature. Thus we carried out a styrene epoxidation at -40 °C with **Ps.Phe.Mo (33)** as catalyst and using a molar ratio of THBP : styrene 3 : 1 and 1,2-DCE as solvent. No styrene oxide was obtained after 4 h. The reaction was repeated reaction at room temperature, 30°C, 40 °C and 80°C. Moderate conversions of styrene were observed only at 80°C and with very poor enantiomeric excess around 0-5%. For example after a 4 h period 87% and 82% of styrene oxide were obtained using **Ps.Phe.Mo (33)** and **Ps.SB.Mo (34)** respectively with enantiomeric excess around 5%. Asymmetric induction with **Ps.Phe.Mo (33)** and **Ps.SB.Mo (34)** in the case of styrene epoxidation, is therefore very poor at 80°C with non-microwave reactions. However it was thought that it might be possible to improve the conversion to styrene oxide by using a microwave assisted technique with also the possibility of increasing the enantiomeric excess.

4.7.2 Asymmetric styrene epoxidation microwave assisted reactions

The results of microwave catalytic epoxidations of styrene using chiral **Ps.Phe.Mo (33)** and **Ps.SB.Mo (34)** activated for 4 h with 1,2-dichloroethane or no solvent are shown in Tables 3.23 and 3.24 respectively. From these, it is evident that the conversion of styrene

to styrene oxide under microwave conditions improves significantly with both (33) and (34). For example 66% and 92% conversion of styrene were obtained at 80°C after 1 h and 2 h respectively with the molar ratio of TBHP : styrene 3: 1 and with (33) used as catalyst and with 1,2-DCE as solvent. In addition the rate of the styrene epoxidation proves to be faster without solvent than with solvent. Thus, 99% conversion of styrene was obtained at 80 °C after 15 min with (33) and no solvent. Similar improvements were also observed with (34) in the absence of solvent. Despite these improved yields of styrene oxides, the enantiomeric excess did not change at all. The best enantiomeric excesses obtained under the microwave conditions were similar to those obtained in without microwaves, around 0-7% ee. Overall it seems that these catalysts require a relatively high temperature to achieve satisfactory rates of reactions, and at these temperatures asymmetric induction is minimal. Other chiral ligands may provide better results.

4.8 Continuous epoxidation of cyclohexene in a Reactive Distillation Column with PBI.Mo as catalyst.

Use of a Reactive Distillation Column (RDC) involves a simultaneous process of reaction and distillation in a single column or vessel. A RDC provides a large number of advantages over the conventional sequential approach of reaction followed by distillation or other separation techniques e.g. improving substantially selectivity and conversion of reactions, solving difficult separations systems where other techniques encounter their limit, reducing capital and running costs etc.

As stated earlier in section 1.4, a RDC separation process is complex interactions between vapor-liquid equilibrium, mass transfer rates, diffusion and chemicals kinetics. Together these pose great challenges to understanding, designing and building a RDC process. Thus, although RDC was invented in 1921, the first industrial application of did not take place before the 1980's.

In this present work, the continuous of the epoxidation of cyclohexene has been carried out at *Loughborough University* on a industrial scale in a packed RDC as shown in 2.28. The results from the epoxidation of cyclohexene using TBHP catalysed by **PBI.Mo** activated 4 h in a RDC are shown in Table 3.25.

From these it is obvious that these results are outstanding and highly relevant. To our knowledge this is the first example of a continuous large scale production of cyclohexene oxide in high conversion and good selectivity. With a mole ratio of cyclohexene : TBHP 3.5 : 1 and with **PBI.Mo** as catalyst, 90% and 92% of TBHP conversion was obtained after 1 h and 2 h respectively in run1. In the first run, TBHP was fed into the top of reaction section whereas cyclohexene was fed into the bottom of reaction section of the RDC. Sometimes the feeding of reagents into a RDC can influence the conversion to the target product. In this case it seems that feeding the top of the reaction section with the high boiling point reagent (TBHP) and the bottom of the reaction section with the low boiling point (cyclohexene) contributes to a excellent conversion possibly because the reagents can react faster because they are both close to reactive section, which means they are close to the catalyst. Bearing in mind that the RDC is running at a pressure at 2 Bar and at a steady-state this means the temperatures are stabilized in the entire column. Thus the whole column is in vapour- liquid equilibrium that this implies that the influence of feeding position should be minimized. In run 2 for example, TBHP was fed under the condenser whereas the cyclohexene was fed into the bottom of the reaction section of the RDC. With this feed protocol 97% TBHP conversion was obtained after 1 h and 2 h respectively using the same mole ratio cyclohexene : TBHP: 3.5 : 1. In addition a total selectivity for cyclohexene oxide formation was always obtained with the **PBI.Mo** catalyst after each run. This result confirms again the potence of **PBI.Mo** as a catalyst in the case of this epoxidation reaction. Similar TBHP conversions were obtained in run 3 and run 4. After run 3, 97% TBHP conversion was achieved after respectively 1 h and 2 h when TBHP was fed into the top of reaction section and cyclohexene was fed above the reboiler using the same mole ratio cyclohexene : TBHP: 3.5 : 1. In run 4, 98% TBHP

conversion was achieved after respectively 1 h and 2 h when TBHP was fed under the condenser whereas the cyclohexene was fed above reboiler. The success of **PBI.Mo** as the catalyst in the RDC also shows again its long term stability. The sample of **PBI.Mo** was loaded in The RDC for several months, and was run as the catalyst several times. It was still very active and showed negligible lost of activity during this exercise. However the outstanding result is that for the first time, a selective epoxidation of cyclohexene with **PBI.Mo** as catalyst in a reactive distillation column has been carried out successfully. This result also shows the potential of this as an economically viable process with a high feasibility and reproducibility on a large scale. Similar processes involving epoxidation other alkenes catalysed by polymer-supported Mo species are therefore appropriate for further investigation.

REFERENCES

[1]A. Scozzafava, L. Menabuoni, F. Mincione, G. Mincione and C. T. Supuran, *Bioorg. Med. Chem. Lett.* **2002**, 11, 575.

[2]A. Scozzafava, L. Menabuoni, F. Mincione, and C. T. Supuran, *J. Med. Chem.* **2002**, 45, 1466.

[3]C. T. Kresge, M. E. Leonowicz, W. J. Roth, J. C. Vartuli, J. S. Beck, *Nature.* **1992**, 359, 710.

[4]J. S. Beck, C. Vartuli, W. J. Roth, M. E. Leonowicz, C. T. Kresge, K.D. Schmitt, C. T. W. Chu, D. H. Olson, E. W. Sheppard, S. B. McMullen, J.B. Higgins, J.L. Schlenker, *J. Am. Chem. Soc.* **1992**, 114, 10834.

[5]A. Corma, *Top. Catal.*, **1997**, 4, 249.

[6]A. Stein, B. J. Melde, R. C. Schroden, *Adv. Mater.* **2000**, 4, 249.

[7]C. Y. Chen, H. X. Li, M. E. Davis, *Microporous. Mater.*, **1993**, 2, 17.

[8]L. Y. Chen, S. Janicke, G. K. Chuah, *Microporous. Mater.*, **1997**, 12, 323.

[9]R. Ryoo, S. Jun, *J. Phys. Chem.*, **1997**, 101, 317.

[10]D. Das, C. Tsai and S.Cheng, *Chem. Commum.*, **1999**, 473.

[11]W. Lin, Q. Cai, W. Pang, Y. Yue, B. Zou, *Microporous and Mesoporous Matererials.*, **1999**, 33, 187.

[12]A. Ortlam, J. Rathousku, G. Schulz-Ekloff, A. Zukal, *Microporous Mater.*, **1996**, 6, 171.

[13]C. N. Wu, T. S. Tsai, C. N. Liao, K. J. Chao, *Microporous Mater.*, **1996**, 7, 173.

[14]S. Simpson, D. C. Sherrington, *React. Polym.* **1993**, 19, 13.

[15]S. Leinonen, D. C. Sherrington, A. Sneddon, D. McLoughlin, J. Corker, C. Canevali, F. Morazzoni, J. Reedijk, and S. B. D. Spratt, *J. Catal.* **1999**, 183, 251.

[16]M. M. Miller, D. C. Sherrington, S. Simpson, *J. Chem. Soc. Perkin Trans 2,* **1994**, 2091.

[17]M. M. Miller, D. C. Sherrington, *J. Catal.* **1995**, 152, 368.

[18]M. M. Miller, D. C. Sherrington, *J. Chem. Soc. Chem. Commun.* **1994**, 55.

Chapter 5

Summary and Conclusions

5 Summary and Conclusions

This thesis deals with the syntheses of new supported Mo catalysts potentially active, selective and stable for the epoxidation of olefins by tert-butyl hydroperoxide on an industrial scale and also in multi-step fine chemical syntheses.

The first group of catalysts synthesised, **PBI.Mo** and various **Ps.AMP.Mo**, utilised polybenzimidazole and polystyrene resin supported aminomethylpyridine respectively as the supports for the Mo-based catalysts. The polystyrene group were prepared from in-house synthesised resin using vinylbenzyl chloride monomer. This allowed the ligand loading and ligand / Mo ratio in these catalysts to be varied. Earlier versions of these supported catalysts were developed in our group, and the main objective in this work was to focus on the stability, recycling and leaching characteristics of these when used as catalysts in the epoxidation of cyclohexene. These reactions employed conditions typical of a large scale industrial process i.e. excess cyclohexene relative to the oxidant, tert-butylhydroperoxide, and minimal solvent. **PBI.Mo** proved to be a very active and selective catalyst and its stability was demonstrated in 10 cycles of the catalyst during which Mo leaching was shown to fall to a very low level. The **Ps.AMP.Mo** catalysts were also very active and selective and the best performer here was an example with a high ligand / Mo ratio which seemed to minimise Mo leaching. Overall however The **PBI.Mo** species proved to be the optimum catalyst and this was taken on into some studies of a continuous cyclohexene epoxidation process (see later).

In an attempt to develop even more stable catalyst species a number of other ligands were attached to the polystyrene resin precursor and examined as before through a number of epoxidation cycles. Some of the ligands were chosen because of their potentially stronger chelating ability, but in the event though these yielded active catalysts, they were generally less active than the **PBI.Mo** species and were no more stable than this.

One inorganic oxide supported species was also investigated based on the MCM-41 mesoporous precursor. This had thiophene-2-carboxaldehyde attached via reaction with a primary amine located on the support. This performed well as a catalyst and showed good stability suggesting that further work with this would be very valuable.

The various catalysts were also examined in cyclohexene and styrene epoxidations under conditions more typical of fine chemicals syhnthesis i.e. in solvent and with an oxidant / alkene ratio of at least 1/1. In these single batch reactions some of supported catalysts performed extremely well, notably again **PBI.Mo**. In this instance however there was a very strong dependence on the solvent, with 1,2-dichloroethane being the best. The source of this dependence is unclear but does not seem to be polarity alone. These reactions were also improved with microwave assistance and could even be carried out without any solvent.

Attempts to exploit some supported chiral Mo complexes as catalysts in the asymmetric epoxidations of styrene proved to be unsuccessful probably because these were active only at high temperature (80°C). Reactions run at much lower temperatures (down to -40 °C) were simply too slow.

In the final part of the work the use of **PBI.Mo** in a scaled- up cyclohexene epoxidation was investigated. This involved collaboration with Dr. Basu Saha in the Chemical Engineering department at Loughborough University funded by the UK EPSRC. The process is a continuous one carried out a single unit operation in a Reactive Distillation Column (RDC). The **PBI.Mo** was prepared at the University of Strathclyde and, once the rig was complete and commissioned, the present author visited to generate the data reported here. The **PBI.Mo** and RDC rig performed beyond expectation and was operated in successive runs over many months with the same batch of catalyst in the reactor zone of the RDC. Very high conversion to cyclohexene oxide was achieved continuously with very high selectivity, and the process is currently being patented.

6 Future work

It seems unlikely that more active and selective catalysts than the **PBI.Mo** species can be found and future work will focus on carrying out other alkene epoxidations in the RDC rig, particularly alkenes of commercial importance.

However the results with the MCM-41 based catalysed are very encouraging, and this species might be useful in the epoxidations of relevance to the fine chemicals and pharmaceuticals businesses. Further work on microwave enhancement also seems well worthwhile.